

NAVAL POSTGRADUATE SCHOOL
Monterey, California



THESIS

THIS QUALITY IMPROVED

**LASER DOPPLER VELOCIMETRY
IN THE SPACE-SHUTTLE MAIN ENGINE
HIGH-PRESSURE FUEL TURBOPUMP**

by

James D. Southward

March 1998

Thesis Advisor: Garth V. Hobson

Approved for public release; distribution is unlimited.

19980427 159

REPORT DOCUMENTATION PAGE			Form Approved OMB No. 0704-0188	
Public reporting burden for this collection of information is estimated to average 1 hour per response, including the time for reviewing instructions, searching existing sources, gathering and maintaining the data needed, and completing and reviewing the collection of information. Send comments regarding this burden estimate or any other aspect of this collection of information, including suggestions for reducing this burden to Washington Headquarters Services, Directorate for Information Operations and Reports, 1215 Jefferson Davis Highway Suite 1204, Arlington, VA 22202-4312, and to the Office of Management and Budget, Paperwork Reduction Project (0704-0188), Washington, DC 20503.				
1. AGENCY USE ONLY (Leave blank)	2. REPORT DATE March 1998	3. REPORT TYPE AND DATES COVERED Master's Thesis		
4. TITLE AND SUBTITLE LASER DOPPLER VELOCIMETRY IN THE SPACE-SHUTTLE MAIN ENGINE HIGH-PRESSURE FUEL TURBOPUMP			5. FUNDING NUMBERS	
6. AUTHOR(S) CDR James D. Southward, USN				
7. PERFORMING ORGANIZATION NAME(S) AND ADDRESS(ES) Naval Postgraduate School Monterey, CA 93943-5000			8. PERFORMING ORGANIZATION REPORT NUMBER	
9. SPONSORING/MONITORING AGENCY NAME(S) AND ADDRESS(ES)			10. SPONSORING/MONITORING AGENCY REPORT NUMBER	
11. SUPPLEMENTARY NOTES The views expressed in this thesis are those of the author and do not reflect the official policy or position of the Department of Defense or the U.S. Government.				
12a. DISTRIBUTION/AVAILABILITY STATEMENT Approved for public release; distribution is unlimited.			12b. DISTRIBUTION CODE	
13. ABSTRACT (Maximum 200 words) Modifications were made to the Naval Postgraduate School cold-flow turbine test rig to enable integration of a two-component laser-doppler velocimetry (LDV) system. The test turbine was the Space-Shuttle Main Engine, High-Pressure Fuel Turbopump, Alternate-Turbopump Development Model, manufactured by Pratt & Whitney. Flow field measurements were obtained, using a the LDV system, in the first-stage rotor end-wall region of the test turbine, at three axial locations and at three depths from the end wall. For each survey location, velocity ratios, absolute flow angle, turbulence intensities, and correlation coefficients were examined. The laser data exhibited distinct trends with axial position, depth from the end wall, and with circumferential position. In addition to the laser data, velocity profiles were determined at the first-stage stator inlet and rotor exit planes, using a three-hole pressure probe. Both laser and probe data were taken at referred rotational speeds in the range 4815 to 4853 rpm. Phase-locked measurements were recorded using a once-per-revolution signal from a magnetic pick-up as a trigger. TSI Phase-resolved software version 2.06 was used for laser data acquisition and reduction.				
14. SUBJECT TERMS Turbine, Data Acquisition, Laser Doppler Velocimetry, Space Shuttle Main Engine, High Pressure Fuel Turbopump.			15. NUMBER OF PAGES 172	
			16. PRICE CODE	
17. SECURITY CLASSIFICATION OF REPORT Unclassified	18. SECURITY CLASSIFICATION OF THIS PAGE Unclassified	19. SECURITY CLASSIFICATION OF ABSTRACT Unclassified	20. LIMITATION OF ABSTRACT UL	

NSN 7540-01-280-5500

Standard Form 298 (Rev 2-89)
Prescribed by ANSI Std. Z39-18
298-102

Approved for public release; distribution is unlimited

**LASER DOPPLER VELOCIMETRY
IN THE SPACE-SHUTTLE MAIN ENGINE
HIGH-PRESSURE FUEL TURBOPUMP**

James D. Southward
Commander, United States Navy
B.S., University of New Mexico, 1980

Submitted in partial fulfillment of the
requirements for the degree of

MASTER OF SCIENCE IN AERONAUTICAL ENGINEERING

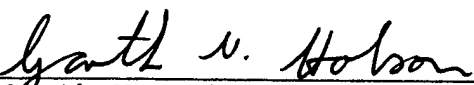
from the

**NAVAL POSTGRADUATE SCHOOL
March 1998**

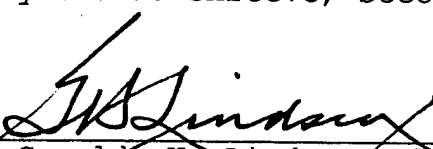
Author:


James D. Southward

Approved by:


Garth V. Hobson, Thesis Advisor


Raymond P. Shreeve, Second Reader


Gerald H. Lindsey, Chairman,
Department of Aeronautics and Astronautics

ABSTRACT

Modifications were made to the Naval Postgraduate School cold-flow turbine test rig to enable integration of a two-component laser-doppler velocimetry (LDV) system. The test turbine was the Space-Shuttle Main Engine, High-Pressure Fuel Turbopump, Alternate-Turbopump Development Model, manufactured by Pratt & Whitney. Flow field measurements were obtained, using a the LDV system, in the first-stage rotor end-wall region of the test turbine, at three axial locations and at three depths from the end wall. For each survey location, velocity ratios, absolute flow angle, turbulence intensities, and correlation coefficients were examined. The laser data exhibited distinct trends with axial position, depth from the end wall, and with circumferential position. In addition to the laser data, velocity profiles were determined at the first-stage stator inlet and rotor exit planes, using a three-hole pressure probe. Both laser and probe data were taken at referred rotational speeds in the range 4815 to 4853 rpm. Phase-locked measurements were recorded using a once-per-revolution signal from a magnetic pick-up as a trigger. TSI Phase-resolved software version 2.06 was used for laser data acquisition and reduction.

TABLE OF CONTENTS

I.	INTRODUCTION.....	1
A.	PURPOSE.....	1
B.	OVERVIEW.....	1
	1. Turbine Description.....	1
	2. Previous Research.....	2
	3. Scope of Research.....	3
C.	LASER DOPPLER VELOCIMETRY BACKGROUND.....	4
II.	EXPERIMENTAL APPARATUS.....	7
A.	OVERVIEW.....	7
B.	AIR SUPPLY SYSTEM.....	7
C.	TEST CELL AND INLET PIPING.....	9
D.	TURBINE TEST RIG ASSEMBLY.....	11
	1. Alternate Turbopump Development.....	11
	2. Turbine-Exit Throttle Valve Assembly..	13
	3. Main Shaft and Bearing Housing.....	14
	4. Quill Shaft.....	15
	5. Shaft Cover.....	15
	6. Dynamometer and Turbine Speed-Control System.....	15
	7. Bearing Lubrication and Cooling System.....	18
	8. Laser Blanks (Optical Windows).....	18
	9. Once-Per-Revolution System.....	19
E.	DYNAMOMETER COOLING SYSTEM.....	20
F.	COBRA PROBE INSTALLATION.....	21
G.	TTR DATA ACQUISITION SYSTEM.....	21
	1. Hardware Components.....	23
	a. 486 PC.....	23
	b. Scanivalve System Components.....	24
	c. Signal Conditioning Unit.....	25
	d. HP Data Acquisition Modules.....	25
	2. LabVIEW Software Package.....	26
	a. General.....	26
	b. Instrument Drivers.....	27
	c. LabVIEW Programs.....	28

H.	LDV SYSTEM.....	29
1.	Laser and Optics Assembly.....	32
2.	Traverse Table System.....	34
3.	Seed Particle Generator.....	36
4.	Electronic Components.....	37
a.	Frequency Shift System.....	37
b.	Photomultiplier System.....	37
c.	Rotating Machinery Resolver.....	38
d.	Digital Burst Correlator.....	38
5.	Phase Resolved Software.....	38
III.	EXPERIMENTAL PROCEDURE.....	41
A.	TTR Operation.....	41
1.	Pre-Start Procedures.....	41
2.	Start Procedures.....	43
3.	Shutdown Procedures.....	44
B.	COBRA PROBE MEASUREMENTS.....	44
C.	LDV PROCEDURES	46
1.	Optics Setup.....	46
2.	System Operation.....	47
a.	Hardware Setup.....	47
b.	Software Setup.....	49
c.	LDV Measurements.....	49
3.	Data Reduction.....	52
IV.	RESULTS AND DISCUSSION.....	55
A.	INLET AND EXIT COBRA PROBE SURVEYS.....	55
1.	First-Stage Stator Inlet.....	55
2.	First-Stage Rotor Exit.....	58
B.	END WALL LDV SURVEYS.....	61
1.	Overview.....	61
a.	Velocity Ratios.....	63
b.	Absolute Flow Angle.....	64
c.	Turbulence Intensities.....	65
d.	Correlation Coefficients.....	66
2.	Data at -0.16 Percent Rotor Tip Chord..	67
3.	Data at 0.35 Percent Rotor Tip Chord..	73
4.	Data at 0.84 Percent Rotor Tip Chord..	75
5.	Window Averaging.....	77
V.	CONCLUSIONS AND RECOMMENDATIONS.....	81
A.	CONCLUSIONS.....	81

B.	RECOMMENDATIONS.....	82
APPENDIX A.	PROJECT PLANNING.....	85
APPENDIX B.	ENGINEERING DRAWINGS.....	87
APPENDIX C.	CALIBRATION DATA.....	97
APPENDIX D.	LabVIEW DAS PROGRAM DOCUMENTATION.....	101
APPENDIX E.	CHECKLISTS.....	107
APPENDIX F.	FORTRAN CODE.....	119
APPENDIX G.	EQUATIONS AND CALCULATIONS.....	123
APPENDIX H.	PRESSURE PROBE DATA.....	127
APPENDIX I.	PHASE MENU SETTINGS.....	131
APPENDIX J.	LDV DATA.....	133
APPENDIX K.	TTR AND SSME DATA.....	141
	LIST OF REFERENCES.....	145
	INITIAL DISTRIBUTION LIST.....	149

LIST OF FIGURES

Figure 1.	Space Shuttle Main Engine.....	2
Figure 2.	Air Supply System.....	8
Figure 3.	Allis-Chambers Compressor.....	8
Figure 4.	Test Cell Plan View and Piping Installation.....	10
Figure 5.	Turbine Test Rig Assembly.....	12
Figure 6.	Turbine Test Rig and Holding Tank.....	13
Figure 7.	Dynamometer and Turbine Speed-Control System.....	16
Figure 8.	Once-Per-Revolution System Schematic..	20
Figure 9.	Data Acquisition System Hardware Schematic.....	22
Figure 10.	Data Acquisition System Workstation...	23
Figure 11.	Laser Orientation in the Test Cell....	30
Figure 12.	LDV System Schematic.....	31
Figure 13.	Laser and Optics Assembly.....	33
Figure 14.	LDV Fringe Pattern and Beam Arrangement.....	34
Figure 15.	Traverse Table.....	35
Figure 16.	Traverse Table/Laser Blank Beam Orientation.....	48
Figure 17.	Turbine Velocity Diagram.....	51
Figure 18.	Probe and LDV Window Locations, Annulus View.....	55
Figure 19.	Probe and LDV Window Locations, Flow-Path View.....	56

Figure 20.	Radial Position vs. Stator Inlet Mach Number.....	57
Figure 21.	Radial Position vs. Stator Inlet Swirl Angle.....	59
Figure 22.	Radial Position vs. Rotor Exit Mach Number.....	59
Figure 23.	Radial Position vs. Rotor Exit Swirl Angle.....	59
Figure 24.	LDV Survey Regions.....	61
Figure 25.	Velocity Ratios for $-0.16c_t$ and 98% Span.....	67
Figure 26.	Absolute Flow Angle for $-0.16c_t$ and 98% Span.....	67
Figure 27.	Turbulence Intensities for $-0.16c_t$ and 98% Span.....	68
Figure 28.	Correlation Coefficient for $-0.16c_t$ and 98% Span.....	68
Figure 29.	Velocity Ratios for $-0.16c_t$ and 93% Span.....	69
Figure 30.	Absolute Flow Angle for $-0.16c_t$ and 93% Span.....	69
Figure 31.	Turbulence Intensities for $-0.16c_t$ and 93% Span.....	70
Figure 32.	Correlation Coefficient for $-0.16c_t$ and 93% Span.....	70
Figure 33.	Velocity Ratios for $-0.16c_t$ and 88% Span.....	71
Figure 34.	Absolute Flow Angle for $-0.16c_t$ and 88% Span.....	71
Figure 35.	Turbulence Intensities for $-0.16c_t$ and 88% Span.....	72
Figure 36.	Correlation Coefficient for $-0.16c_t$ and 88% Span.....	72

Figure 37.	Velocity Ratios for $0.35c_t$ and 93% Span.....	73
Figure 38.	Absolute Flow Angle for $0.35c_t$ and 93% Span.....	73
Figure 39.	Turbulence Intensities for $0.35c_t$ and 93% Span.....	74
Figure 40.	Correlation Coefficient for $0.35c_t$ and 93% Span.....	74
Figure 41.	Velocity Ratios for $0.84c_t$ and 93% Span.....	75
Figure 42.	Absolute Flow Angle for $0.84c_t$ and 93% Span.....	75
Figure 43.	Turbulence Intensities for $0.84c_t$ and 93% Span.....	76
Figure 44.	Correlation Coefficient for $0.84c_t$ and 93% Span.....	76
Figure 45.	Velocity Ratios for $-0.16c_t$ and 93% Span (Window Averaging On/Off).....	77
Figure 46.	Absolute Flow Angle for $-0.16c_t$ and 93% Span (Window Averaging On/Off)....	78
Figure 47.	Turbulence Intensities for $-0.16c_t$ and 93% Span (Window Averaging On/Off)....	78
Figure 48.	Correlation Coefficient for $-0.16c_t$ and 93% Span (Window Averaging On/Off)....	79
Figure B1.	Quill Shaft (Drawing No. 4120).....	87
Figure B2.	Shaft Cover (Drawing No. 4127).....	88
Figure B3.	Three Hole Blank (Drawing No. 4137)...	89
Figure B4.	Laser Blank with Pressure Taps (Drawing No. 4133).....	90
Figure B5.	Laser Window (Drawing No. 4134).....	91

Figure B6.	Laser Window Holder (Drawing No. 4138).....	92
Figure B7.	Window (Drawing No. 4139).....	93
Figure B8.	Laser Window Covers (Drawing No. 4140).....	94
Figure B9.	Target Disk (Drawing No. 4139).....	95
Figure C1.	Lebow Load Cell Calibration.....	97
Figure C2.	Cox Flow Meter Calibration.....	97
Figure C3.	Type-J Thermocouple Calibration.....	98
Figure C4.	Cobra Probe Calibration.....	99
Figure D1.	SSME_TTR.VI Icon Hierarchy.....	101
Figure D2.	SSME_TTR.VI Front Panel.....	102
Figure D3.	TTR_TEST.VI Front Panel.....	104
Figure D4.	ACTUATOR.VI Front Panel.....	104
Figure D5.	VEL_PRFL.VI Front Panel.....	105

LIST OF TABLES

Table 1.	Scanivalve Port Assignments.....	24
Table 2.	LDV System Characteristics.....	30
Table 3.	TTS Specifications.....	35
Table 4.	Transducer Calibration.....	42
Table 5.	TTR Operating Limits.....	44
Table 6.	Traverse Table System Coordinates for Span Position.....	49
Table 7.	Window Width/Sector Delay Values.....	52
Table A1.	Thesis Milestone Chart.....	85
Table D1.	SSME_TTR.VI Description of SubVI's....	103
Table I1.	I/O Port and Processor Selection.....	131
Table I2.	Processor Settings.....	131
Table I3.	Manual Override Settings.....	131
Table I4.	Optics Configuration.....	131
Table I5.	Rotary Encoder Setup.....	132

LIST OF ACRONYMS, ABBREVIATIONS, SYMBOLS, SUBSCRIPTS AND SUPERSSCRIPTS

ACRONYMS & ABBREVIATIONS:

2-D	Two Dimensional
3-D	Three Dimensional
ADC	Analog-to-Digital Converter
ATD	Alternate Turbopump Development
CFD	Computational Fluid Dynamics
DAS	Data Acquisition System
deg.	Degrees
DMA	Direct Memory Access
DPT	Differential Pressure Transducer
DVM	Digital Volt Meter
ft-lb.	Foot-pounds
GPIB	General Purpose Information Bus
HP	Hewlett-Packard, Horse Power
HPFTP	High Pressure Fuel Turbopump
hr.	Hours
ID	Inside Diameter
in.	Inches
inHg	Inches of Mercury
I/O	Input/Output
LabVIEW	Laboratory Virtual Instrument Engineering Workbench
LDV	Laser Doppler Velocimetry
NPS	Naval Postgraduate School
OPR	Once Per Revolution
PC	Personal Computer
PHASE	Phase Resolved
PLL	Phase-Locked Loop
PS	Pressure Side
psi	Pounds Per Square Inch

psia	Pounds Per Square Inch Absolute
psig	Pounds Per Square Inch Gauge
PVC	Polyvinyl Carbonate
RMR	Rotating Machinery Resolver
RMS	Root Mean Square
RPM	Revolutions Per Minute
SCU	Signal Conditioning Unit
SDIU	Scanivalve Digital Interface Unit
sec.	Second
SS	Suction Side
SSME	Space Shuttle Main Engine
TTR	Turbine Test Rig
TTS	Traverse Table System
VAC	Volts Alternating Current
VDC	Volts Direct Current
VI	Virtual Instrument

SYMBOLS:

%	Percent
.R	PHASE raw data file
.S	PHASE statistics file
.V	PHASE velocity file
α	Absolute flow angle
β	Dimensionless pressure coefficient; Relative flow angle
ϵ	Turbulence intensity referenced to component velocity
ϕ	Angle difference between TTS and LDV access hole
γ	Specific heat ratio
κ	Half angle
λ	Wavelength
π	Pi

θ	Temperature ratio
ρ	Density
A	Area
c	Absolute velocity; Correlation coefficient; Chord
C	Centigrade
C_p	Specific heat at constant pressure
d	Spacing distance; Diameter
D	Distance (depth) from end wall
$D_{e^{-2}}$	Beam diameter of parallel beams measured in beam expander prior to entering final lens
f	Frequency
kg	Kilograms
kPa	Kilopascals
K	Kelvin
l	Length
m	Meter
M	Mach number
N	Number; Rotational speed
P	Static pressure
P1	Cobra probe total pressure
P23	Cobra probe differential pressure
R	Rankine; Gas constant per mole; Radius
s	Seconds
S	Blade spacing
T	Turbulence intensity referenced to inlet total velocity, Static temperature
U	Wheel speed
V	Velocity
w	Relative velocity
X	Dimensionless velocity

SUBSCRIPTS:

o	Stagnation quantity
---	---------------------

1	Station upstream of stator
2	Station between stator and rotor
3	Station downstream of rotor
θ	Tangential direction
D	Doppler
f	Fringe
h	Hub
i	Unspecified component direction
m	Mean value
REF	Reference
s	Shifted
t	Total condition; Tip
z	Axial direction

SUPERSCRIPTS:

'	Fluctuating component; Coordinate axis relative to LDV access hole
°	Degrees

ACKNOWLEDGMENT

First and foremost I would like to thank Dr. Garth Hobson for his instruction and guidance during this thesis research. Without his endless patience, pro-active involvement, and oversight this research would never have been completed. Rick Still also deserves a special mention for his many hours of shop support and overall professionalism. I would also like to especially thank my wife, Martine Greco, for her dedicated support and understanding during this long endeavor.

I. INTRODUCTION

A. PURPOSE

The purpose of this research was to conduct two-dimensional (2-D) laser-doppler velocimetry (LDV) flow-field measurements in the rotor end-wall region of the test turbine. Modification of the existing cold-flow Turbine Test Rig (TTR), located at the Naval Postgraduate School Turbopropulsion Laboratory, was required to integrate the LDV system. Also included in this thesis was the measurement of the velocity profiles at the first-stage stator inlet and rotor exit planes.

Both the LDV and velocity profile data will be useful in the development and validation of three-dimensional (3-D) Computational Fluid Dynamics (CFD) computer codes. These codes are viscous models which are designed to account for the case-wall boundary layer and secondary flow effects. Typically, these effects are included using empirical parameters which require an extensive experimental database. Tip leakage flows typically account for approximately 30 percent of the aerodynamic losses in turbines.

B. OVERVIEW

1. Turbine Description.

The test turbine was the first-stage turbine of the High Pressure Fuel Turbopump (HPFTP) of the Space Shuttle Main Engine (SSME). The HPFTP consists of a two-stage, axial flow turbine, driven by a mixture of steam and gaseous Hydrogen, which drives a three-stage liquid Hydrogen pump. Figure 1, from Sutton [Ref. 1: 1992], shows a diagram of the SSME. The particular turbine, or Alternate Turbopump Development model (ATD) was designed by Pratt & Whitney and produces approximately 73,000 horsepower, which is remarkable

considering the blade tip diameter is only 11 inches. The turbine was designed to operate at an inlet temperature of approximately 1900 degrees Rankine ($^{\circ}\text{R}$) and an inlet pressure of 5200 psia.

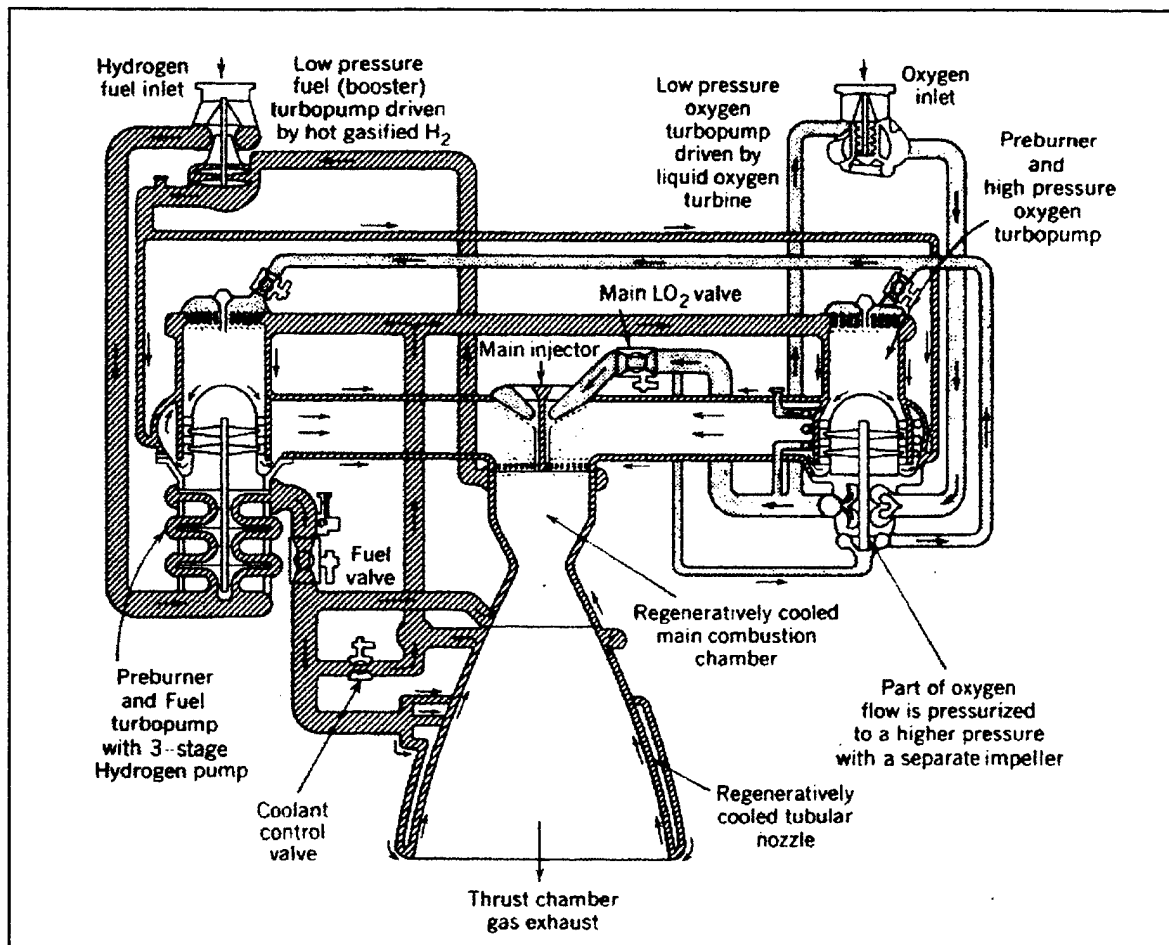


Figure 1. Space Shuttle Main Engine

2. Previous Research.

The work reported here is part of an on-going project and follows three previous efforts. Studevan [Ref. 2: 1993] was responsible for the initial design and installation of the turbine into the cold-flow test facility. His developments included the turbine inlet piping, turbine assembly (casing and bearing), incorporation of a hydraulic dynamometer, and the turbine control and instrumentation system. He also made preliminary estimations of turbine

performance. Rutkowski [Ref. 3: 1994] made modifications to the turbine installation which included redesigned bearings, an oil-mist cooling system, temperature and vibration monitoring systems, and the incorporation of a outer casing access hole and probe mount. Numerical modeling to predicted flow field characteristics of the first-stage turbine stator, using a 3-D viscous flow code, was also reported. Greco [Ref. 4: 1995] completed further modifications to the TTR to include the addition of a turbine throttle valve, upgraded turbine outer casing, dynamometer automatic speed-control system, turbine tachometer system, and a Cobra probe system. He also constructed the TTR data acquisition system, mapped the first-stage turbine performance, and used a 3-D viscous flow code to simulate the flow through the first-stage.

3. Scope of Research

The primary research goal was to obtain LDV measurements in the end-wall region of the turbine rotor. Before this could be accomplished however, the test cell and TTR required modification. The LDV system needed to be integrated into the test cell, and the Rotating Machinery Resolver (RMR) and Phase Resolved (PHASE) Software needed to be validated on the system.

Specific modifications included repositioning the TTR within the test cell, installation of an inlet piping extension, a dynamometer system heat exchanger, a new quill-shaft design, safety-wired retaining nuts and shims on the bearing housing, a shaft cover access hole, and the installation of a once-per-revolution (OPR) system. A complete description of these hardware changes can be found in Chapter II, Experimental Apparatus.

Shakedown runs were conducted over a period of three months to verify proper operation of the system components. During these runs, valuable experience was gained on

operating the newly-configured TTR, and on using the LDV system and PHASE software to reference data to the rotating frame of reference. The velocity surveys of the stator inlet and rotor exit were also measured during this period.

In the final phase of the study, LDV surveys were conducted at three positions relative to a selected rotor passage; forward of the leading edge, mid passage, and near the trailing edge.

Appendix A, Table A1 presents the program time-line and milestones.

C. LASER DOPPLER VELOCIMETRY BACKGROUND

Prior to the introduction of LDV, flow field studies of turbomachinery generally used pressure probe or hot-wire techniques. In the end-wall region of a turbine rotor, complex secondary flows exist which are the result of unsteadiness, boundary layer separation, tip vortices, and blade wakes. Probe techniques are not only exceedingly difficult to apply in this region, but probes are intrusive in nature and tend to disrupt the flows they are trying to measure.

LDV techniques measure the fluid velocity by detecting the Doppler frequency shift of laser light scattered by sub-micron particles moving with the flow. LDV has several advantages over other techniques. It is non-intrusive, independent of thermophysical properties of the flow, provides an unambiguous measurement of velocity components, and is independent of fluctuation intensities. There are, however, some disadvantages associated with LDV techniques. Optical access to the flow region is required and the flow field must be seeded. LDV does not measure the flow velocities directly, but measures the velocities of seeding particles within the flow. Seed particle size must be small enough to closely follow the flow. Accuracy of LDV

measurements can be as high as 0.1 percent for the mean flow values.

Over the last 15 years, a number of papers have been published on LDV measurements in turbomachinery. The primary focus of these papers, however, has been on compressors. Malak et al [Ref. 5: 1987] conducted 3-D LDV measurements in a radial-inflow turbine scroll. Stauter et al [Ref. 6: 1991] conducted 2-D LDV measurements in a two-stage axial compressor. Their data contained temporally and spatially resolved flow velocities of the rotor and stator wake structure. Stauter [Ref. 7: 1992] later published results of 3-D LDV measurements conducted on the same axial compressor. This time, however, measurements were made both between compressor blade rows and within the tip region of the rotating blades. Most recently, Skoch et al [Ref. 8: 1997] published a paper on single-component LDV measurements in a centrifugal impeller. They compared their data to predictions from a 3-D viscous steady flow analysis code. Only two papers were found which published LDV data taken in axial flow turbines. Binder et al [Ref. 9: 1985] used laser anemometry to measure two components of velocity and resolved unsteadiness at four axial planes inside of the nozzle-rotor space. Zaccaria et al [Ref. 10: 1995] used a 2-D LDV system to measure the steady and unsteady flow field at midspan within a turbine rotor. Their measurements were taken at 37 axial locations from just upstream of the rotor to one chord downstream of the rotor, and at six tangential locations equally spaced across one nozzle pitch. This reference was the only paper found that actually conducted measurements within the rotating blade space.

II. EXPERIMENTAL APPARATUS

A. OVERVIEW

All testing was conducted at the Naval Postgraduate School (NPS) High Speed Turbopropulsion Laboratory. Primary components of the experimental apparatus consisted of an air supply system, test cell and inlet piping, TTR assembly, dynamometer and its associated cooling system, TTR Data Acquisition System (DAS) and LDV system.

B. AIR SUPPLY SYSTEM

Compressed air from the air supply system was used to operate the TTR. The air supply system had a maximum flow rate of 10,000 cubic feet per minute which was supplied by an Allis-Chambers twelve-stage axial compressor. A 1250 horsepower (HP) electric motor drove the compressor, through a speed-increasing gear box, at 12,000 revolutions per minute (RPM). The maximum pressure ratio of the compressor was three-to-one. A schematic of the air supply system is presented in Figure 2, and a photograph of the Allis-Chambers compressor is shown in Figure 3.

Air at atmospheric pressure and temperature entered the air supply system through a filtered intake and was ducted directly to the twelve-stage axial compressor. Following compression, the air was cooled to approximately 560°R as it flowed through a water-air heat exchanger or aftercooler. Before leaving the compressor room, air passed through a moisture trap and then through a metering orifice plate where the mass flow was measured. Air was then piped to the test cell where it passed through a plenum chamber, followed by the test cell valve and finally to the turbine inlet piping.

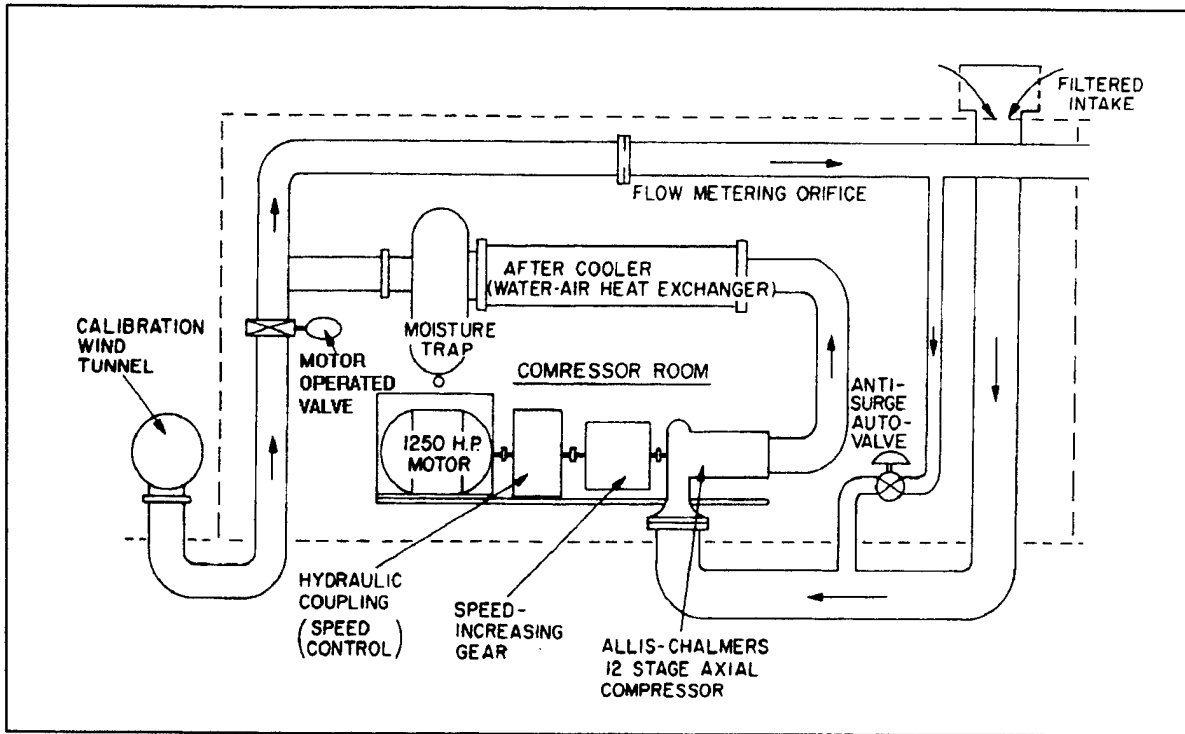


Figure 2. Air Supply System



Figure 3. Allis-Chambers Compressor

Two remotely-controlled dump valves allowed compressed air to be vented to the atmosphere, while operating the system in the standby mode. Both of the dump valves and the test cell supply valve were butterfly type valves which were electrically actuated and remotely controlled from the adjacent control room.

C. TEST CELL AND INLET PIPING

The test cell contained all of the experimental apparatus except the air supply system, controls, and DAS. An explosion-proof window, between the test cell and control room, enabled safe viewing of the apparatus during turbine operation. The layout of the test cell was changed significantly to allow incorporation of the LDV system. The entire TTR bench was moved to the east side of the cell, a heat exchanger was added, the dynamometer holding tank was relocated, a Scanivalve was brought into the cell from the control room, and 220 VAC three-phase power was installed for the laser. A test cell plan view and piping installation diagram, reflecting these changes, is shown in Figure 4.

The inlet piping consists of seven primary components; a control valve, an eight inch inside diameter (ID) piping extension, an eight inch ID double-elbow section, two vertical pipe supports, an eight-to-ten inch ID pipe coupling, and a ten-inch ID tapered section. The pipe coupling contained an internal honeycomb and screen arrangement for flow straightening purposes. Installation of the four-foot inlet piping extension was a configuration change required to repositioning the TTR to make room for the LDV system.

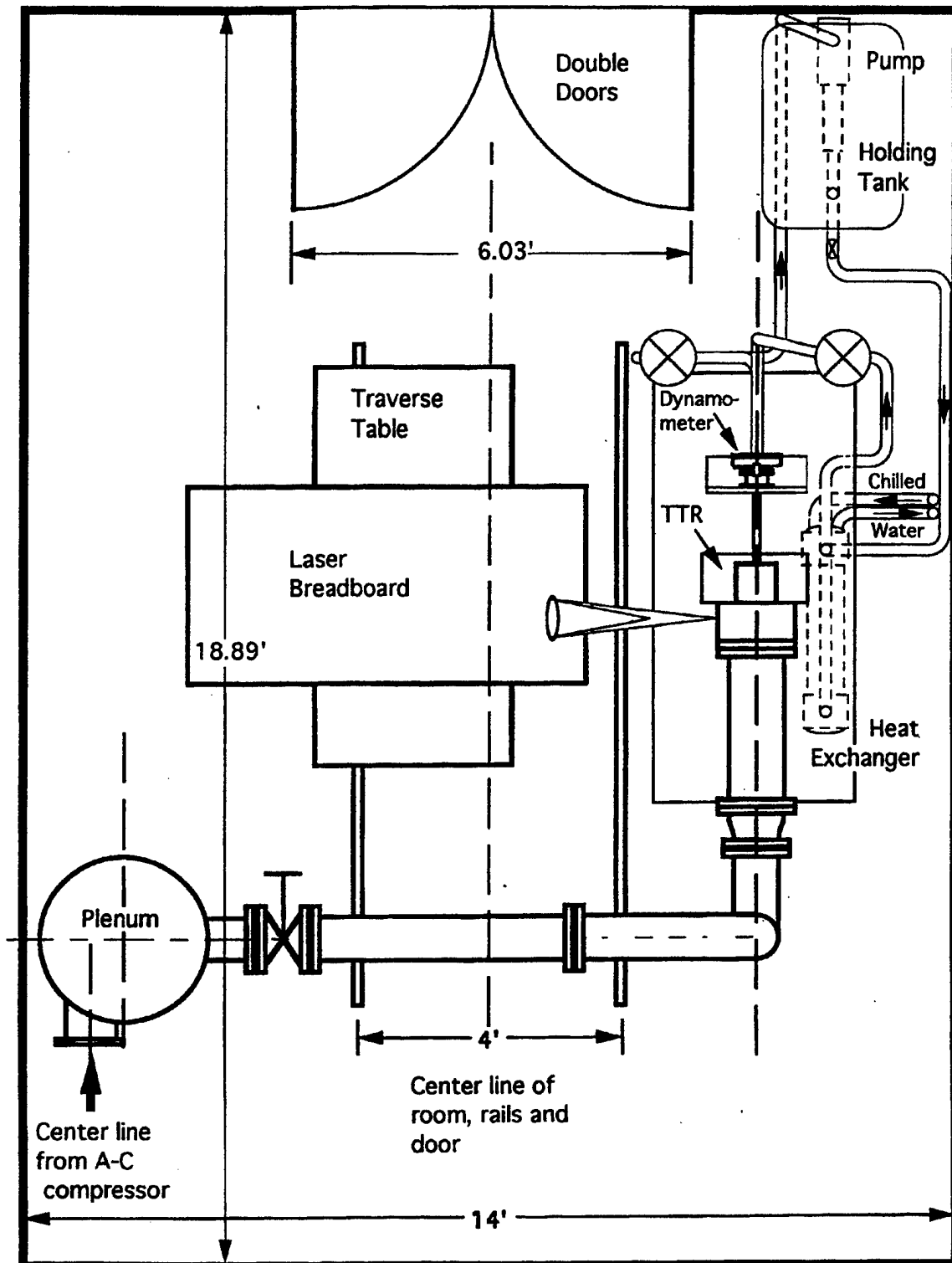


Figure 4. Test Cell Plan View and Piping Installation

Another configuration change was the installation of two vertical pipe supports on the double elbow section. They were required to carry the additional load generated by the piping extension, especially when the pipe coupling was removed during TTR maintenance. The final tapered section of the inlet piping incorporated a 2.1 degree taper on the last 10.1 inches. The taper expanded the ID to that of the turbine inlet and allowed this section to be attached directly to the TTR.

D. TURBINE TEST RIG ASSEMBLY

The TTR assembly is shown in Figures 5 and 6. It consisted of the ATD, turbine-exit throttle valve assembly, main shaft and bearing housing, quill shaft, shaft cover, dynamometer and turbine speed control system, bearing lubrication/cooling system, laser blanks, and OPR system.

1. Alternate Turbopump Development

The test SSME HPFTP ATD consisted of an inlet strut housing, first-stage stator and rotor, retaining ring, and modified outer casings. Since the initial phase of turbine testing was intended to examine only the first-stage, the second-stage rotor blades were machined down to the root. The first-stage outer casing incorporated an inlet probe slot and an access hole for the LDV window. The rotor tip gap was 0.020 inches, as measured during TTR assembly. The second-stage outer casing, included an exit probe slot and four axially aligned static pressure ports. High pressure air, from the inlet piping, flowed through the inlet struts and was turned off-axis and accelerated by the first-stage stator. Flow energy was transferred to the first-stage rotor blades as they turned in reaction to the pressure. Exit air was exhausted into the test cell.

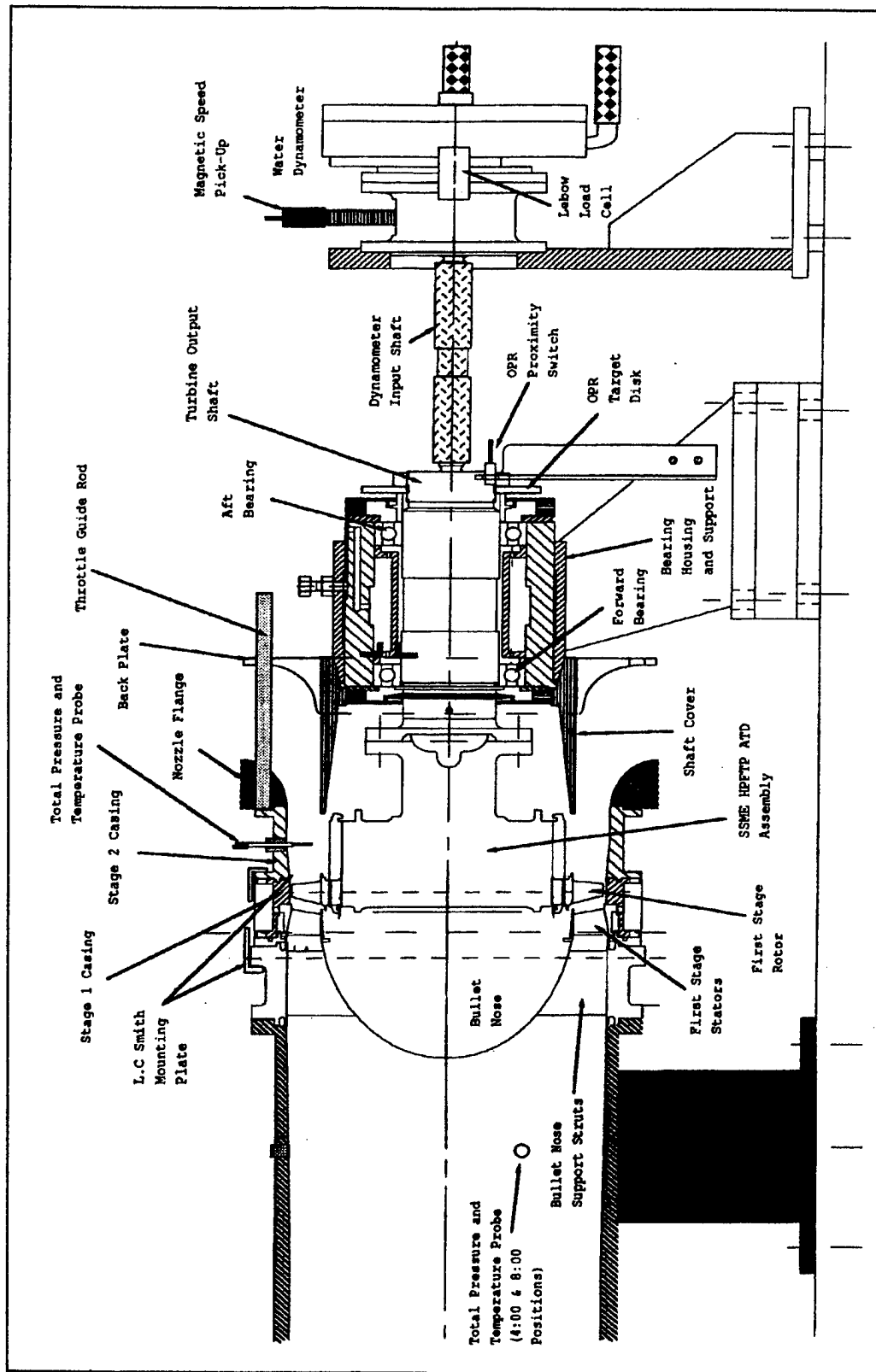


Figure 5. Turbine Test Rig Assembly

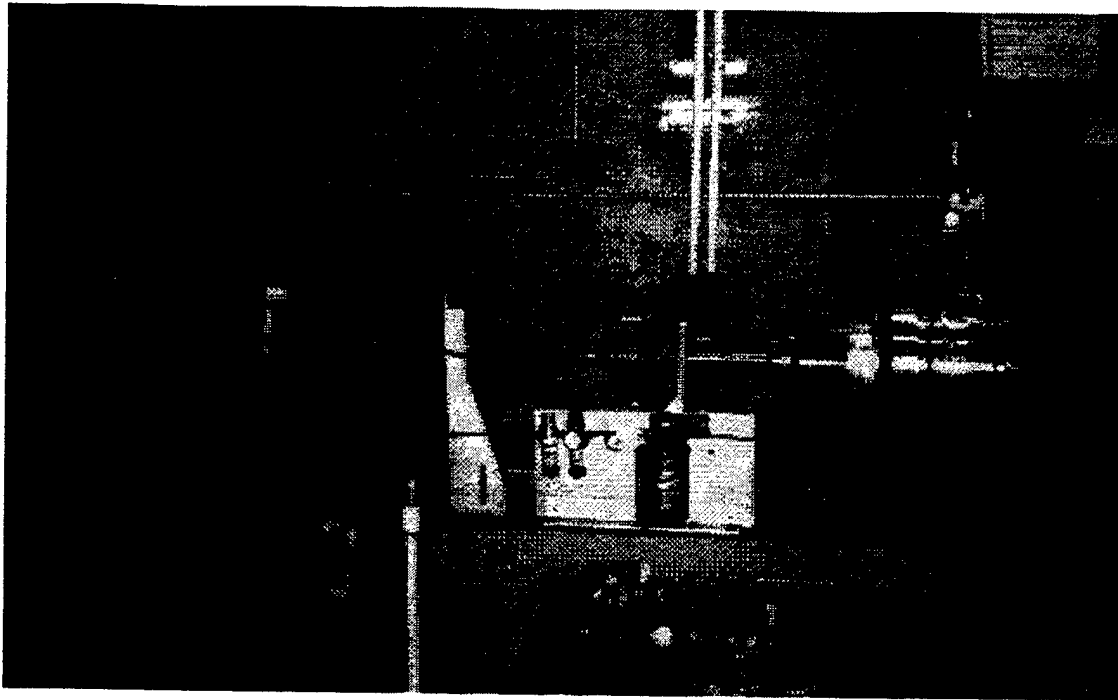


Figure 6. Turbine Test Rig and Holding Tank

2. Turbine-Exit Throttle Valve Assembly

The turbine-exit throttle valve assembly was designed to increase the total pressure upstream of the turbine and allow control of the turbine pressure ratio for performance mapping purposes. Use of the throttle valve assembly caused the exit flow to be directed outward. Turbine exit area was adjusted by positioning a back-pressure plate using a linear ball-drive actuator. The actuator was mounted between the dynamometer and the back-pressure plate. A single throttle guide rod was used to keep the back-pressure plate aligned during normal operation. For the present study, however, the back-pressure plate was set at the full open position (2.6 inches open) which resulted in slightly reduced main bearing temperatures. Additionally, the first-stage outer casing was rotated to place the laser access hole in a position compatible with the LDV system.

3. Main Shaft and Bearing Housing

The main shaft was 10.52 inches in length and was constructed of heat treated SAE 4340 hot-rolled steel. The aft end incorporated a splined fitting for the quill shaft, and was also externally threaded to accept a circular bolt to secure components, such as the OPR target disk, onto the shaft. The forward end was internally threaded and connected to a flange which bolted directly to the ATD. There were two bearing surfaces on the main shaft, which each supported Fafnir high-precision bearings. The bearing housing contained the bearings, an outer bearing spacer, oil-mist lubrication channels, and front and rear oil seal assemblies. The main shaft and bearing housing remained unchanged from that reported by Rutkowski [Ref. 3: 1994], except for two modifications. First, a 0.002 inch brass shim was added between the main shaft and flange in order to relieve stress on the lock pins, one of which had previously failed. Second, the twelve cap screws securing the front oil seal and bearing retainer to the housing, were replaced with bolts that could be safety wired. This change resulted because of minor damage which occurred to the shaft-cover inner surface when two bolts backed off.

In order to ensure safe operation of the TTR, the bearing housing incorporated both temperature and vibration monitoring systems. Thermocouples were installed at each bearing outer race and wired to digital output meters at the control panel. Two accelerometers were attached to the bearing housing support and wired to an analog Ballantine Laboratories RMS indicator, also located in the control room.

4. Quill Shaft

The quill shaft was a 7.50 inch long aluminum shaft which connected the bearing assembly main shaft to the dynamometer. The quill shaft remained unchanged except for wrench flats that were machined in the middle of the shaft. Previous TTR disassemblies required the shaft to be destroyed because no flats were present. By design, the quill shaft was manufactured of softer material than that of either the dynamometer or main shaft splines. Therefore, it needed to be routinely inspected and replaced when excessively worn. An engineering drawing of the redesigned quill shaft is presented in Appendix B, Figure B1.

5. Shaft Cover

The shaft cover provided a guiding surface for the back-pressure plate and also provided a smooth flow path for turbine exhaust air. It attached to the bearing housing oil seal end-plate with six setscrews. The shaft cover was slightly modified from the configuration presented by Greco [Ref. 4: 1995], in that the lock pin access slot was enlarged to provide easier access to the lock pins during TTR assembly. An engineering drawing for the modified shaft cover is provided in Appendix B, Figure B2.

6. Dynamometer and Turbine Speed-Control System

The dynamometer and turbine speed-control system consisted of a hydraulic dynamometer, load cell, magnetic speed pickup, tachometer, inlet and outlet control valves, manual valve regulator, electronic controller, and flow meter. Figure 7 presents a schematic of this system. Turbine power was absorbed by a 250 HP hydraulic dynamometer, which was connected to the quill shaft. Water entered the dynamometer housing at its center and was accelerated

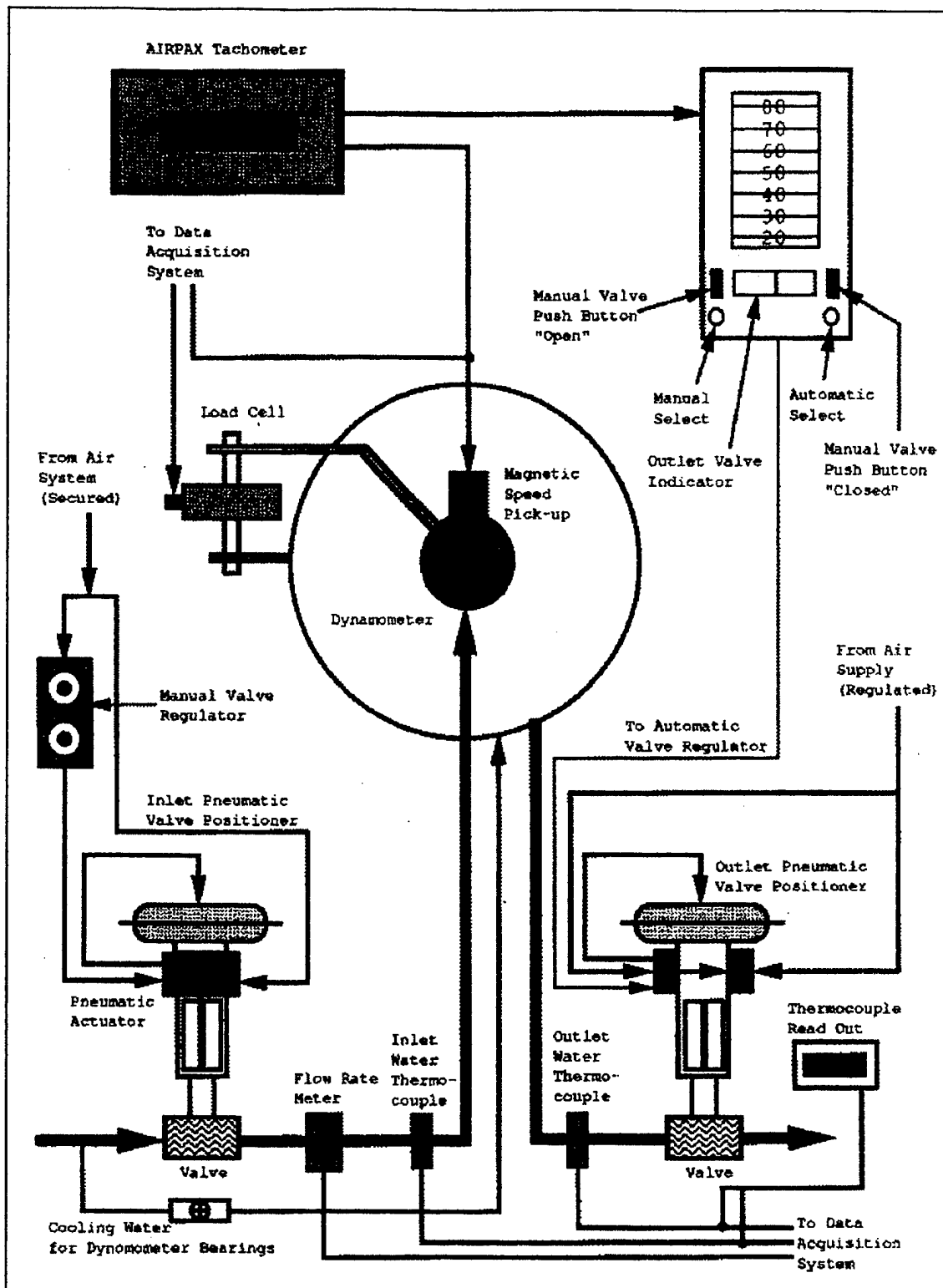


Figure 7. Dynamometer and Turbine Speed Control System

outward over a perforated disk rotating between a set of perforated stators. Centrifugal pressure and gravity caused the water to exit through a discharge hole in the bottom of the housing. Torque was generated on the dynamometer housing by the resistance created from water flow over the perforated disks. Additional information on the dynamometer can be found in the instructional manual [Ref. 11: 1976]. A Lebow load cell was incorporated on the housing to measure torque. A calibration curve for the load cell was constructed by Greco [Ref. 4: 1995] and verified during the present study. The curve is presented as Appendix C, Figure C1.

Turbine speed was measured by a magnetic pickup located over a thirty-tooth gear mounted on the dynamometer input shaft, and was displayed by a digital readout AIRPAX TACHTROL 3 Tachometer [Ref. 12: 1994]. Turbine speed was controlled with the dynamometer system, either automatically or manually. Water level in the dynamometer housing was adjusted to set the turbine load. A Fischer pneumatic control valve was incorporated on the inlet and outlet lines and were used to maintain the dynamometer water at a prescribed level. Valve control pressure was provided by regulated shop air at 20 psig. For the present study, the exit valve was set manually to 50 percent. The inlet valve remained full open during all TTR operations.

A Cox flow meter was installed on the inlet line to measure the dynamometer water flow rate. Additionally, two thermocouples measured the inlet and outlet water temperature. As power was absorbed by the dynamometer, the water temperature increased. This heat was removed from the water by the dynamometer cooling system. A Cox flow meter calibration curve was developed by Greco [Ref. 4: 1995] and is presented in Appendix C, Figure C2.

7. Bearing Lubrication and Cooling System

Bearing lubrication and cooling was provided by a Norgren Micro-Fog unit which was powered by filtered shop air. This oil-mist system injected a small stream of air-borne atomized oil particles into a port on the bearing housing sleeve. Subsequent ports within the outer bearing spacer routed the oil-mist to the ball bearings. Used oil was drained from the open system into a waste bucket below the TTR bench and was not recirculated.

8. Laser Blanks (Optical Windows)

Three types of laser blanks or optical windows were designed to conduct LDV measurements; a non-pressurized three-hole blank, a laser blank with pressure taps, and a laser window. The laser blanks were secured by two cap screws into a 0.75 inch circular hole located in the first stage outer casing at approximately the 09:30 position, as viewed from the inlet. The bottom surface of the laser blanks were mounted flush with the inner surface of the turbine outer casing.

The non-pressurized three-hole blank contained two 0.013 inch alignment holes and three 0.052 inch optical access ports in the bottom surface. Appendix B, Figure B3 presents the engineering drawing for this blank.

The laser blank with pressure taps was a chambered device that was designed to prevent flow through the optical access ports. It incorporated a 0.25 inch thick optical-grade acrylic window, sealed with an O-ring. Three 0.050 inch diameter stainless-steel tubes were epoxied into the pressurized blank. One tube passed through the blank at an angle and provided a static source for the end-wall pressure. Two other tubes passed into the blank horizontally

and were used for pressurizing and sensing chamber pressure. Engineering drawings for the laser blank with pressure taps and its laser window are presented in Appendix B, Figures B4 and B5.

A laser window assembly was also designed which incorporated three components; a laser window holder, window, and laser window cover. Engineering drawings for the laser window assembly are presented in Appendix B, Figures B6, B7 and B8.

9. Once-Per-Revolution System

An OPR system was installed to provide an input signal to the LDV system Rotating Machinery Resolver (RMR). The OPR system consisted of an radio frequency (RF) probe, angle-iron bracket, target disk, and digital signal conditioner. The RF probe was an Electro Sensors Model 608 solid state device [Ref. 13: 1991]. It utilized an oscillator circuit to radiate a high frequency field from the tip of the switch. The OPR signal was generated as the radiated field passed over a 1/2 inch hole machined into the target disk. The target disk was manufactured from 0.25 inch thick stainless steel stock and was balanced by removal of material from the opposite edge to the target hole. The inside diameter of the disk was machined to 2.875 inches, which allowed it to be installed over the dynamometer end of the main shaft. Appendix B, Figure B9 presents the engineering drawing for the OPR target disk.

The digital signal conditioner was an Electro Sensors Model SA420A [Ref. 14: 1997] and was only used as a power supply for the RF probe. As illustrated in Figure 8, the signal conditioner outputs (terminals 3, 4, 8 & 9) were not used, and the OPR signal was taken directly from the RF probe output (terminal 6). To boost the output signal voltage, a 550 ohm resistor was connected between the RF

probe supply and signal lines (terminals 5 & 6). The resulting output signal was a 1.0 volt square-wave pulse which was provided to the RMR. The RMR required an OPR signal strength of 0.4 to 1.4 volts.

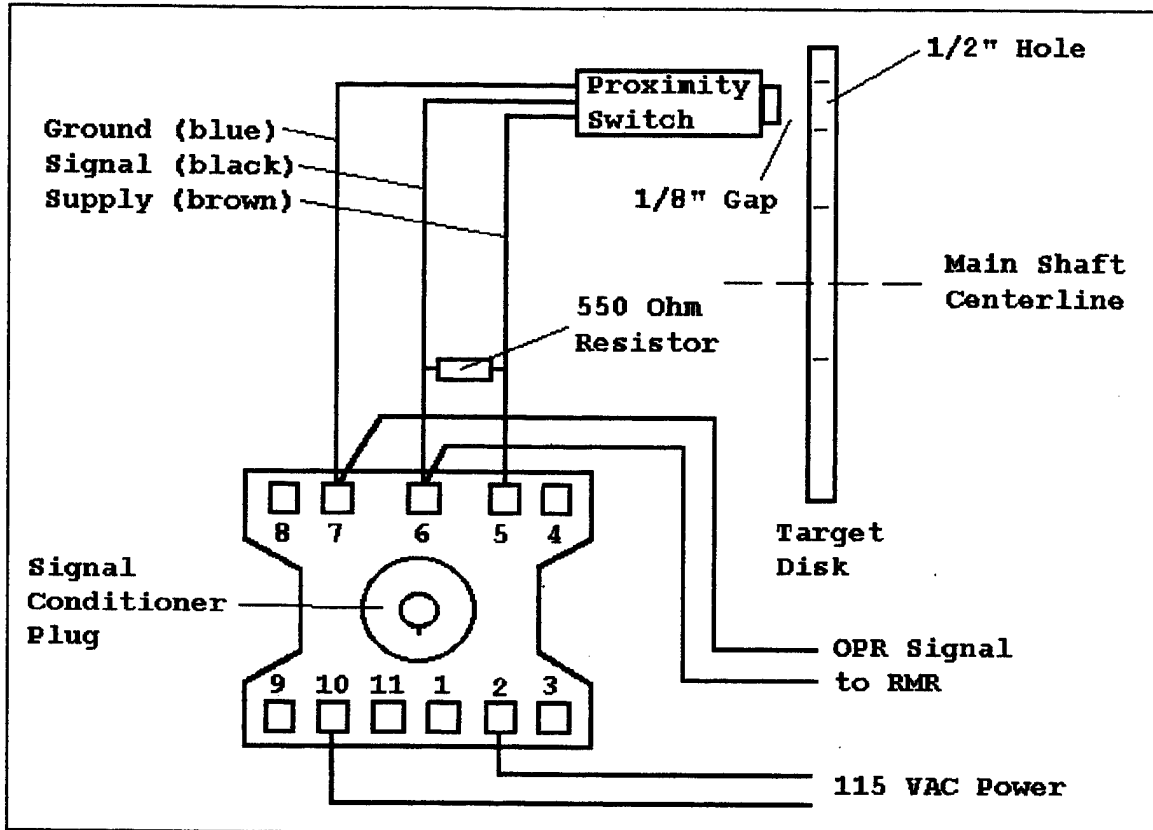


Figure 8 Once-Per-Revolution System Schematic

E. DYNAMOMETER COOLING SYSTEM

The dynamometer cooling system was designed to remove excess heat from the recirculation water. Water temperature increased as the dynamometer absorbed power from the turbine during operation. A discrepancy in the dynamometer cooling system was reported by Greco [Ref. 4: 1995]. While operating at high RPM, he noted that the chilled-water pressure, used to cool the Allis-Chalmers compressor, could easily fluctuate, causing the system to pop its pressure relief valve. This problem was solved by the installation of a liquid-to-liquid ITT Bell & Gossett Model CHX636-2S shell and tube type heat exchanger, which created a closed-circuit

recirculating system for the dynamometer. The new heat exchanger was bolted to the test cell floor below the TTR bench and plumbed with Polyvinyl Carbonate (PVC) piping as shown in Figure 4. Chilled water from the Allis-Chalmers cooling system flowed through the heat exchanger at 50 psig, and cooled the water from the dynamometer recirculation system.

F. COBRA PROBE INSTALLATION

A three-hole Cobra probe and L.C. Smith probe actuator were used to survey the first-stage stator inlet and rotor exit velocities. The probe was mounted on a bracket attached to the turbine outer casing, and its probe tip was carefully inserted through a 1/8 inch hole machined at the casing flange. Probe position was controlled with a switch box located at the DAS station, which was electrically connected to the two L.C. Smith drive motors. One motor controlled depth and the other controlled yaw position. Potentiometers on each motion actuator provided an output voltage signal to channels 13 and 14 of the PC-LPM_16 I/O board in the DAS 486 PC (Figure 9). Mach number, yaw angle, and total pressure were obtained using this installation and were recorded automatically with a computer-controlled DAS. A Cobra probe calibration was completed by Greco [Ref. 4: 1995] using the free jet calibration rig at the TPL. He plotted dimensionless velocity (X) against dimensionless pressure coefficient (β) and fit the data with a sixth-order curve fit. Appendix C, Figure C4 presents the calibration curve, polynomial fit, and explanation of the calibration dimensionless variables.

G. TTR DATA ACQUISITION SYSTEM

Figure 9 shows a schematic of the Data Acquisition System. With the exception of the Scanivalve, the TTR DAS

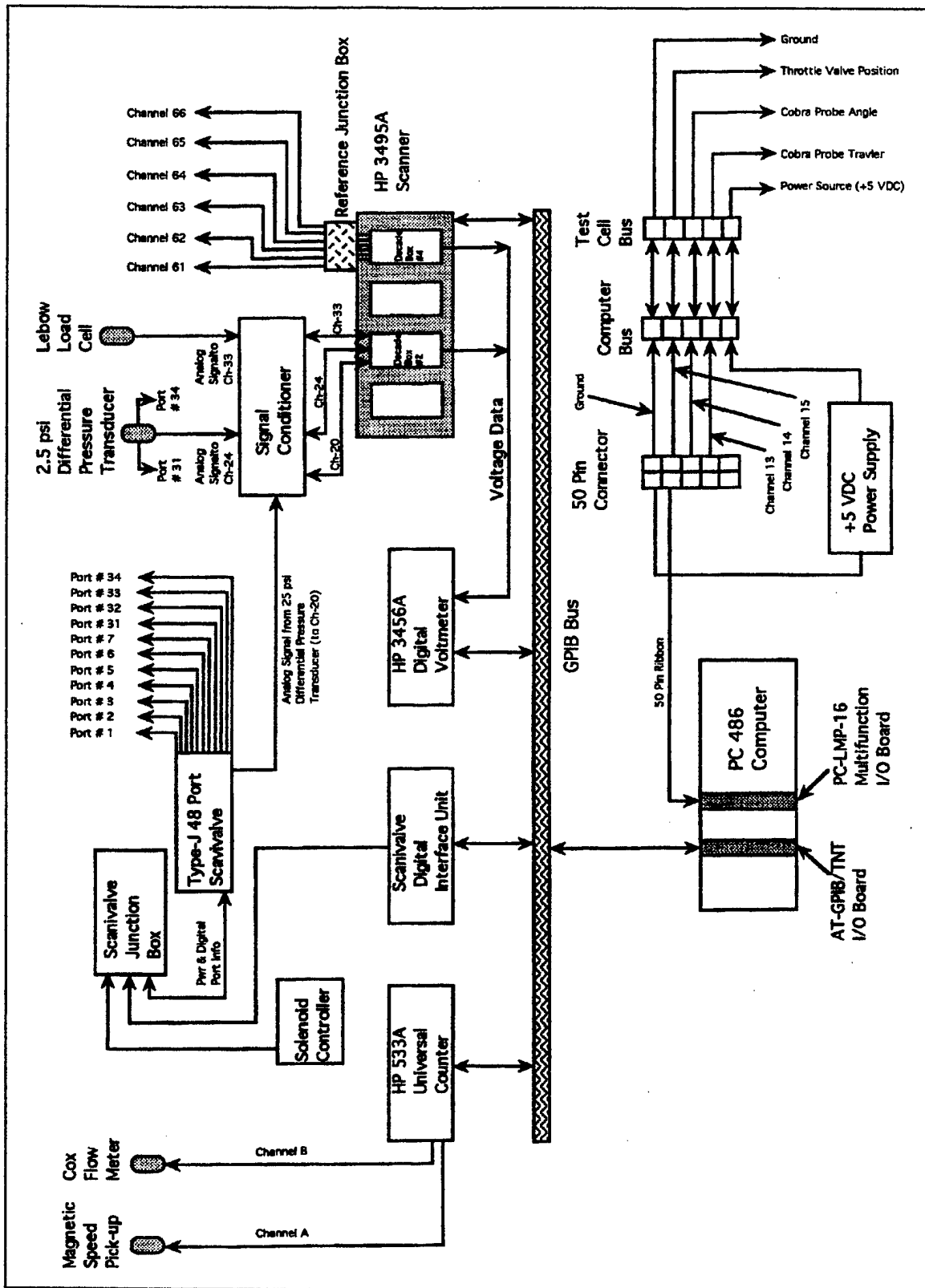


Figure 9. Data Acquisition System Hardware Schematic

was located outside the test cell in the lower control room. Figure 10 shows a photo of the DAS workstation. The TTR DAS consisted of both hardware and software components, and was developed by Greco [Ref. 4: 1995].

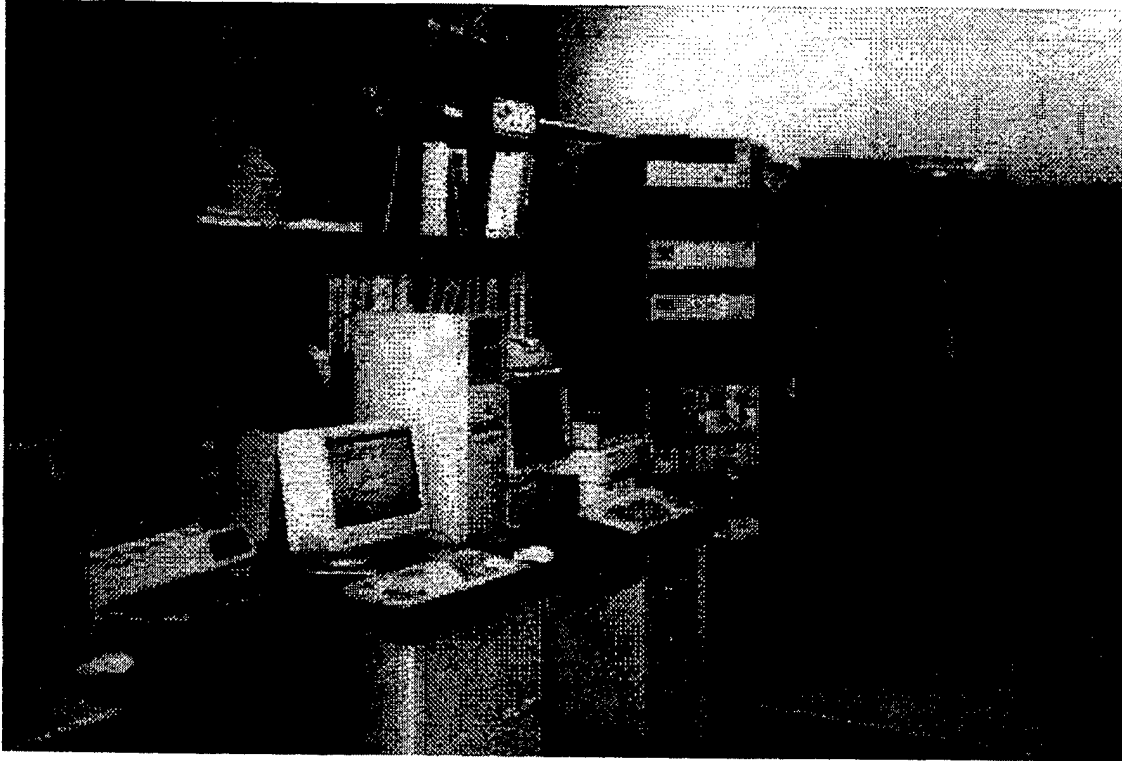


Figure 10. Data Acquisition System Workstation

1. Hardware Components

Major hardware elements included a personal computer (PC) with two interface boards, Scanivalve Digital Interface Unit (SDIU), 48-port Scanivalve, Signal Conditioner Unit (SCU), and three Hewlett-Packard (HP) data acquisition modules. The PC, HP data acquisition modules and SDIU were all connected via a General Purpose Interface Bus (GPIB), a standard digital data bus.

a. 486 PC

A 486 PC, with Laboratory Virtual Instrument Engineering Workbench (LabVIEW) software, provided interactive control of system components, near real-time

data display, and data reduction capability. Two internal boards were incorporated for interface functions. An AT-GPIB/TNT Interface Board [Ref. 15: 1994] enabled the PC to communicate with the GPIB digital data bus. A PC-LPM-16 Multifunction Input/Output (I/O) board [Ref. 16: 1993] contained a low power self-calibrating analog-to-digital converter (ADC) with sixteen analog inputs, two 16-bit timing/counter I/O channels, and eight digital I/O lines. This board was used to control and monitor the position of the Cobra probe and back-pressure plate. Power was provided by a +5 VDC power supply wired directly to pin 50 of the computer bus.

b. Scanivalve System Components

Scanivalve system components included a type-J 48-port Scanivalve, Scanivalve interface box, CTRL2/S2-S6 solenoid controller, and a Scanivalve Digital Interface Unit (SDIU). The Scanivalve contained a single differential pressure transducer, pneumatically switched to 48 port locations. Scanivalve port assignments are shown below in Table 1.

Assignment	Scanivalve Port #
Tare	1
Calibration	2
Turbine Inlet (8 O'clock) (1)	3
Turbine Outlet	4
Turbine Inlet (4 O'clock) (1)	5
Cobra Probe P1	6
Cobra Probe P23	7
Vena Contractor (2)	31
Flange (2)	32
Flange (2)	33
Vena Contractor (2)	34

Notes: (1) As viewed from inlet, looking aft
(2) Orifice plate mass flow rate

Table 1. Scanivalve Port Assignments

In the configuration reported by Greco [Ref. 4: 1995], the Scanivalve pressure ports were connected to lines spliced into a bank of Mercury manometers and routed through a manifold system into the test cell. Several of these lines, however, were found to be leaking. Additionally, Cobra probe pressure measurements were sensitive to the surface tension in the Mercury manometers. Therefore, in an effort to reduce complexity and increase data confidence, the Scanivalve was relocated in the test cell. This configuration greatly reduced the length of the pressure lines and the number of connections.

c. Signal Conditioning Unit

Four channels of the Signal Conditioning Unit (SCU) were used. Each channel contained a Wheatstone Bridge which was calibrated by adjusting its zero and span prior to operation. Channel 20 was used for the ± 25 psi Scanivalve differential pressure transducer (DPT), channel 22 for the ± 1 psi Cobra probe null-yaw DPT, channel 24 for the ± 2.5 mass-flow DPT, and channel 33 for the Lebow load cell.

d. HP Data Acquisition Modules

HP data acquisition modules included a HP 3456A Digital Voltmeter (DVM) [Ref. 17: 1982], HP 3495A Scanner [Ref. 18: 1978], and a HP 5335A Universal Counter [Ref. 19: 1988]. Each module interfaced with the PC controller via the GPIB digital data bus.

The DVM measured voltage inputs received from the various instrumentation channels and output the signals to the GPIB bus. Following commands from the controller, the HP Scanner acted as a switch box for routing input signals to the DVM.

Temperature and pressure inputs were wired into two decade boxes which provide inputs to the Scanner. Decade

box #2 connected channels 20, 24 and 33 from the SCU, and decade box #4 connected six thermocouple leads to channels 61 through 66. Type-J Iron-Constantan thermocouples were used for all temperature measurements. Temperatures were determined by measuring the voltage between the thermocouple and a reference junction. The voltage was compared to a calibration curve which was developed by Greco [Ref. 4: 1995] and is presented in Appendix C, Figure C3.

The Universal Counter was used to receive frequency signals from the magnetic speed pick-up and Cox flow meter. Inputs were connected to channels A and B on the Counter front panel.

2. LabVIEW Software Package

a. General

The software programs were LabVIEW PC-based graphical data-acquisition programs. LabVIEW for windows version 3.0 was used to run the programs. Programs were created in block diagram form using the graphical programming language G. Virtual instruments (VI) imitated actual instruments in both appearance and operation. Each VI had three features; an interactive user interface (front panel), a source code equivalent (block diagram), and a programmatic interface (icon and connector). The front panel of a VI simulated the panel of a physical instrument and contained push buttons, knobs, graphs, and other interactive controls and indicators. The front panel was used to input data and view results, and behind it was the block diagram which was analogous to the instrument circuitry. VI's received instructions through the G source code of the block diagram. Block diagrams were constructed by wiring together icons and connectors and they indicated the flow of data. VI's were also hierarchal, in that they could be used as

top-level programs or as subroutines (subVI); top level VI's contained groups of subVI's which represented application functions. A VI was run by clicking an arrow icon in the upper left hand corner of the front panel. A detailed description of LabVIEW can be found in the user manual [Ref. 20: 1993].

b. Instrument Drivers

LabVIEW VI's were developed as for the DVM, Scanner, Universal Counter, and SDIU.

The DVM and Scanner instrument drivers were designed as a combined VI, with the Scanner (SCANNER2.VI) being a subVI or subroutine to the DVM (HP_DVM.VI). This combined VI connected Scanner channels to the DVM to record a specific voltage measurement. Items wired to the ten scanner channels of SCANNER2.VI included inputs from seven thermocouples, two DPT's, and the Lebow load cell. Information input to HP_DVM.VI included scanner channel number, measurement function, range, and measurement output.

The HP 5335 Universal Counter instrument driver (HP_5335.VI) was used to control and measure frequencies for turbine RPM and dynamometer water flow rate. Information input to HP_5335.VI included function, channel A and B coupling, channel A and B impedance, channel A and B attenuation, mean on/off, and output measurement.

The SDIU instrument driver (SVCONTROL.VI) was used to step or home the Scanivalve to the desired port and display the port number on the front panel. Information input to SVCONTROL.VI included acquisition rate, Scanivalve port number, pressure measurement, count, and time delay.

c. LabVIEW Programs

Four labVIEW programs were used in the present study; SSME_TTR.VI, TTR_TEST.VI, ACTUATOR.VI and VEL_PRFL.VI. All of these programs were developed by Greco and a detailed description of each can be found in [Ref. 4: 1995].

SSME_TTR.VI was the main TTR data acquisition program. It controlled the DAS hardware to measure and display raw and reduced turbine performance data. Data were saved to two spreadsheet files; TTRdata.dat for the raw data and SSMEdata.dat for the reduced data. Atmospheric pressure in inches of mercury (inHg) was the only keyboard input required. An Icon Hierarchy Diagram and Front Panel for SSME_TTR.VI are presented in Appendix D, Figures D1 and D2. Descriptions of SubVI's used in SSME_TTR.VI are provided in Appendix D, Table D1.

TTR_TEST.VI was used during TTR start-up and shutdown to provide a near real-time display of turbine RPM, dynamometer flow rate and torque. It could not be operated concurrently with other programs and was secured, by pressing the stop button, prior to running SSME_TTR.VI. A diagram of the TTR_TEST.VI Front Panel is provided in Appendix D, Figure D3.

ACTUATOR.VI was used to position the TTR back-pressure plate, and set the radial position and yaw angle of the Cobra probe. Since the back-pressure plate was set at a single position during all LDV measurements, this program was mainly used for Cobra probe control during inlet and exit velocity surveys. ACTUATOR.VI incorporated warning and stop indicators to alert the operator when the probe tip was within either 0.2 or 0.1 inches of the hub. The calibration offset in the block diagram (source code) needed to be adjusted so that the full-down position corresponded to the

Cobra probe head being at the rotor hub with the program readout indicating zero inches. A calibration offset value of 2.66 inches was used for the stator inlet position, and 2.79 inches for the rotor exit position. A copy of the ACTUATOR.VI Front Panel is provided in Appendix D, Figure D4.

VEL_PRFL.VI was used to measure the stator inlet and rotor exit velocity, once the position and yaw angle were established using ACTUATOR.VI. Raw and reduced data were saved to a spreadsheet file Vel_prfl.dat for data analysis. Cobra probe calibration coefficients developed by Greco [Ref. 4: 1995] and used in the program, are presented in Appendix C. Calibration off-set values were also adjusted, as described above for ACTUATOR.VI. A copy of the VEL_PRFL.VI Front Panel is shown in Appendix D, Figure D5.

H. LDV SYSTEM

The LDV system used in the present study consisted of a laser and optics assembly, traverse table system, seed particle generator, electronic components, and system software. The laser was set up in the test cell perpendicular to the TTR, and was directed into the first stage turbine through a circular laser blank optical window. Three-phase 220 VAC electrical power and filtered cooling water were installed in the test cell to support laser operation. Figure 11 is a photo showing the orientation of the laser in the test cell, with respect to the TTR. Figure 12 presents an overall system schematic for the LDV and Table 2 provides a summary of the LDV system configuration.

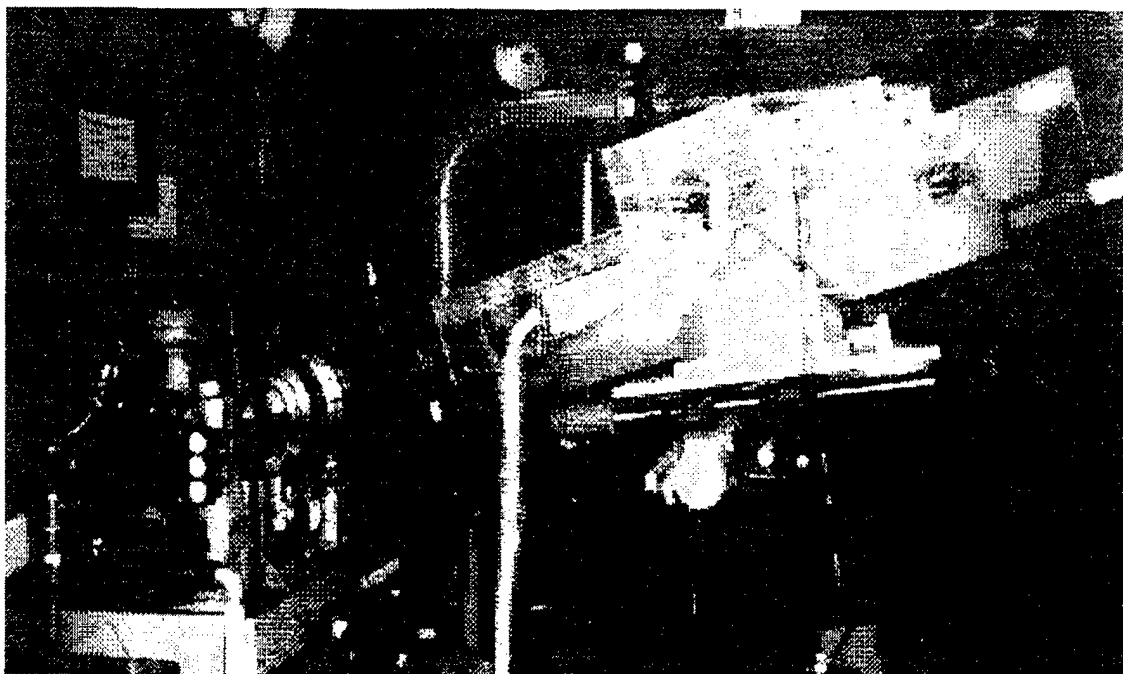


Figure 11. Laser Orientation in Test Cell

LASER:		MEASURING VOLUME:	
Type	Argon-Ion	Length	2.5 mm
Manufacturer	Lexel	Diameter	133.0 μm
Nominal Power	2.0 watts		
WAVELENGTH:		FREQUENCY SHIFT:	
Blue	488.0 nm	Range	2-40 kHz
Green	514.5 nm	Increments	1,2,5,10 MHz
FRINGE SPACING:		SIGNAL PROCESSOR:	
Blue	4.51 μm	Type Counter	IFA 750
Green	4.76 μm	Manufacturer	TSI
FOCAL LENGTH:		HALF ANGLE:	3.1 deg.
	762.0 mm	NO. OF FRINGES:	28

Table 2. LDV System Characteristics

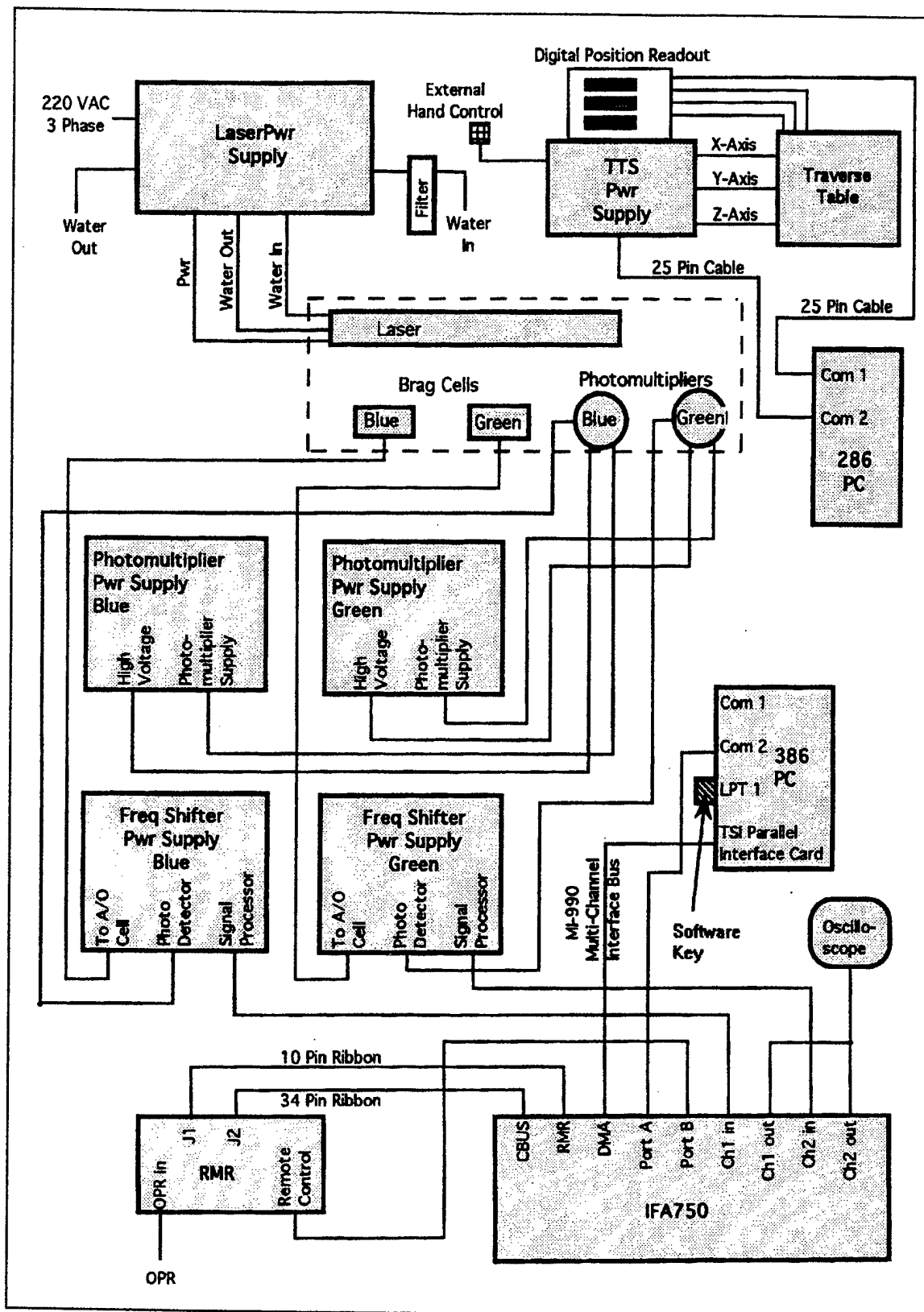


Figure 12. LDV System Schematic

1. Laser and Optics Assembly

The laser and optics assembly consisted of a TSI Model 9100-7 four-beam, two-color system. Figure 13 shows a diagram of the assembly, which was mounted on a three by six foot aluminum breadboard base. A Lexel Model 95 four-Watt Argon-ion laser was used. It produced a beam that was processed through the optical components shown in Figure 13, before being directed into the turbine rotor section. The beam first passed through a collimator which ensured the minimum diameter of the beam was at the focal point of the transmitting lens. Next, the beam passed through a multi-color separator and was split into four beams; two green of wavelength 514.0 nm and two blue of wavelength 488.0 nm. The four beams then passed through a series of components that displaced, polarized, and conducted frequency shifting. A beam expander was used to increase the incident beam diameter by a factor of 3.75 before being refocused with a 762 mm focal length lens. The technique of expanding and refocusing the beams reduced the signal-to-noise ratio by about fifty, and also decreased the size of the measuring volume. Figure 14 from Murray [Ref. 21: 1989] shows the resulting fringe pattern and beam arrangement.

Scattered laser light, from the seeding particles, was refocused by the receiving optics. Returning light was separated by a color-splitter into green and blue wavelengths, and then routed to separate photomultipliers. The photomultipliers converted the Doppler frequency of the optical signal into an electrical signal for processing. A detailed description of the laser and optics assembly can be found in [Ref. 22: 1984] and [Ref. 23: 1990].

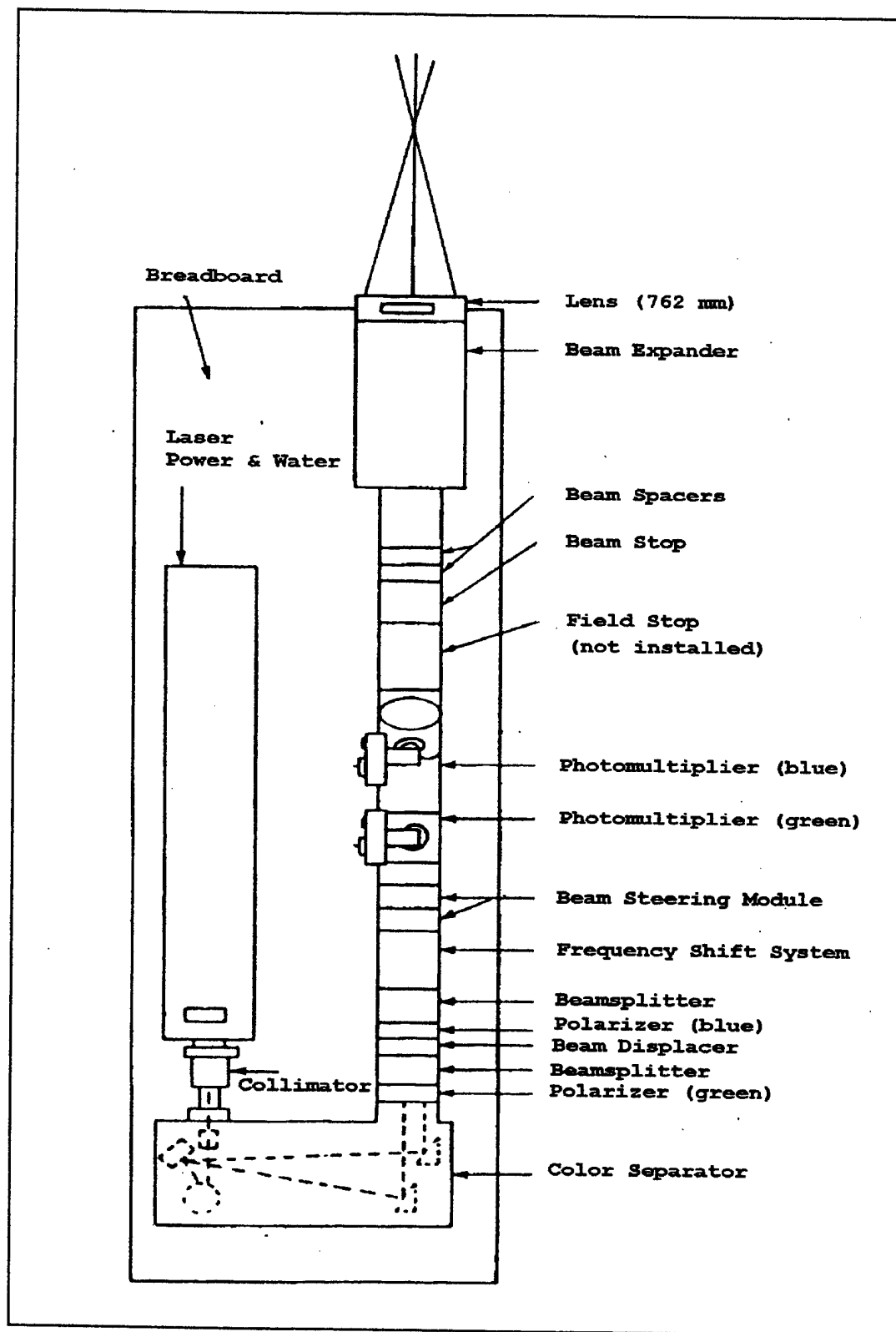


Figure 13. Laser and Optics Assembly

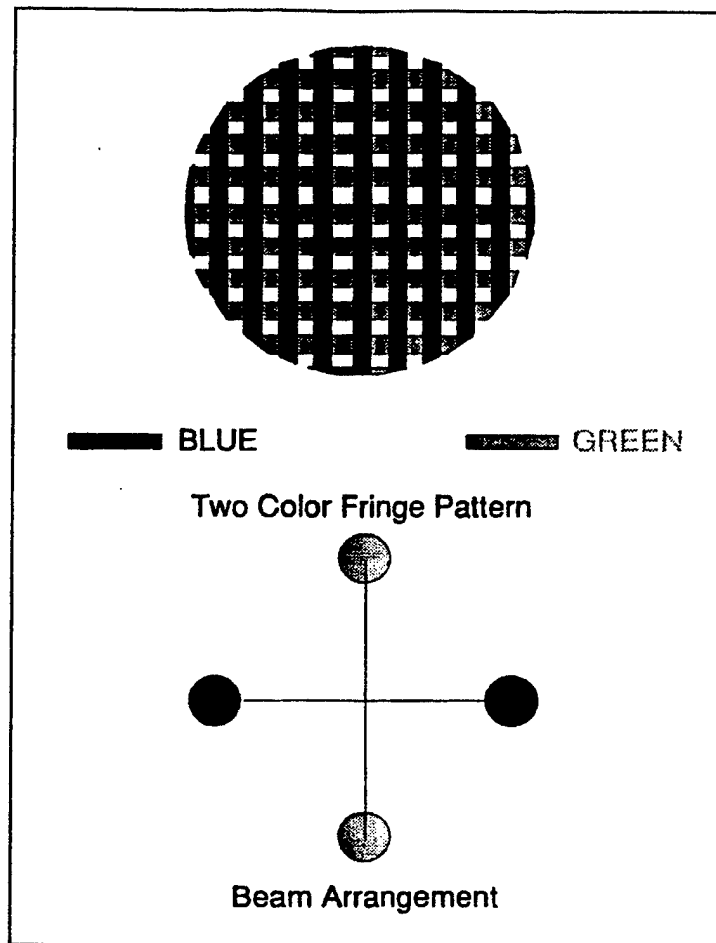


Figure 14. LDV Fringe Pattern and Beam Arrangement

2. Traverse Table System

The Traverse Table System (TTS) used was a Model 9500 manufactured by TSI and is shown in Figure 15. TTS specifications are presented in Table 3. It was an automated three-axis system which could be computer controlled in the x (axial), y (perpendicular) and z (vertical) axes. An external hand controller was also incorporated to allow manual positioning. Table movement was driven by stepper motors connected through a control box. Precision linear encoders sensed movement in each axis. A yaw table was added to the TTS, as reported by Murray [Ref. 21: 1989], which fitted between the traverse mechanism and the optical

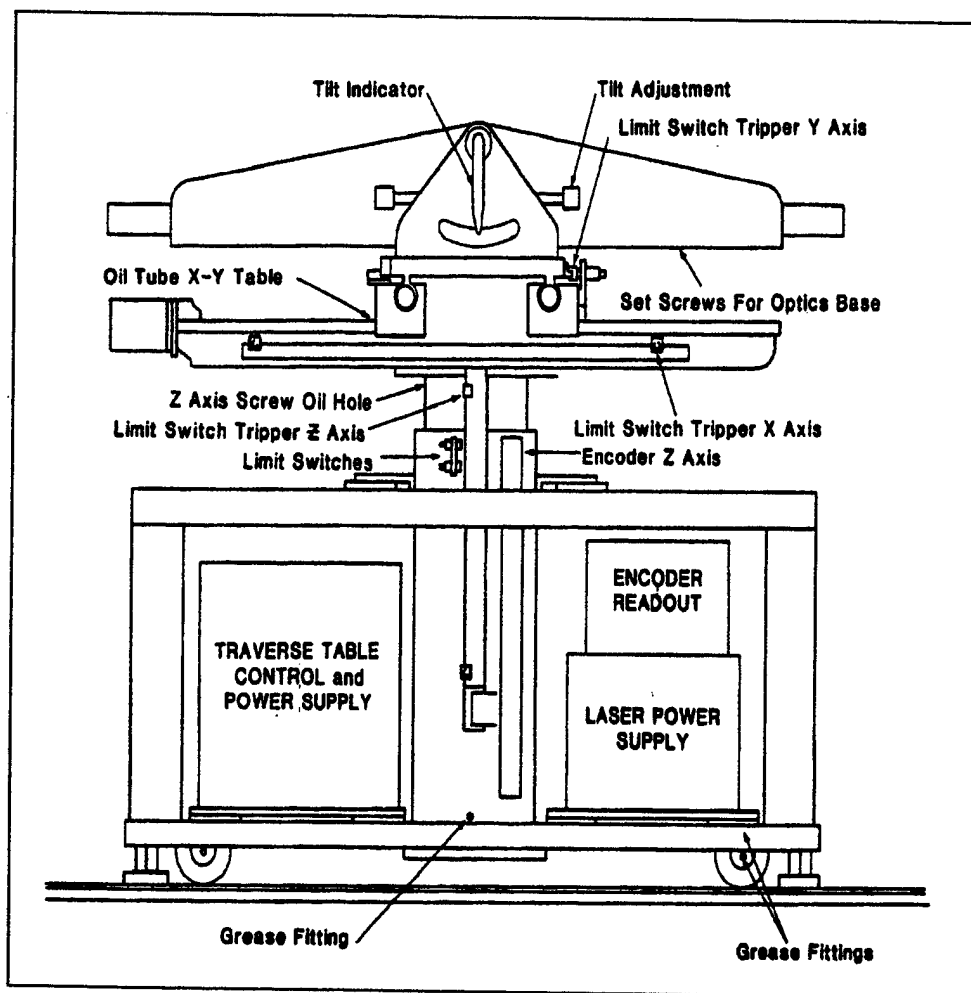


Figure 15. Traverse Table

x axis translation	38 in.
y axis translation	19 in.
z axis translation	19 in.
Tilt of optics base	± 9 deg.
Minimum movement	0.0001 in.
Readout resolution	0.0001 in.
Repeatability	0.0001 in.
Nominal Traverse rate	0.2 in./s
Load capacity	200 lb.

Table 3. TTS Specifications

platform support arms. The yaw table could accommodate up to +6 degrees of yaw.

Because of the laser blank orientation in the turbine outer casing, 14.9 degrees of tilt were required of the laser. Breadboard tilt was adjusted manually, but was limited to nine degrees. Therefore, the rear supports of the TTS were raised by 3.5 inches to meet the orientation requirements. A detailed description of the traverse table can be found in [Ref. 24: 1987].

3. Seed Particle Generator

A TSI Six-Jet Atomizer Model 9306 was used for the present experiment. It incorporated a pressure regulator, dilution system, and the capability to select from one to six atomizer jets. Anhydrous glycerin was selected as a seeding material because of its small particle size, water solubility, and tendency to not build up on flow surfaces to the same extent as oil-based materials. It was atomized using 35 to 50 psig shop air with all six jets operating, and with a dilution air setting of 80. In general, seed particle size could vary from 0.1 to 10 μm , but in the present work was typically about 1 μm [Ref. 25: 1992], so that the particles would closely follow the flow. The seeding wand injected atomized particles into the inlet piping 31.0 inches from the measurement window. It was important to introduce the seeding material far enough upstream so that the wand did not interfere with the flow in the measurement section. For some measurements, two atomizers were connected in parallel through a manifold system to increase seed particle density, in an effort to increase data rate. A detailed description of the Six-Jet atomizer can be found in [Ref. 25: 1992].

4. Electronic Components

The electronic components consisted of two frequency shifters, two photomultipliers, a RMR, digital burst correlator, and two PC controllers. Figure 12 shows a schematic of the electronic components. All items were located in the test cell except the main computer system, which was located in the upper control room. That computer received digital inputs from the signal processor via a TSI Model MI-990 Multi-Channel Interface Bus, and the other computer was used in the test cell for initial set-up. An oscilloscope was also connected to the signal processor to provided real-time monitoring of the Doppler-burst signal quality.

a. Frequency Shift System

Frequency shifting allowed the measurement of high speed flow by moving the Doppler frequency to a more optimum range for the digital burst correlator. Shifting was accomplished using two TSI Model 9180-3A Frequency Shift Systems. Each system consisted of an acousto-optic modulator, power supply, and down mixer for the photodetector signal. One shifter was used for the green beam and another was used for the blue beam. A detailed description of the frequency shift system can be found in [Ref. 26: 1984].

b. Photomultiplier System

Two TSI Model 9160 Photomultiplier systems were used to convert the received optical signal to an electrical signal suitable for processing. Each system consisted of a photomultiplier with removable aperture, power supply, and a 50-ohm termination box. One photomultiplier system was used for each of the two beams (green and blue).

c. Rotating Machinery Resolver

A TSI Model 1989A High-Speed RMR provided the capability to precisely correlate LDV measurements to a desired angular position on the rotating turbine. A signal from the RMR allowed the digital burst correlator to latch the angular position to a corresponding velocity measurement. The angular position and velocity data were sent to the computer as a matched set. Angular positions were based on a Phase-Locked-Loop (PLL) frequency multiplication of the OPR signal. The OPR was multiplied by a factor of 3600, which provided an angular position resolution of 0.1 degrees. Four PLL sensitivities were available to the operator; 90, 180, 360, and 720 minutes of arc. Data was disregarded if the phase-lock was broken at any time during a measurement. A detailed description of the RMR can be found in [Ref. 27: 1992].

d. Digital Burst Correlator

The signal processor used was a TSI Model IFA 750 digital-burst correlator. It was a fully automatic digital unit which distinguished the signal bursts from the noise based solely on signal-to-noise ratio. Signals were received from the photomultipliers via the frequency shifters from which it extracted information such as phase, frequency, burst time of arrival, and burst transit time. A detailed description of the IFA 750 can be found in [Ref. 28: 1997].

5. Phase Resolved Software

PHASE version 2.06 consisted of three subroutines; a data acquisition program, statistical program, and traverse table control program. A detailed description of the Phase software package can be found in [Ref. 29: 1992].

The data acquisition program controlled data collection from the IFA 750 and enabled phase-angle tagging for

specific velocity measurements. As data events were collected, they were associated with specific bins, each corresponded to 0.1 degrees in the rotating frame. A real-time histogram could be displayed of either frequency or velocity information.

The statistical analysis program reduced the raw data, collected by the data acquisition sub-routine, and constructed velocity and statistic files for each raw data set. Statistical parameters included, among other items, mean flow velocity, turbulence intensity, mean flow angle, Reynolds stress, and correlation coefficient. Data could be displayed in either tabular or graphical format.

The traverse table program was a seven option subroutine that could independently control movement of the traverse table. It allowed the user to compile a list of coordinate positions which the data acquisition program could then use as a predetermined path for automatic data collection.

III. EXPERIMENTAL PROCEDURE

A. TTR OPERATION

The TTR was operated on a weekly basis during a six month period when system shakedown and data runs were performed. Preheating of the lubrication system for the Allis-Chambers compressor was necessary prior to compressor start-up. Approximately one hour was needed to start and stabilize the compressor rotational speed before operating the TTR. A target referred rotation speed of 4825 RPM was chosen to conduct both Cobra probe and LDV measurements. This RPM provided a stable speed for taking data, as well as giving acceptable main-bearing temperatures and low vibration levels. Typical runs would last from four to five hours. A TTR operation checklist, provided in Appendix E, was used to conduct pre-start, start, and shut-down functions.

1. Pre-Start Procedures

Pre-start procedures included setting up the shop air supply, Cobra probe, throttle actuator, dynamometer cooling system, TTR DAS, plenum valves, and the oil mist lubrication system. If LDV measurements were to be conducted, the Cobra probe was removed from the TTR to prevent clogging with seeding material. Otherwise, the probe was retracted into the case wall prior to start. The throttle actuator was set at the full open position (2.6 inches) for all TTR operations. This position provided cooler main-bearing temperatures than other positions due to increased air flow over the bearing housing. Pre-start checks of the DAS involved calibrating the Scanivalve pressure transducer and load cell transducers, starting the LabVIEW software, and initializing data save files. Shop air, through a

calibration regulator, provided the reference pressure for the DPT calibrations. A reference pressure of 10 inHg was used for the Scanivalve and 5 inHg for the mass flow transducer. A reference moment of 67.53 ft-lb. was applied for the Lebow load cell by hanging a 31.44 lb. weight on a calibration arm, 24.0 inches from the dynamometer housing centerline. For each calibration, a test lead was attached from the output of the appropriate signal conditioning channel to the DVM. The Wheatstone bridge zero was set, after which the reference pressure or moment was applied. The bridge span was then set to the correct voltage. Since a span adjustment would slightly change the zero, this procedure was iterated until no further change of either the zero or span were required. Table 4 summarizes the transducer calibration values used.

Transducer	Channel	Reference	Voltage (VDC)
\pm 2.5 psi Mass Flow DPT	24	5.0 inHg	0.006785
\pm 25 psi Scanivalve DPT	20	10.0 inHg	0.013609
Lebow Load Cell	33	67.53 ft-lb.	0.002197

Table 4. Transducer Calibration

The LabVIEW software programs SSME_TTR.VI and TTR_TEST.VI were set up and tested. Current atmospheric pressure was entered into SSME_TTR.VI by first clicking the edit mode button on the front panel toolbar and then typing in the new value. Raw and reduced data from SSME_TTR.VI were automatically saved to two spreadsheet files; SSMEdata.dat and TTRdata.dat. Both of these data files, however, needed to be initialized before measurements could be recorded. This was accomplished by opening the data files with Windows Notepad and entering the date in the left column below the

previous entry. The cursor was returned to the next line and the changes saved before exiting Notepad.

2. Start Procedures

The first item on the start checklist, was to run TTR_TEST.VI to provide a real-time indication of RPM, torque, and water flow rate during the start-up process. An intermediate RPM of approximately 1500 was set by opening the test cell valve to twenty percent and then closing the downstream dump valve. At this condition, the mass flow rate indication from the orifice plate was accurate. Prior to increasing RPM above 1500, the test cell was inspected for any abnormal indications, such as leaks, noises, or vibrations. The test cell valve was then opened to 50 percent and the upstream dump valve was set as required to achieve about 3000 RPM. At this point another test cell inspection was conducted and final adjustments to the Cobra probe or LDV system were made. For safety reasons, personnel were not authorized in the test cell at TTR RPMs above 3000. To set the measurement RPM of approximately 5000, the upstream dump valve was slowly closed until the desired RPM was reached. RPM changes above 3000 were made slowly to avoid surging the Allis-Chambers compressor. RPM for the Allis-Chambers was indirectly monitored by a counter at the control station, and was maintained within 50 units of 3950 during speed changes. During steady-state operations, the dynamometer water temperature, main-bearing temperatures, oil-mist drip rate, and accelerometers were monitored to ensure that acceptable limits were not exceeded. TTR operating limits are presented in Table 5. TTR operating conditions were recorded each hour using a data sheet obtained from Greco [Ref. 4: 1995]. Prior to taking measurements, the LabVIEW program TTR_test.VI was run to confirm a stable operating state.

Dynamometer Water Temperature	125 °C
Main Bearing Temperature	130 °C
Accelerometers	0.01
Oil-Mist Drip Rate	1 drop/sec

Table 5. TTR Operating Limits

3. Shut-Down Procedures

Shut-down procedures were essentially an abbreviated reversal of the start and pre-start procedures. They consisted mainly of securing valves for the air supply and cooling water systems, turning off the scavenge pump, and closing the LabVIEW programs. A post shut-down inspection of the hardware was also conducted.

In the event of an equipment failure, an emergency shut-down procedure was developed. It consisted of opening both dump valves and closing the test cell valve, all simultaneously, and then securing the scavenge pump in the test cell.

B. COBRA PROBE MEASUREMENTS

A three-hole Cobra probe was used to measure the velocity profile at the first-stage stator inlet and rotor exit planes. Probe depth and yaw angle were monitored with the LabVIEW program ACTUATOR.VI, which received voltage inputs from potentiometers attached to the L.C. Smith probe actuators. Cobra probe position was manually controlled with a switch box located at the DAS station. The first task, after installing the probe on the TTR, was to verify the accuracy of the ACTUATOR.VI position readout. The calibration off-set values in the source code required modification, as described in paragraph II-G-2-c. No mechanism was in place to prevent inadvertent actuation of the probe tip into the turbine hub. Contact of the probe tip with the hub would either damage the probe or, at a minimum,

change its calibration. Radial position was measured from zero inches at the hub to 1.1 inches at the stator inlet casing and 1.0 inches at the rotor exit casing. Yaw angle was measured from -90 degrees (left yaw) to +90 degrees (right yaw) with zero degrees indicating axial flow.

The LabVIEW program VEL_PRFL.VI was used to record pressure data and calculate dimensionless velocity (X), dimensionless pressure coefficient (β), and Mach number (M). Probe total pressure (P_1) was connected to Scanivalve port number six and the differential pressure port (P_{23}) was connected to port number seven. Absolute flow angle (α) was determined by null-yawing the P_{23} pressures using a ± 1 psi DPT connected to the SCU channel 23. Note that the Cobra probe data presented in this thesis were measured with the Scanivalve located at the DAS station. This configuration not only required long pressure lines to reach the test cell, but also routed the lines through numerous connections, a switching manifold, and a Mercury manometer board. Because of the small size of the Cobra probe ports and high sensitivity of the null-yaw setup, the long pressure line runs and surface tension in the Mercury manometers were found to adversely effect the measurements. Large changes in flow velocity required up to 10 minutes for P_1 to stabilize and null-yaw values were in error up to five degrees. To mitigate these adverse effects, the P_{23} line to the Scanivalve was clamped in the test cell during flow angle measurements and was unclamped when running VEL_PRFL.VI. After completing the survey measurements, the Cobra probe was removed from the TTR and mounted in the free-jet calibration rig. Its calibration was validated up to 0.4 M by comparing the VEL_PRFL.VI output to known flow Mach number.

C. LDV PROCEDURES

1. Optics Setup

In order to obtain maximum performance from the LDV system, the laser optical components were removed from the breadboard and meticulously cleaned. Cleaning was accomplished by hand using methyl alcohol and lens cleaning tissues. Particular care was taken to avoid scratching the lens and ensuring that no "water" marks remained on the optics. During reassembly, the system components were aligned using the procedures detailed in [Ref. 22; 1984].

Once reassembly was complete, the tuning process was started by first adjusting the beam crossings. The beams were focused into a microscope objective which projected the beam pattern onto a wall surface. In this way, the beam arrangement could easily be seen with magnification and without the use of filtered goggles. Adjustments were made so that all four beams converged simultaneously to a single circle, as the y-axis of the TTR was traversed through the focal point.

After the beam crossing was properly adjusted, the receiving optics were then tuned. A scatter plate was placed at the beam crossing to provide an adequate amount of returning scattered light for the tuning process. The blue and green portions of the returning light were precisely focused onto their respective photomultiplier. To do this, each photomultiplier was removed from its mount and an alignment eyepiece was inserted in its place. The eyepiece was used to focus the returning light and adjust the focal point to the correct position. Final adjustments to the photomultipliers were made by measuring the flow velocity of an external seeding arrangement and by making minor adjustments to maximize the observed data rate, as required.

2. System Operation

Procedures used during the set-up and operation of the LDV system are documented below for the hardware, software, and LDV measurements. Appendix E contains an LDV system operation checklist which was used as a guide for routine operations. The checklist includes procedures for start-up, measurement preparation, and shut down.

a. Hardware Setup

The LDV hardware setup was completed prior to starting the TTR and was done in accordance with the start-up portion of the LDV checklist. During the set-up process, laser power was set at an eye-safe power level of 0.5 Watts, or less, to minimize the risk of eye injury. The last item on the start-up portion of the checklist was to establish the beam reference position and orient the beam through the appropriate laser-blank access hole.

The beam reference position was established manually using the TTS hand controller. A zero reference was established by centering the beam crossing through the upstream laser-blank alignment hole and adjusting the measurement volume diameter until it was minimized on the surface plane of the hole opening. Laser safety goggles were used to observe the beam arrangement and focal point during this process. The TTS used a rectangular coordinate system; therefore, once the reference position was correctly established, the digital encoder x, y and z axes were reset to zero. The x-axis was oriented in the turbine axial direction, with positive being in the upstream direction. The y and z-axes were relative to the TTS table structure, which in this application was tilted 6.0 deg toward the TTR.

The beam crossing was positioned through one of the three laser-blank access holes by traversing the laser

breadboard with respect to the TTS coordinate system. The x coordinate simply set the axial position of the measurement volume. However, because of the 8.9 degree difference between the traverse table and the laser blank, both the y and z-axes required adjusting to set the measurement volume depth. A y' -axis was defined to measure depth. It corresponded to the radial axis of the access hole and also originated on the surface plane of the hole opening. Note that the breadboard was tilted such that it aligned perfectly with the y' -axis. Figure 16 shows the beam orientation with respect to the traverse table and laser-blank access hole.

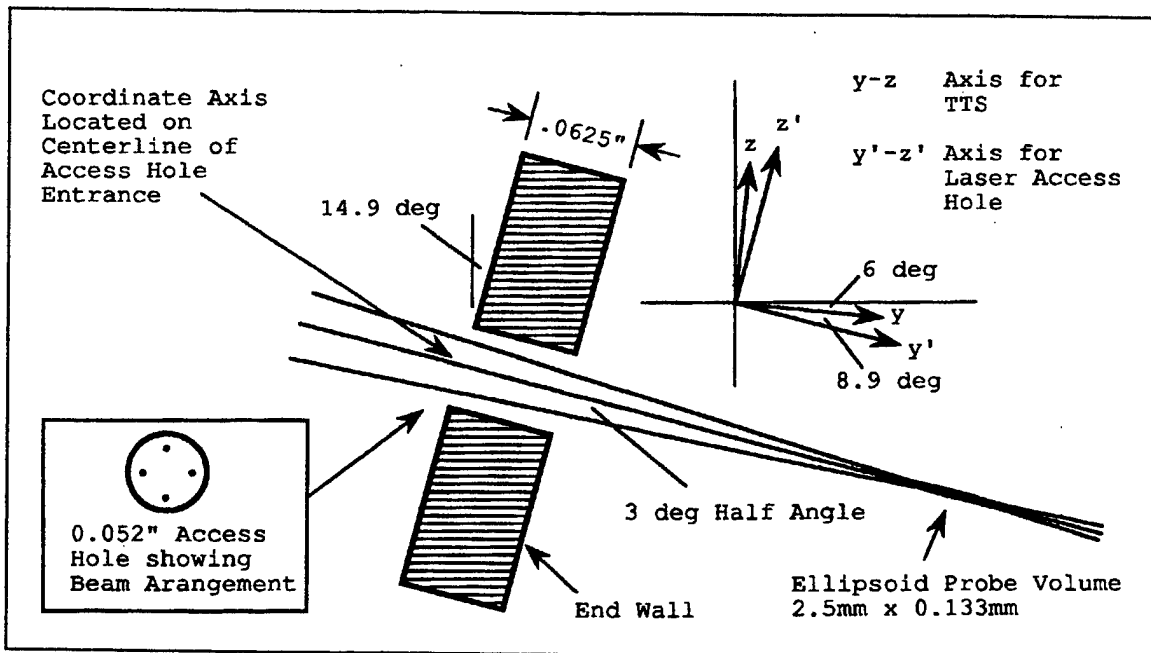


Figure 16. Traverse Table/Laser Blank Beam Orientation

Appendix G equation (1) was used to calculate the distance of the measurement volume from the inside case wall. At the inner surface of the case wall, for example, y' was equal to the thickness of the laser-blank access holes or 0.0625 inches. Coordinate positions for the y and z-axes were calculated using the transformations presented in Appendix G, equations (2) and (3). The angle ϕ was defined

as the tilt angle of the breadboard with respect to its table base ($\phi = 8.9$ deg.). Prior to starting the TTR, the beam crossing was manually positioned to verify adequate beam clearance from the access hole sides. Since the TTR had a tendency to "grow" slightly in the axial direction as it reached a stable operating temperature, minor adjustments of the x coordinate were usually required to maintain a centered position through the access hole. Table 6 presents the TTS coordinates used to position the LDV system with respect to span position.

Radial Position (% Span)	y' (1) (in.)	D (2) (in.)	y (in.)	z (in.)
98	0.0812	0.0187	0.0822	-0.0127
93	0.1313	0.0688	0.1329	-0.0205
88	0.1815	0.1190	0.1837	-0.0284

Notes: (1) y' is depth measured from the outer surface plane of the laser blank access hole.

(2) D is depth measured from the inner case wall.

*Table 6. Traverse Table System Coordinates
for Span Position*

b. Software Setup

The PHASE resolved software was set up by making the appropriate entries into the relevant data acquisition program menus. Appendix I, Tables I1 through I4 summarize these entries for the I/O port and processor selection, processor settings, optics configuration, and rotary encoder set-up. A key element in obtaining an adequate data rate was the use of the IFA 750 in the manual override mode. The signal to noise ratio was set at very low and the threshold optimization was turned off.

c. LDV Measurements

After a slow climb up an extensive learning curve, a total of five survey data sets were obtained. Three sets

were recorded at each depth for the $-0.16c_t$ location and one set was recorded at the middle depth position for both the $0.35c_t$ and $0.84c_t$ locations. All axial positions were referenced to the rotor tip chord (c_t). The three axial positions mentioned above corresponded to the location of the 0.052 inch diameter laser access holes of the unpressurized three-hole laser blank. The three depths (D), measured from the end wall, were 0.019 in. (98% span), 0.069 in. (93% span), and 0.119 in. (88% span). Maximum depth from the end wall was limited by the access hole diameter. Depths greater than 88 percent span resulted in too much backscatter, which was caused by beam interference with the access hole.

Since the LDV system was stationary with respect to the rotating frame of the turbine rotor, absolute velocities were measured. Figure 17 was adapted from Hill and Peterson [Ref. 28; 1992] to illustrate the relationship between absolute velocities (c) and relative velocities (w) within a turbine. The absolute flow angle (α) is the angle between the axial coordinate axis and the absolute velocity vector.

The PHASE software divided the rotating space into windows and bins, thereby enabling measurements to be taken around the entire rotor or in only one blade passage. One 360 degree rotation was divided into 3600 bins, or 0.1 degrees per bin. The SSME HPFTP ATD has 50 first-stage rotor blades, which equates to one blade per 7.2 degrees of

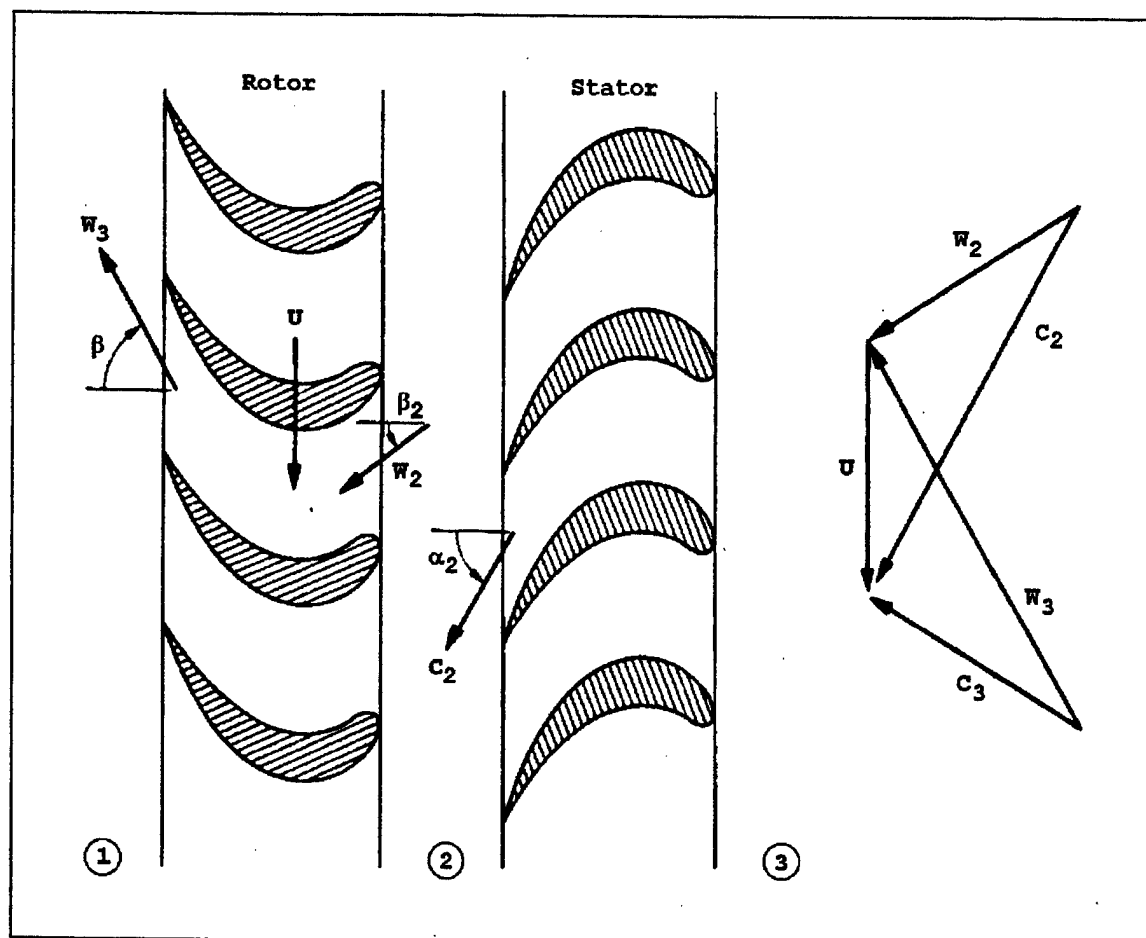


Figure 17. Turbine Velocity Diagram

rotation. In the present study, a total of fifty windows were used, which resulted in one window per blade section. The data presented in this thesis were taken across one window, consisting of between 15 and 72 bins, depending on the measurement position. A delay to first sector entry, in the rotary encoder set-up menu, allowed the desired measurement window to be centered exactly over the blade passages. Window width and sector delay values were functions of both axial position and depth. These values are presented in Table 7 for each measurement location.

Radial Position (% Span)	Axial Position (% c_t)		
	-16.0	35.0	84.0
98	72/0	-	-
93	72/0	15/15	30/40
88	72/0	-	-

Table 7. Window Width/Sector Delay Values

Measurements within the blade space were particularly sensitive to background reflections from the rotor hub and blade surfaces. This problem was solved by reducing the laser output power to approximately 0.25 Watts, vice the normal 2.0 Watts, thereby minimizing unwanted reflection and increasing data rate. It was also required to sometimes make minor adjustments to the photomultipliers in order to optimize the data rate. Because of the narrow clearance between the beams and the access hole, it was critical to keep the hole completely free of seeding material or dirt accumulations. The laser blank was frequently removed from the case wall for cleaning, especially if a decreased data rate was noted. A total of 20,000 points were recorded for each survey, giving an average of 278 data points per bin. Test conditions, such as RPM, inlet temperatures and inlet pressures, were recorded concurrently with the LDV measurements using the LabVIEW SSME_TTR.VI data acquisition program.

3. Data Reduction

The data acquisition program produced raw data files (*.R*) that consisted of the Doppler frequency information for each of the points collected during a run. Velocities were calculated from the *.R* files, using the statistical

analysis subroutine, and saved to velocity files (*.V*). Next, statistics information was calculated and saved to corresponding statistics files (*.S*). Data collected at the $-0.16c_t$ axial location were obtained from one representative blade space. Because of the difficulty obtaining an adequate (greater than 20Hz) data rate within the rotating blade space, window averaging of all 49 blade spaces was used during the PHASE data reduction process, for measurements taken at the $0.35c_t$ and $0.84c_t$ axial locations. In all cases, data were smoothed slightly by combining bins in groups of two, prior to computing statistics. For each data set, the target number of data points was 20,000; however, not all data sets achieved this value due to the combination of low data rate, and a DMA time-out limitation of 999 seconds.

The principle equations used in the PHASE LDV data reduction process are presented in Appendix G, equations (4) through (13). To account for variations in TTR operating conditions, mean velocities and turbulence intensities were non-dimensionalized with respect to inlet total velocity. Equations used for data normalization are presented in Appendix G, equations (14) through (18). Referred rotation speed was defined by Appendix G, equation (19).

Data contained in the PHASE statistics were not in a format that could be read directly with a PC based spreadsheet program. PHASE statistics data were arranged in one long column consisting of a 230-line header containing software menu settings, and was followed by single processor statistics in 20 line blocks, and then multiprocessor statistics in 7 line blocks. A FORTRAN program, presented as Appendix F, was written to extract the specific items of interest from the statistics files, and organize them into an ASCII format that could then be read by Microsoft Excel.

Items of interest in the present study included tangential mean velocity, tangential turbulence intensity, axial mean velocity, axial turbulence intensity, mean absolute flow angle, and correlation coefficient. Prior to compiling and running the program, its source code was modified for each data set to account for different file names and different number of blocks.

IV. RESULTS AND DISCUSSION

A. INLET AND EXIT COBRA PROBE SURVEYS

First-stage stator inlet and rotor exit velocity profiles were measured using a 2-D Cobra probe setup and VEL_PRFL.VI program, as discussed in sections II-G-2-c and II-F. Tabular data obtained from the program was transferred into an Excel spread sheet for plotting and is presented in Appendix H.

1. First-Stage Stator Inlet

First-stage stator inlet data were taken at a referred rotational speed of 4853 RPM. The survey position was located 0.41 inches forward of the stator leading edge plane and 11.3 degrees clockwise from the twelve o'clock position. Figure 18 shows the stator inlet probe location with respect to the turbine annulus, as viewed from upstream looking aft, and Figure 19 shows the location with respect to the flow-path.

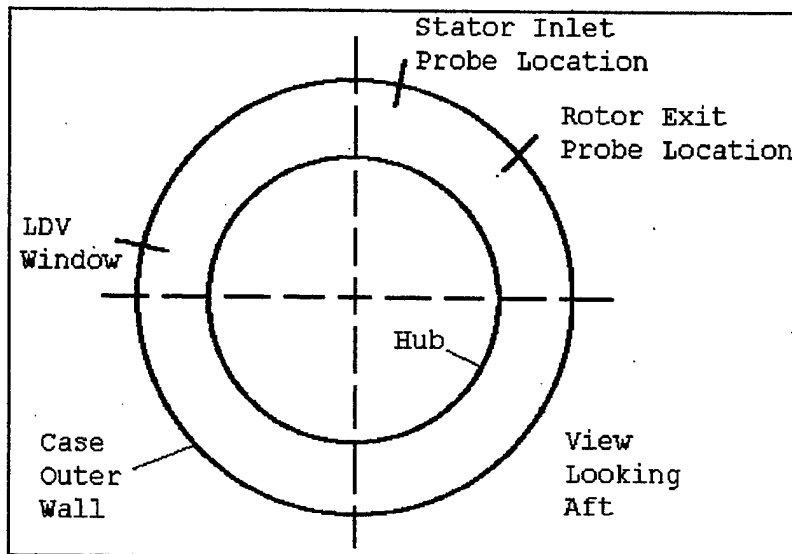


Figure 18. Probe and LDV Window Locations, Annulus View

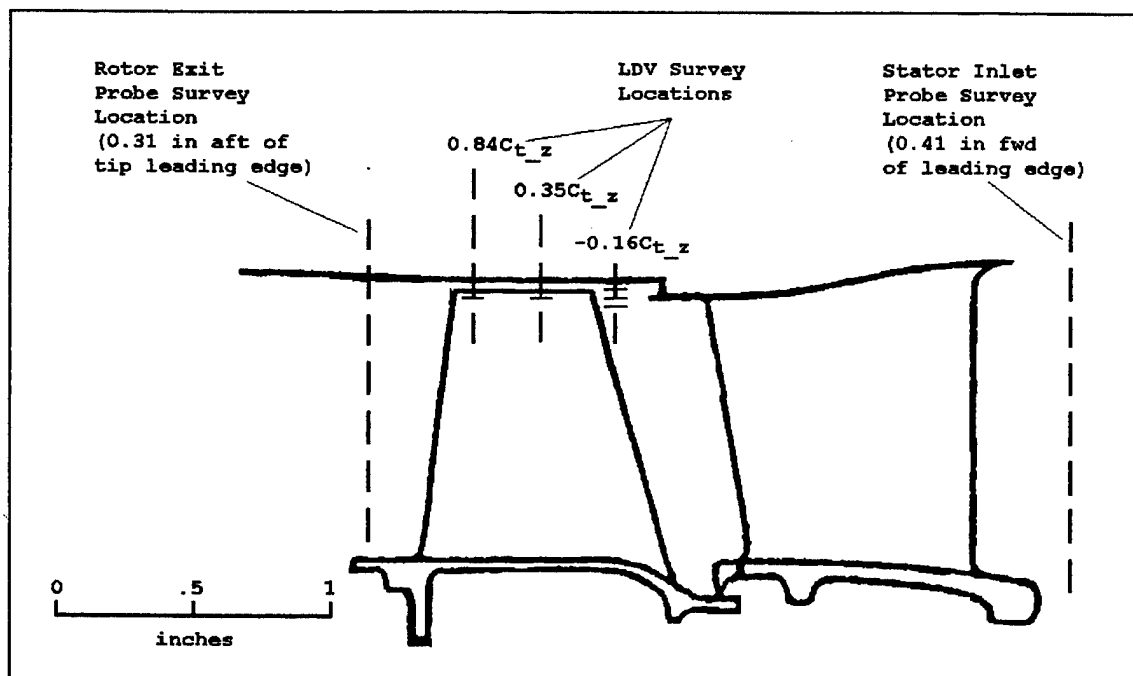


Figure 19. Probe and LDV Window Locations, Flow-Path View

This position was halfway between two of the smaller inlet struts and directly forward of a stator leading edge. The SSME HPFTP ATD incorporated sixteen inlet struts; four large struts and twelve smaller struts, all equally spaced and of symmetric profile. Note that all clock angles were referenced from the inlet end of the turbine looking aft. Mach number (M) and absolute flow angle (α) were plotted against radial position and are presented in Figures 20 and 21.

Inlet flow exhibited a uniform plug-type characteristic, in that both Mach number and flow angle were essentially uniform with radial position. Mach number was approximately constant at 0.17 across the inlet annulus. Boundary layer effects were qualitatively assessed as very thin, in that values of decreasing Mach number with decreasing distance to the wall were not noted, despite

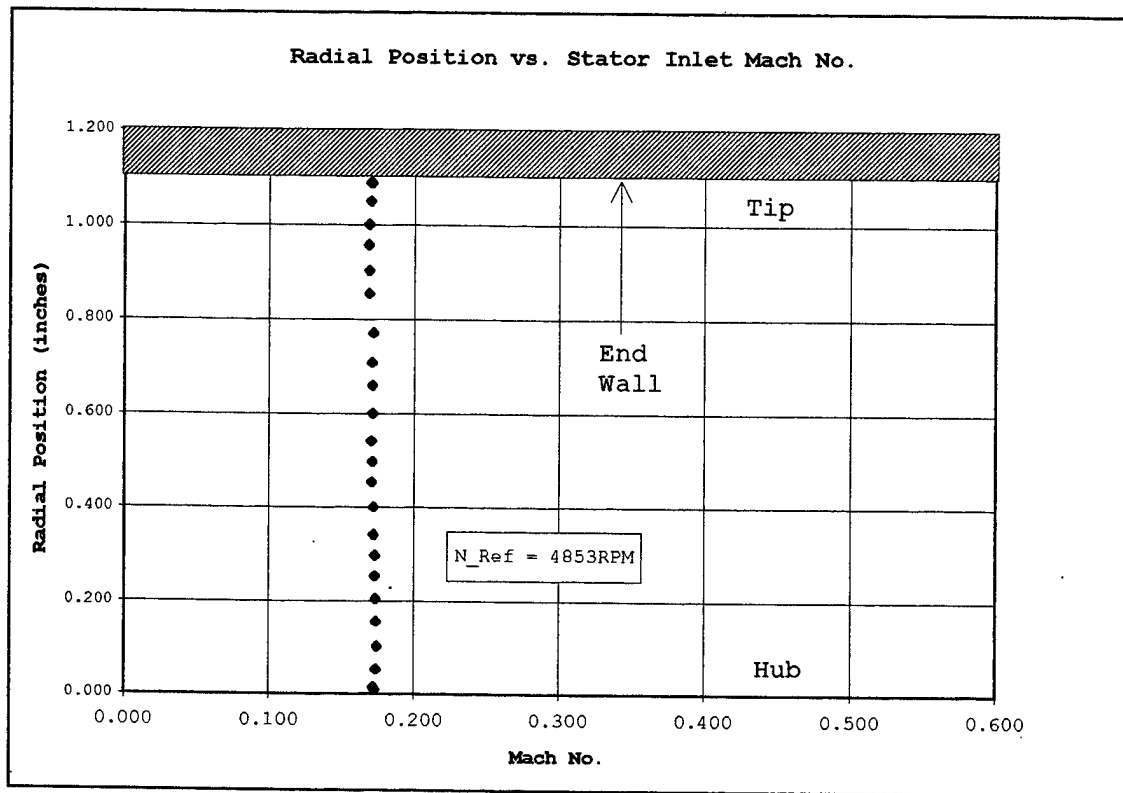


Figure 20. Radial Position vs. Stator Inlet Mach Number

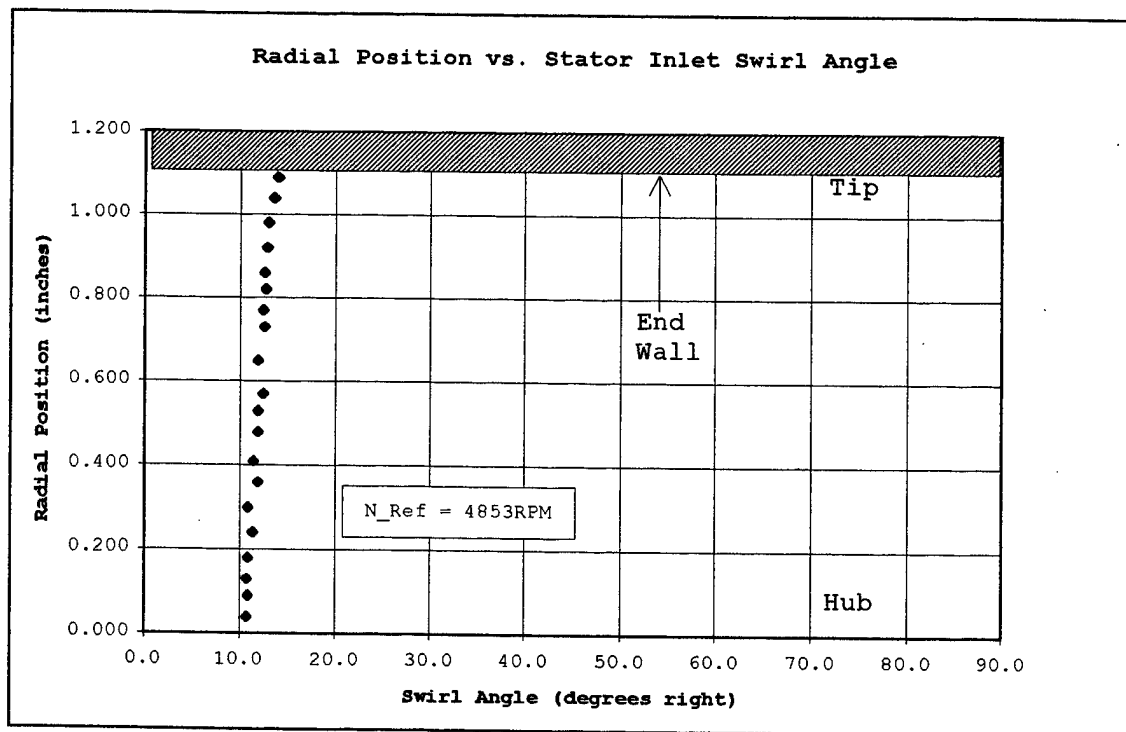


Figure 21. Radial Position vs. Stator Inlet Swirl Angle

taking measurements to within 0.01 inches of the hub and case wall. Absolute flow angle varied only slightly from 11 degrees at the hub to 14 degrees at the case wall. Note that positive swirl angle is from the right when looking upstream. Most likely, the flow was being influenced by the close proximity of the stator, where the flow turned to the right ahead of the leading edge, as a result of potential effects, before being turned back to the left.

It was noted in the tabular data of Appendix H, that the Cobra probe total pressure (P_1) was generally about eight percent lower than the inlet total pressure (P_t). P_1 was also observed to be constant across the radial span. This difference may have been the result of a small radial component in the flow field, which the three hole Cobra probe was not designed to measure. The hub radius increased slightly at the probe location, therefore, the presence of a radial component was possible.

2. First-Stage Rotor Exit

First-stage rotor exit data were taken at a referred RPM of 4839. A radial survey was conducted at an exit plane location 0.31 inches aft of the rotor tip trailing edge (0.19 in. aft of the rotor hub trailing edge) and 50.0 degrees clockwise from the twelve o'clock position. Figure 18 shows the rotor-exit probe location with respect to the turbine annulus, and Figure 19 shows the orientation with respect to the flow-path. Mach number and absolute flow angle were plotted against radial position and are presented in Figures 22 and 23. Both profiles exhibited a complex structure and suggested the presence of secondary-flow effects, such as tip-leakage vortices generated by

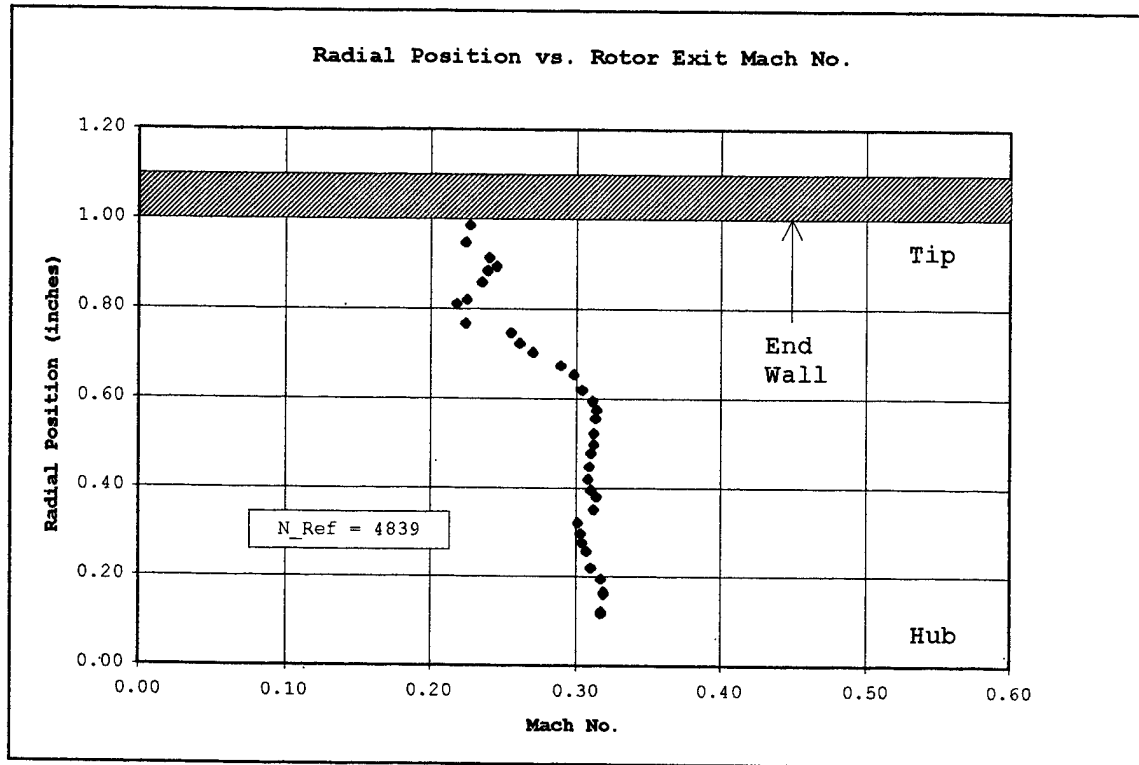


Figure 22. Radial Position vs. Rotor Exit Mach Number

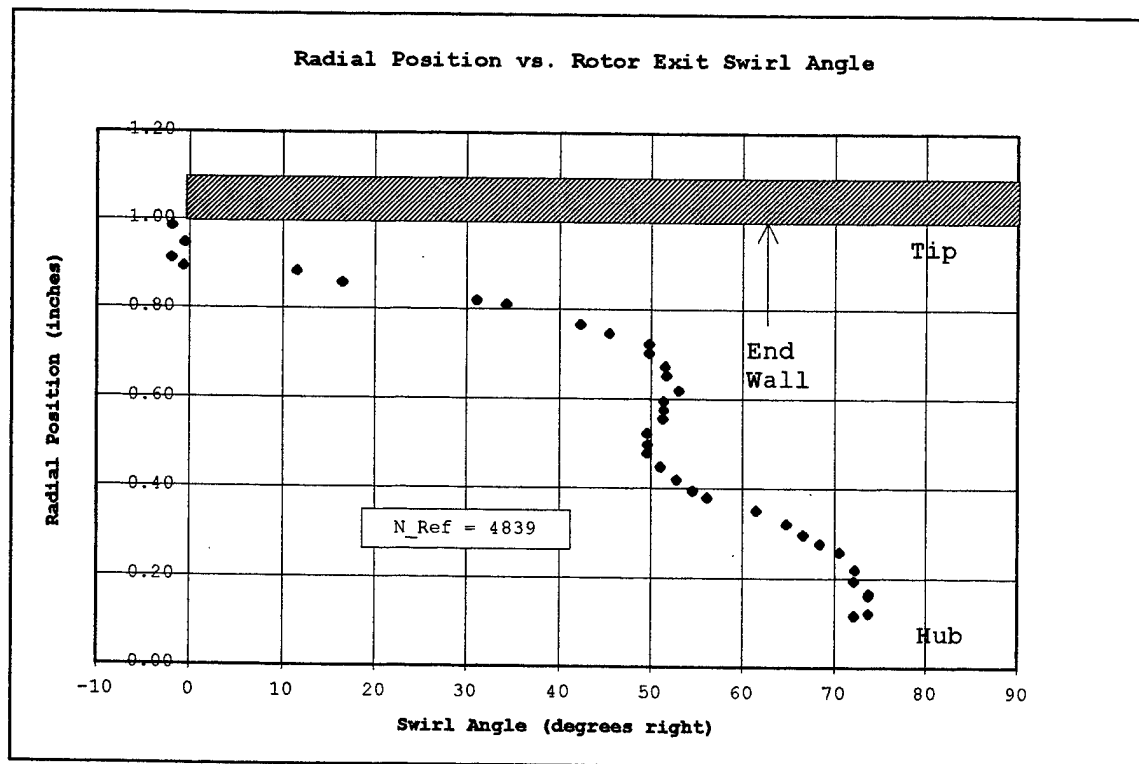


Figure 23. Radial Position vs. Rotor Exit Swirl Angle

the rotor tip gap. The tip gap was measured at 0.020 inches during TTR assembly.

Mach number remained approximately uniform at a value of approximately 0.31 for radial positions extending from the hub to 60 percent span. Between 60 and 80 percent span, Mach number dropped off smoothly to approximately 0.22, and then remained at approximately 0.23 for the remainder of the measured span. As with the inlet survey, boundary layer effects appeared to be negligible, in that they were not observed within the measured region. Measurements were taken to within 0.01 inches from the case wall and to within 0.12 inches from the rotating hub.

Absolute flow angle varied from a maximum of 74 degrees-right near the hub to two degrees-left near the case wall. The profile exhibited a serpentine type behavior that was similar in overall character to data reported by Greco [Ref. 4; 1995]. Specific differences between the two sets of data, however, can be attributed partly to the RPM difference, but more predominately to circumferentially non-uniform flow effects due to the inlet guide vane configuration. A velocity triangle analysis was conducted at 0.6 span to predict the rotor-exit absolute flow angle (α_3) based on the stator inlet Mach number and flow angle. Calculations are presented in Appendix G and resulted in an exit flow angle of 60 degrees. When compared to the 0.6 radial position value from Figure 24 of 53 degrees, the two values are within seven degrees. This is within reasonable agreement considering the highly variable nature of the rotor exit swirl. As the case wall was approached, the exit swirl angle dropped off very rapidly from the 53 degree mid span value near to zero degrees. The angle remained between zero and -2.0 degrees for the last 10 percent of span. This

behavior would be consistent with tip leakage effects, which would tend to washout the swirl angle as the end wall region was approached.

B. END WALL LDV SURVEYS

1. Overview

LDV surveys were conducted in the rotating blade passages, within the rotor end wall region, at three axial locations relative to the rotor tip chord; forward of the leading edge ($-0.16c_t$), mid-chord ($0.35c_t$), and aft-chord ($0.84c_t$). Figure 24 illustrates the survey regions with respect to the rotor blade tip.

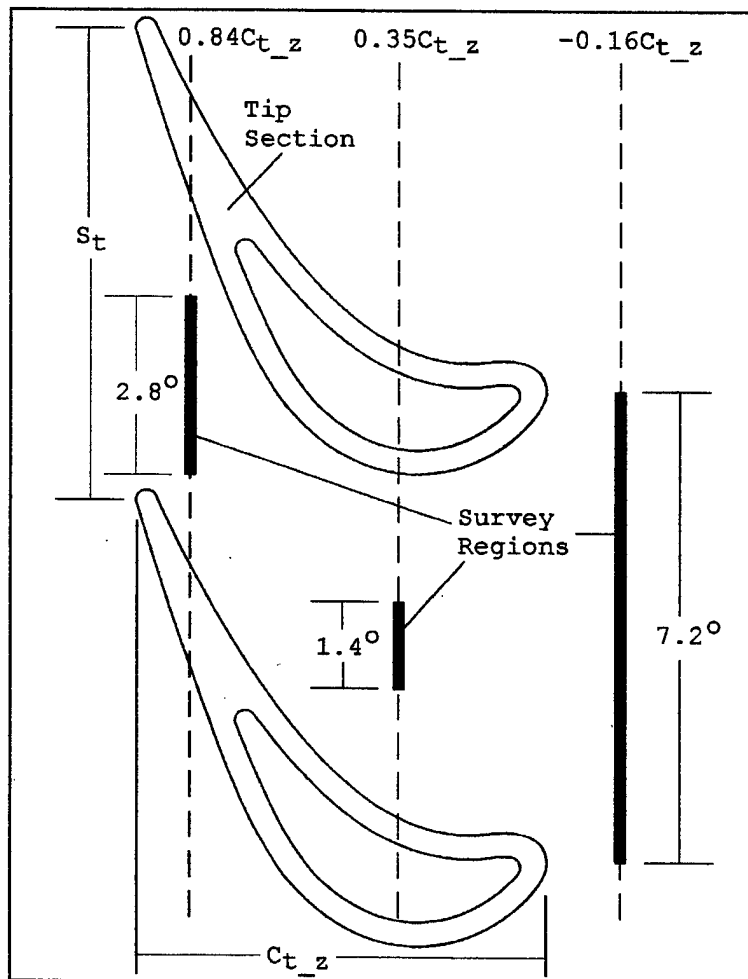


Figure 24. LDV Survey Regions

At the forward location, data were taken at three depths from the end wall; 0.019 inches (98% span), 0.069 inches (93% span), and 0.119 inches (88% span). At the middle and aft-chord locations, data were only taken at 93 percent span. At these two locations, blade interference with the LDV system limited data acquisition to a narrow section the blade passage. Data repeatability was examined for the three spanwise positions at the forward axial location. Repeatability of the middle and aft-chord locations was not checked; therefore, this data should be considered preliminary until further tests can be conducted.

The three-hole laser blank, which was used as the laser window, was located 75 degrees counter-clockwise from the twelve o'clock position. Figure 18 shows the LDV window location with respect to the turbine annulus, as viewed from upstream looking aft. Additionally, Figure 19 is a representation of the first-stage flow path showing the axial orientation of the LDV survey locations. Since the laser-access window was fixed on the turbine casing, the survey location was located at a fixed circumferential location within the stator exit flow. Data are presented in Figures 25 through 44 for each of the five survey locations mentioned above. Each data set included velocity ratios, absolute flow angle, turbulence intensities, and correlation coefficient plotted against circumferential angle (θ). Measurements were conducted at referred turbine RPMs between 4810 and 4853, and a total inlet velocity of between 792.8 and 799.1 m/sec. LDV tabular data are provided as Appendix J. Specific test conditions are listed in the header of each LDV tabular data set. Additionally, the corresponding TTR and SSME flow condition data are provided as Appendix K, for reference purposes.

a. Velocity Ratios

Axial velocity ratios were essentially constant across the blade passage for each survey location. At the forward axial position ($-0.16c_t$), a slightly decreasing trend was noted with increasing span. This was expected and most likely a result of end wall boundary layer. Some of the velocity decrease, however, may have been due to radial flow escaping through the unpressurized laser-blank access hole. Repeatability of the axial data was qualitatively assessed as marginal, in that, a four to 17 percent variation was noted between the data sets. Repeatability of the tangential velocity ratio data, however, was qualitatively assessed as very good. Most data points repeated to within two percent, although several showed differences up to seven percent. The cause of these variations is unknown, but does not appear to be a function of differences in RPM or flow condition (V_t). With increasing aft axial position a slightly decreasing trend in axial velocity ratio (0.079 to 0.067) was noted. This variation represented a 15 percent decrease in axial velocity, but may not be significant in view of the above-mentioned data set variations.

Tangential velocity ratios were higher in magnitude than the corresponding axial ratios. At the forward axial position, the maximum velocity ratio occurred in front of the blade leading edges and was essentially constant with span position at 0.18. This seemed to indicate that the flow was turning as it accelerated over the leading edges of the "approaching" blades. Tangential velocity ratios decreased to a minimum value between the blades, creating a "bucket" region in the data. The minimum value in the bucket region, however, varied slightly with both span and axial position. At the forward location, the minimum value

decreased from 0.15 to 0.13 as the end wall was approached (increasing span). As before, this behavior would be consistent with end wall boundary layer effects.

With axial position, the tangential velocity ratio decreased to approximately 0.1 at the middle and aft-chord axial locations. This reduction in tangential velocity corresponded to a reduction in total velocity as well as a decrease in turning angle. Additionally, data at the aft axial location exhibited a circumferential velocity deficit, between four and five degrees circumferential angle, where the velocity ratio dropped suddenly by 88 percent to 0.25. Although the precise causes of these effects are unknown, it was likely the result of three dimensional effects caused by tip leakage vortex and secondary-flow. Figure 19 shows a step feature in the case wall, just aft of the stator, which may have also contributed to 3-D flow effects in the tip region.

b. Absolute Flow Angle

Absolute flow angle varied across the blade passage, as well as with both span and axial survey location. The absolute flow angle entering the first-stage rotor passage was that of the stator exit flow, which had a design value at the tip of 66 degrees. Because of the close proximity of the forward survey location to the rotor leading edges, however, the stator exit flow was influenced by the "approaching" blades, thereby creating the characteristic "bucket" shape observed in the data. Flow angle near the leading edges was approximately seven degrees higher than in the center passage. This finding is consistent with flow turning and accelerating around the blade leading edges. The trend with increasing span position showed a slight increase in absolute flow angle as the end wall was approached. This effect is consistent with

secondary-flow induced overturning in the end wall region. The trend with increasingly aft axial position showed a significant 13 percent drop in the flow angle at the mid-chord position, and then a slight six percent increase at the aft-chord position. Additionally, at the aft-chord position, the flow angle dropped off suddenly at the same circumferential angle where the velocity ratio deficit was noted. The precise causes of the observed trends are surely very complex in nature, but are most likely the combined result of the end wall boundary layer, unmeasured radial flow components, secondary-flows, and tip leakage vortex effects. Repeatability of the absolute flow angle data was qualitatively assessed as marginal. Since the absolute flow angle was calculated from the velocity components using Appendix (G), equation (10), the differences between the data sets is directly related to the corresponding differences in axial velocity ratio, which was previously discussed.

c. Turbulence Intensities

Axial and tangential turbulence intensity components (T_z & T_θ) were plotted for each survey location. Distinct trends were noted across the blade passage, with span position, and with axial survey location. Generally speaking, the component values were similar in overall magnitude, which is characteristic of isotropic turbulence. Across the blade passage, axial turbulence was generally constant, whereas the tangential component exhibited a serpentine character. A slight increase in turbulence was noted with increasing span position, which would be expected as the end wall is approached. Repeatability of the axial turbulence data was qualitatively assessed as poor, in that, the data sets varied by approximately 30

percent at all three span locations. On the other hand, repeatability of the tangential components were very good.

d. Correlation Coefficients

As defined by Appendix G, equation (13), the correlation coefficient is a non-dimensional measure of the turbulent Reynold stresses. For each of the survey locations, the correlation coefficient deviated only slightly from zero (within ± 0.1) and exhibited no notable characteristics other than random scatter. Since the data were near zero, this would suggest that the survey location, in the fixed frame of reference, was in the free stream stator exit flow and not directly within a wake zone. Within a stator wake, either a positive or negative mean value would be expected. The near-zero values for the correlation coefficients further supports the presence of isotropic turbulence. No trends were noted with changes in either axial or span location.

2. Data at -0.16 Percent Rotor Tip Chord

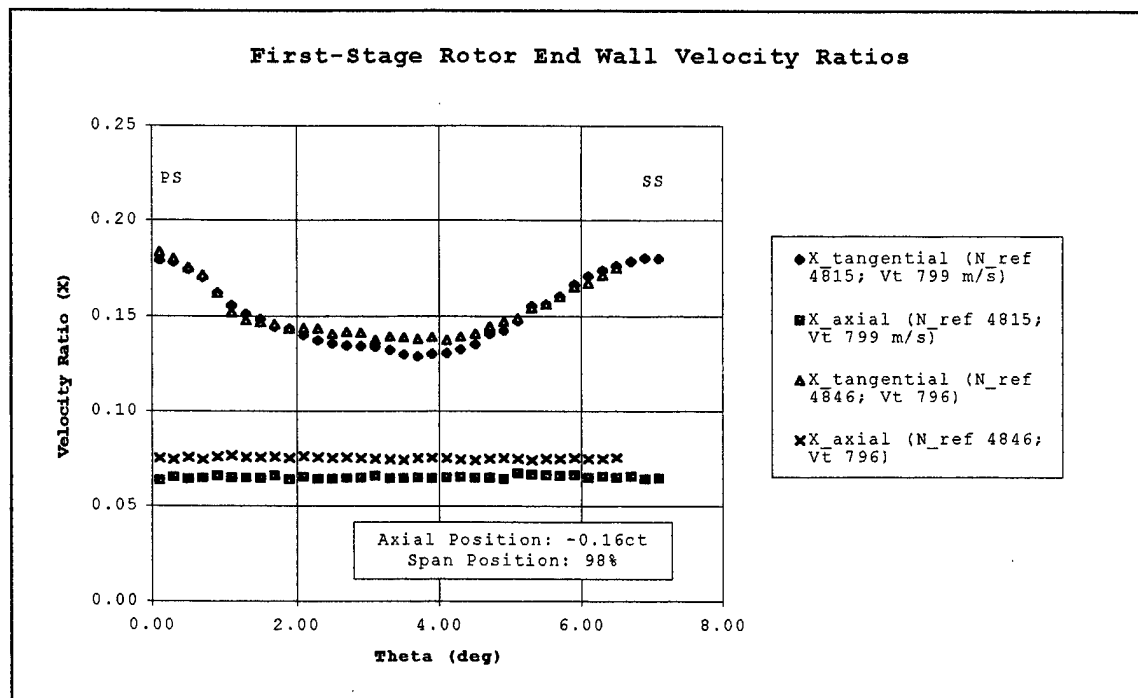


Figure 25. Velocity Ratios for
-0.16 c_t and 98% Span

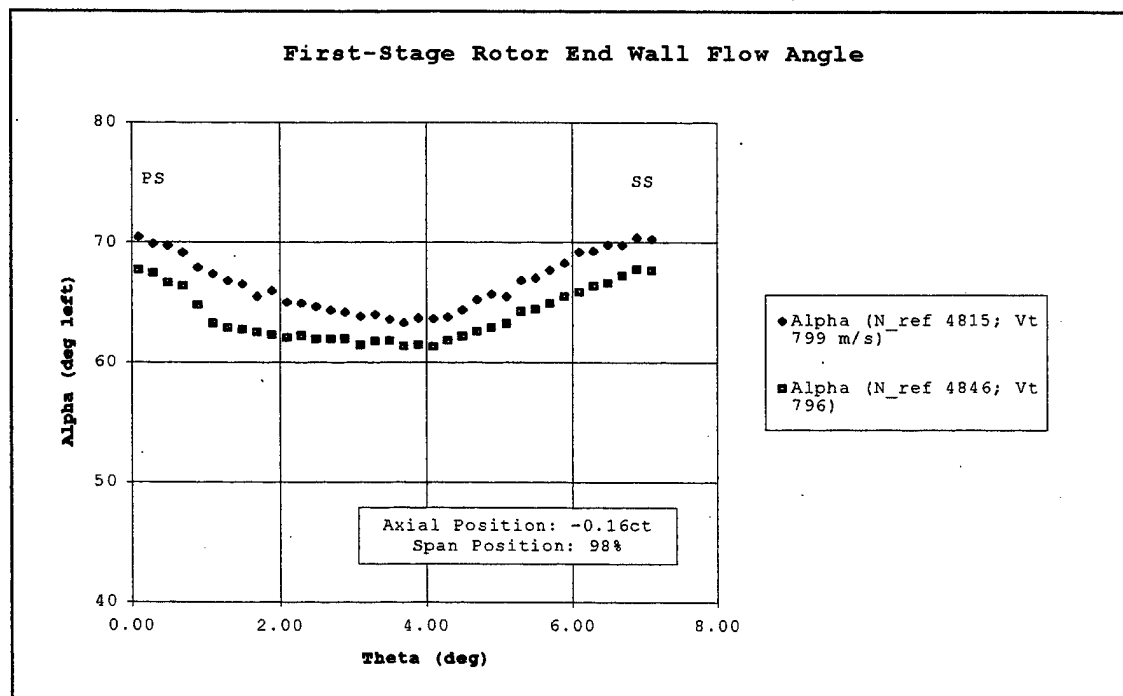


Figure 26. Absolute Flow Angle for
-0.16 c_t and 98% Span

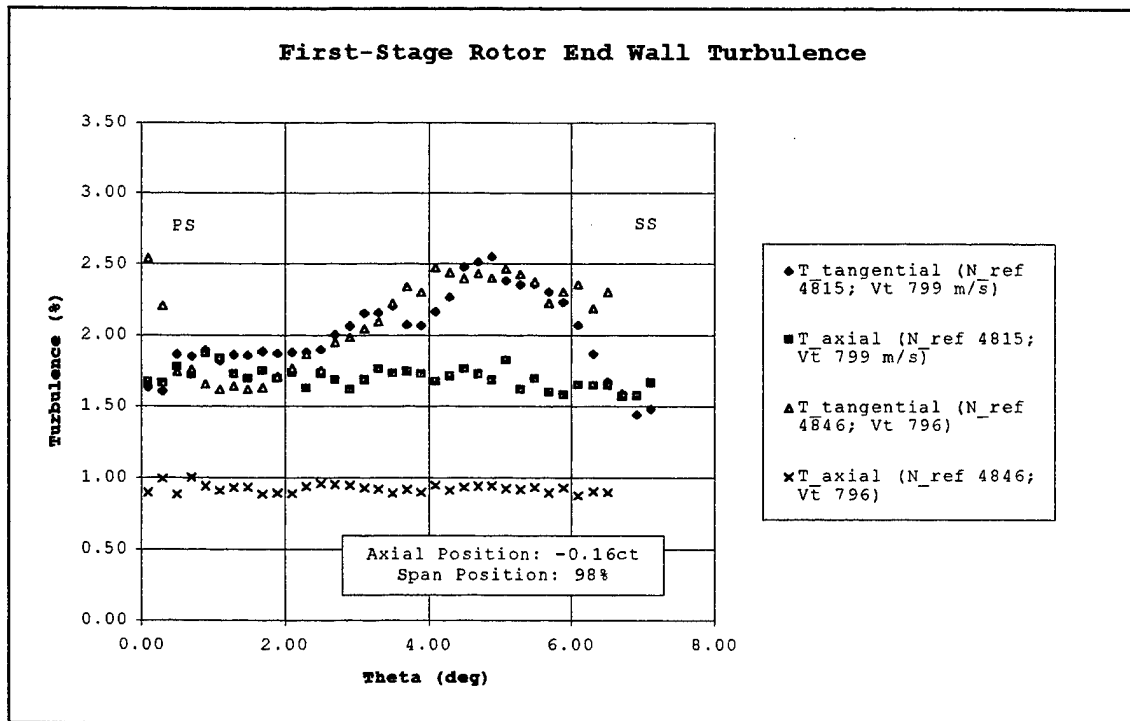


Figure 27. Turbulence Intensities for
 $-0.16c_t$ and 98% Span

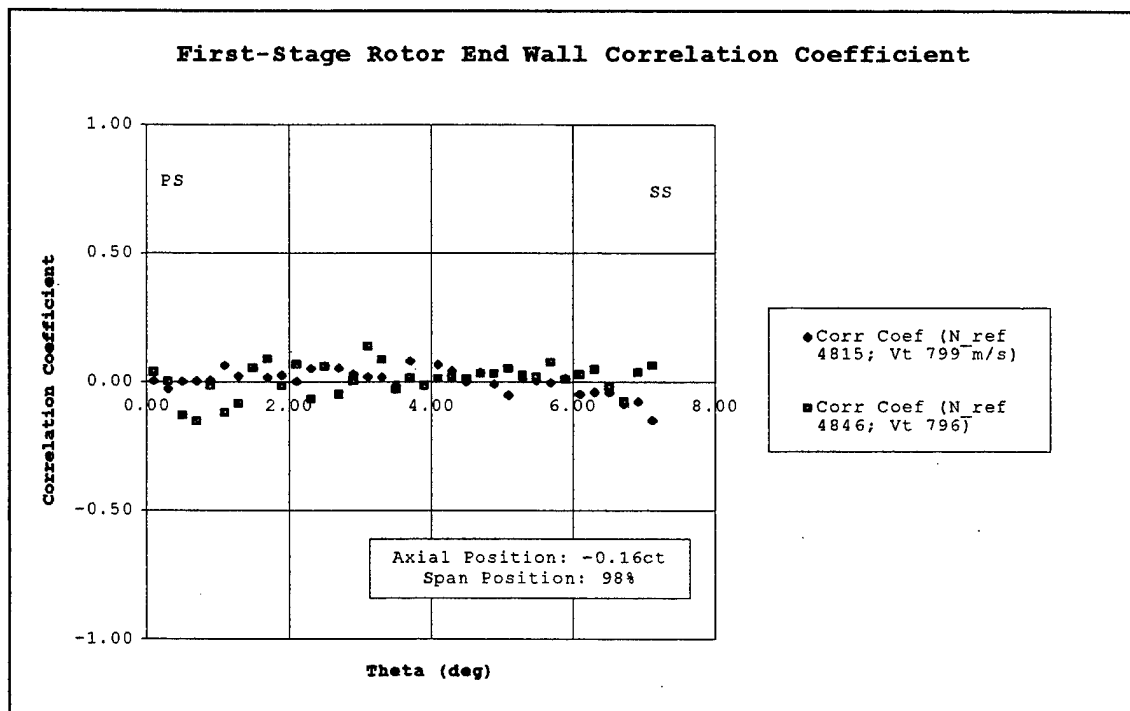


Figure 28. Correlation Coefficient for
 $-0.16c_t$ and 98% Span

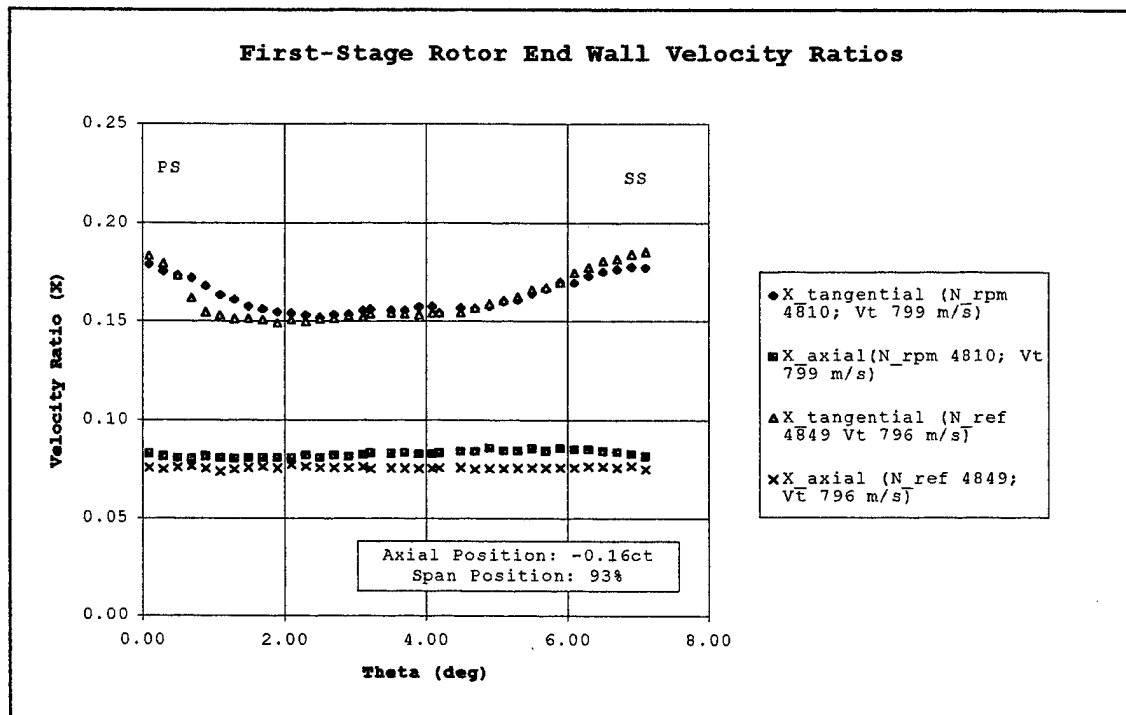


Figure 29. Velocity Ratios for
 $-0.16c_t$ and 93% Span

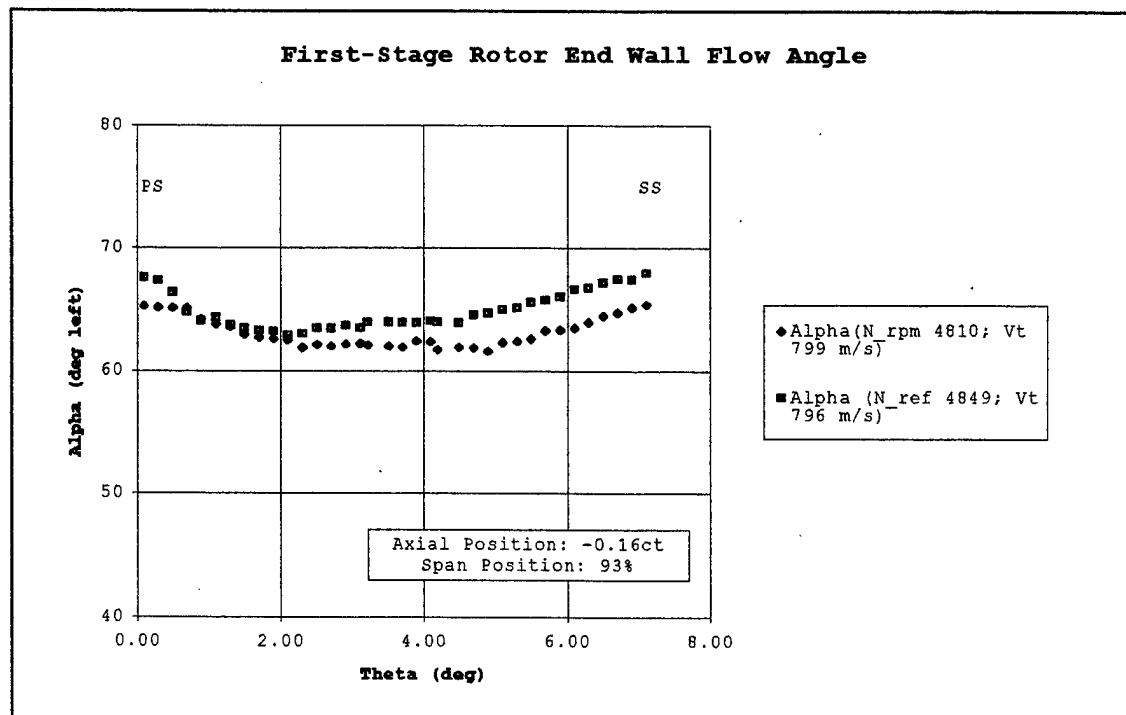


Figure 30. Absolute Flow Angle for
 $-0.16c_t$ and 93% Span

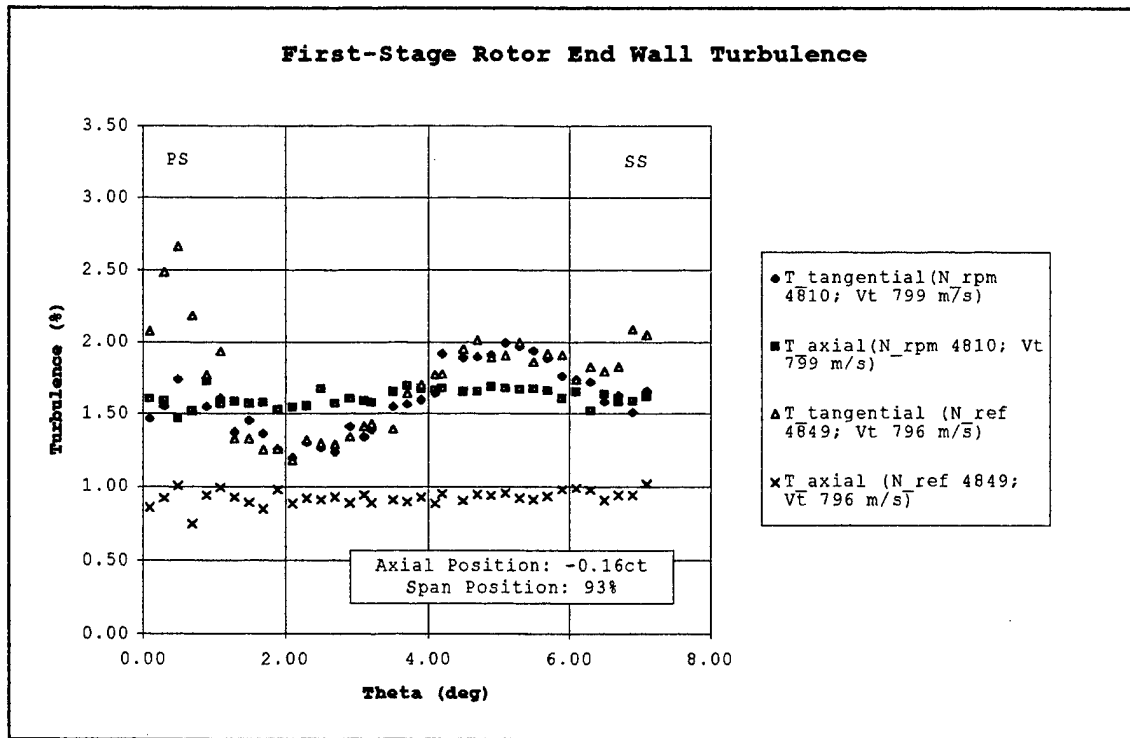


Figure 31. Turbulence Intensities for
 $-0.16c_t$ and 93% Span

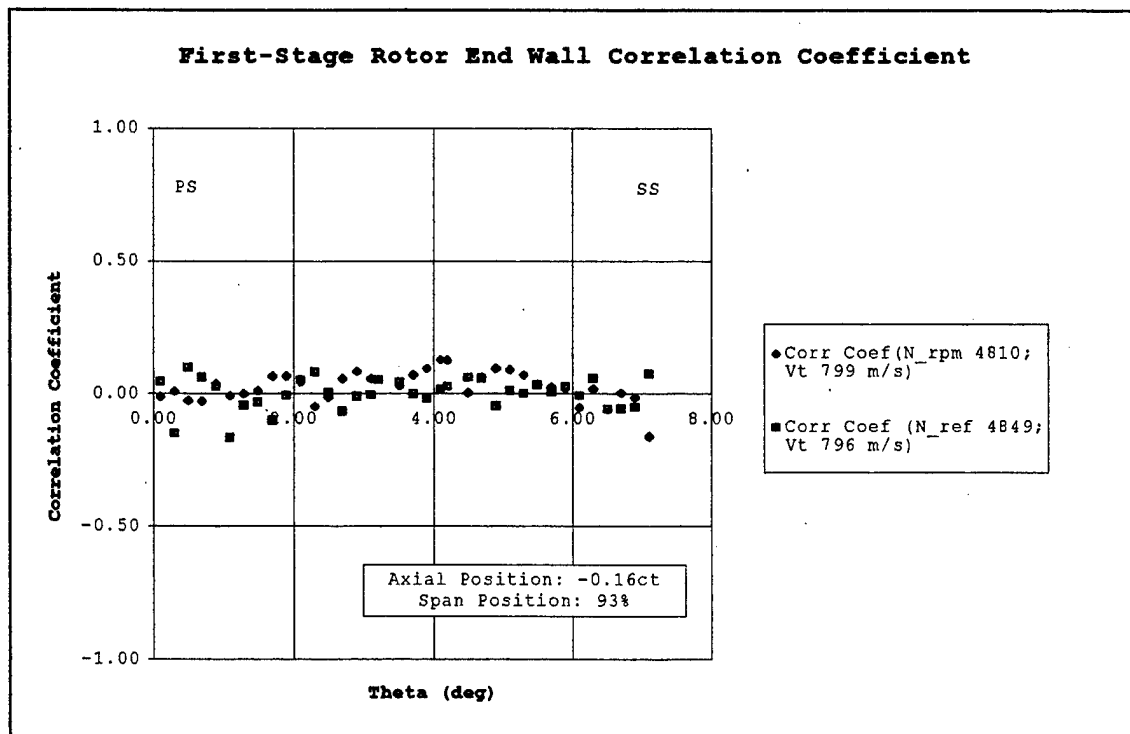


Figure 32. Correlation Coefficient for
 $-0.16c_t$ and 93% Span

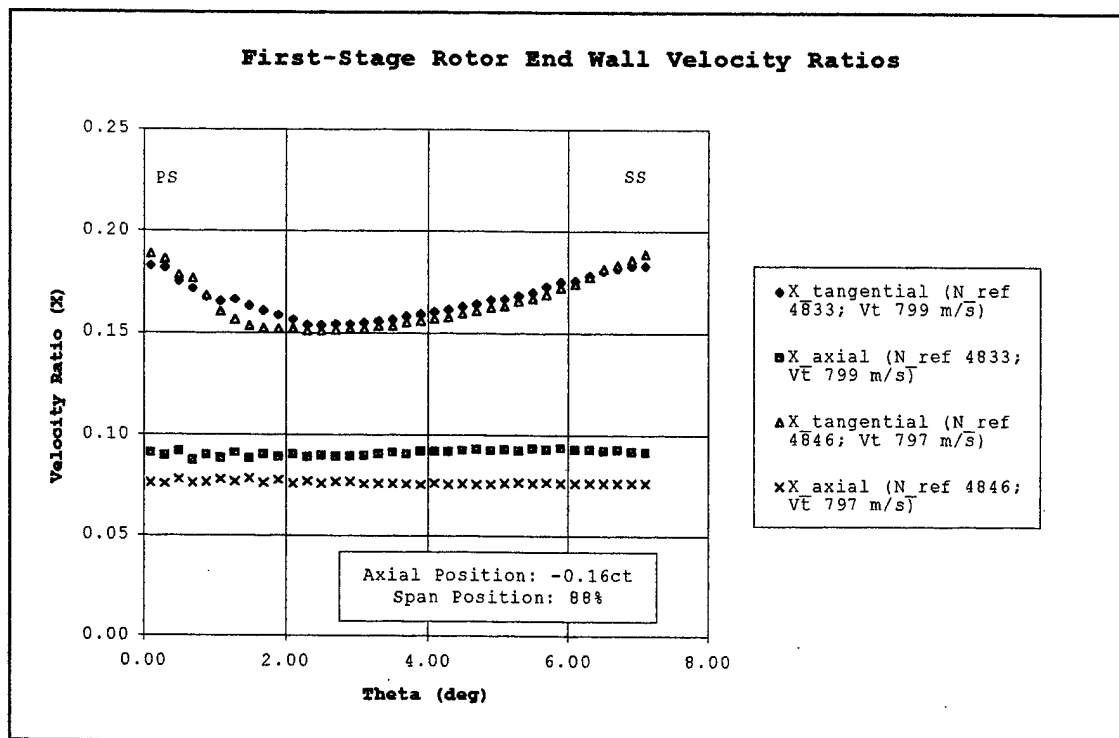


Figure 33. Velocity Ratios for
 $-0.16c_t$ and 88% Span

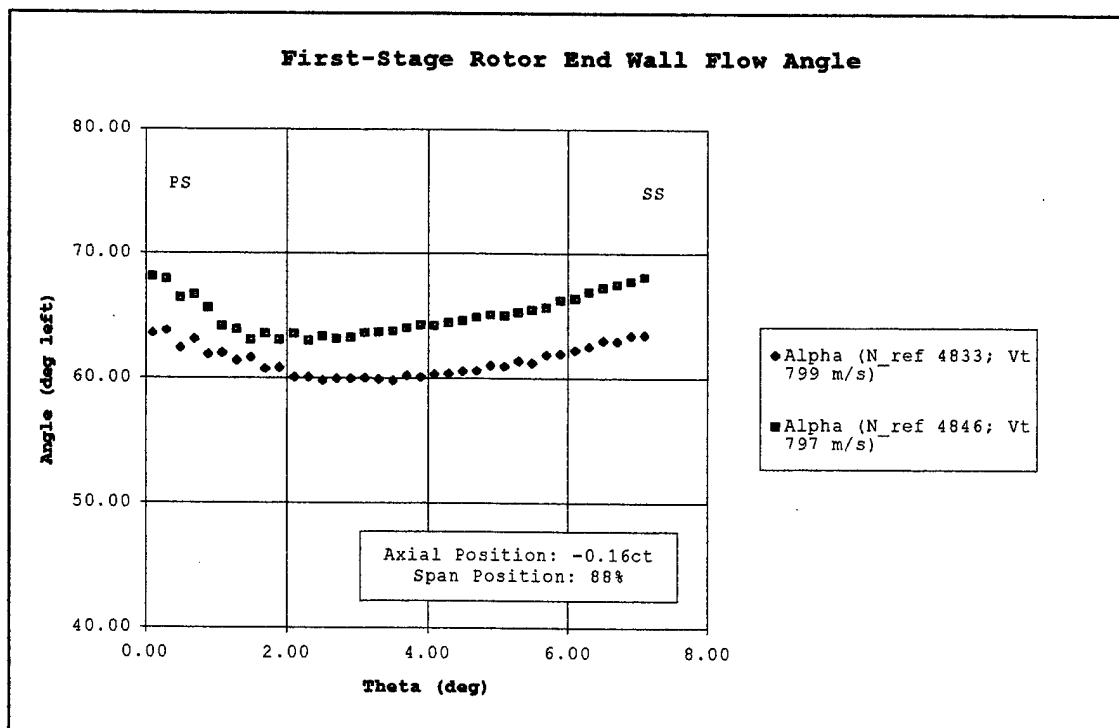


Figure 34. Absolute Flow Angle for
 $-0.16c_t$ and 88% Span

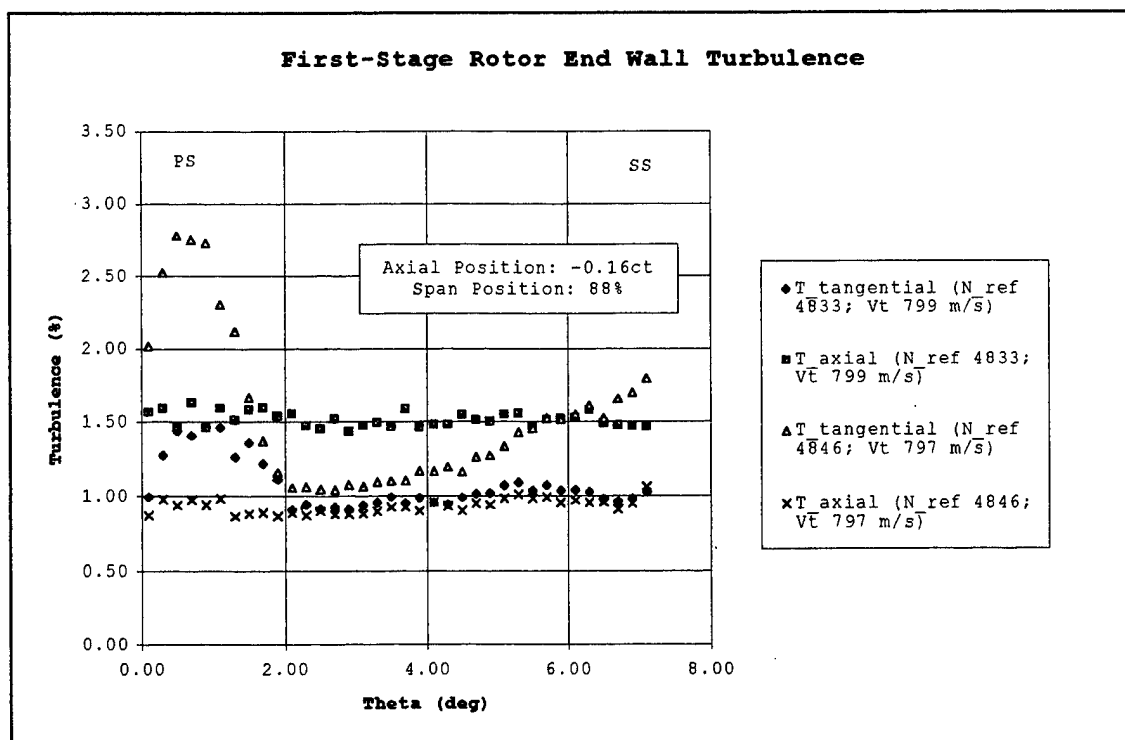


Figure 35. Turbulence Intensities for
 $-0.16c_t$ and 88% Span

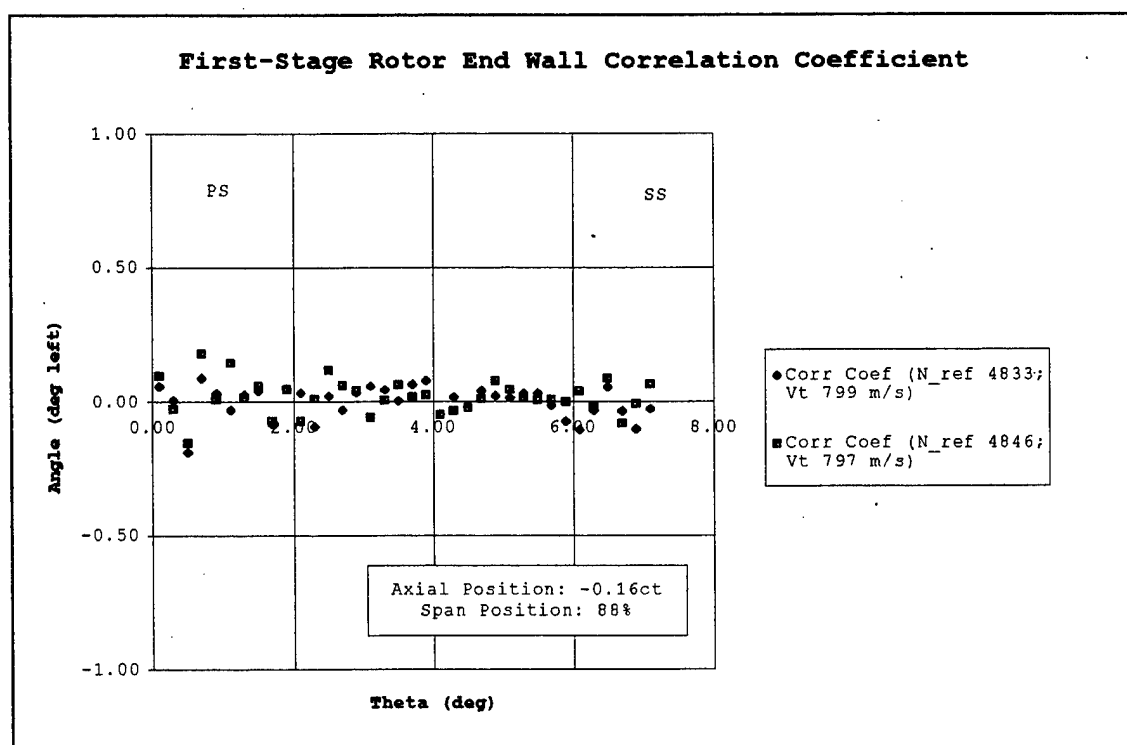


Figure 36. Correlation Coefficient for
 $-0.16c_t$ and 88% Span

3. Data at 0.35 Percent Rotor Tip Chord

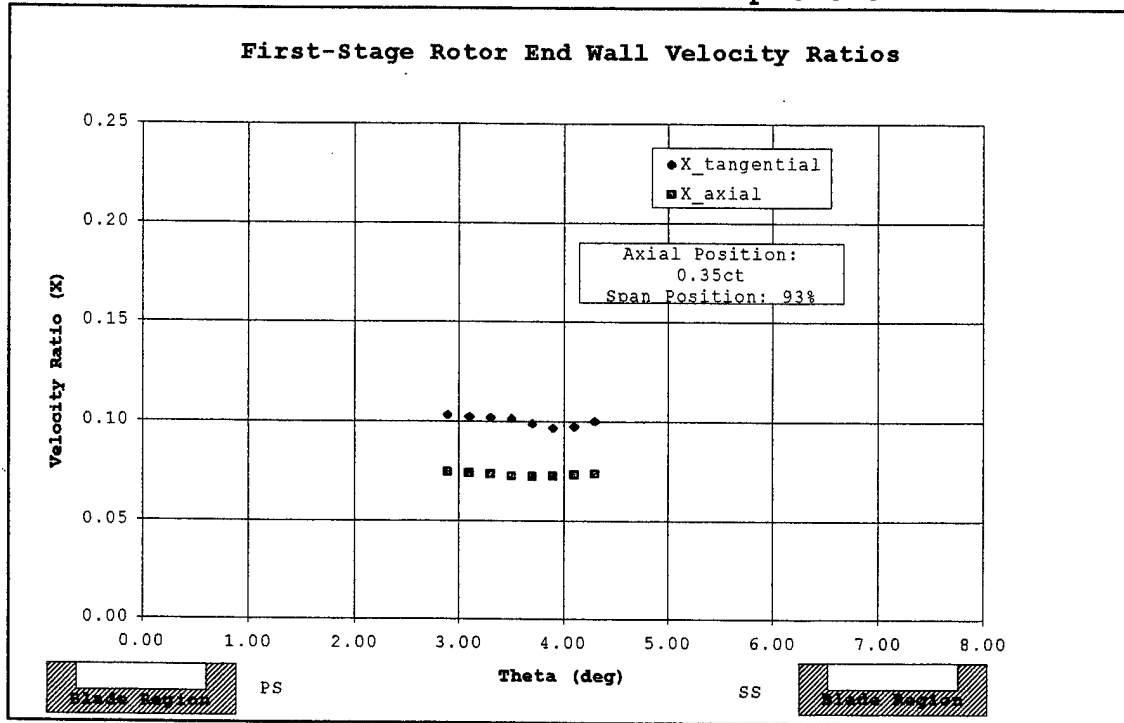


Figure 37. Velocity Ratios for
 $0.35c_t$ and 93% Span

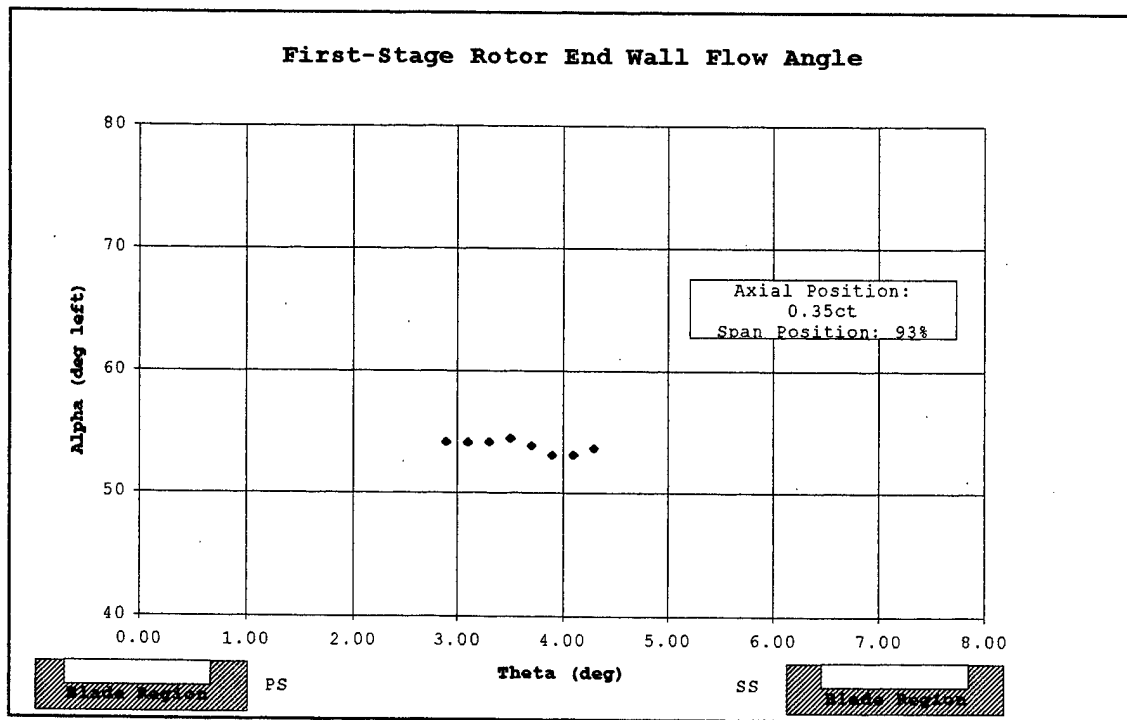


Figure 38. Absolute Flow Angle for
 $0.35c_t$ and 93% Span

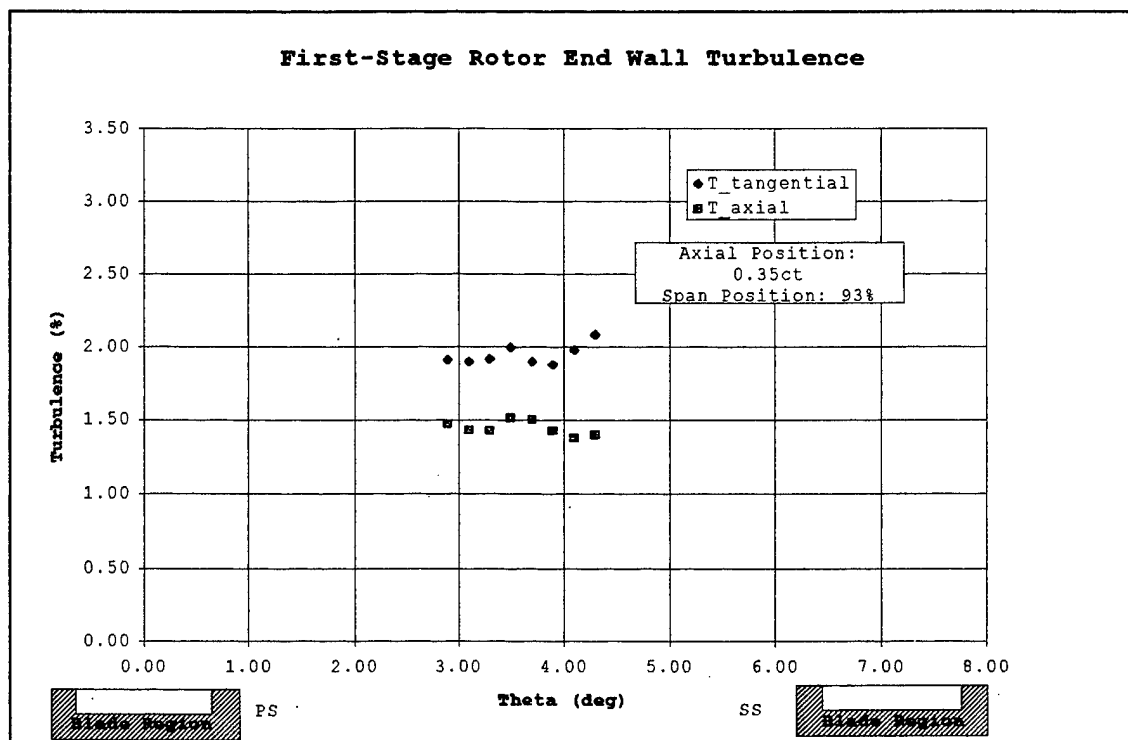


Figure 39. Turbulence Intensities for
0.35c_t and 93% Span

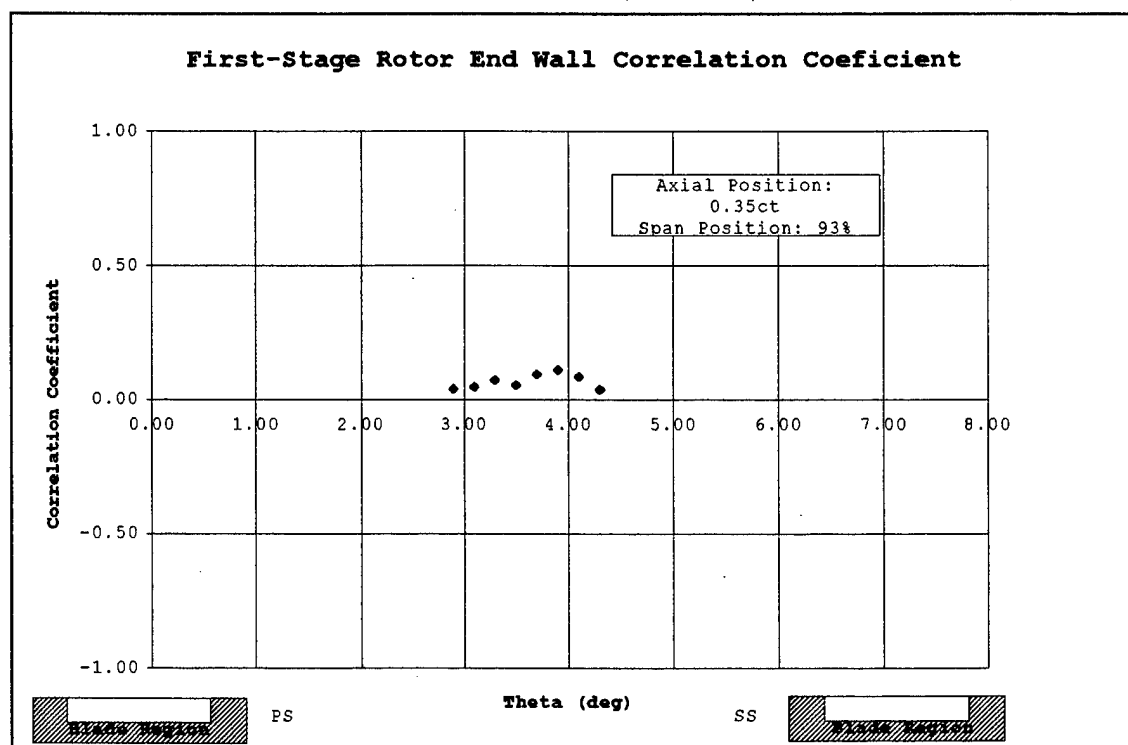


Figure 40. Correlation Coefficient for
0.35c_t and 93% Span

4. Data at 0.84 Percent Rotor Tip Chord

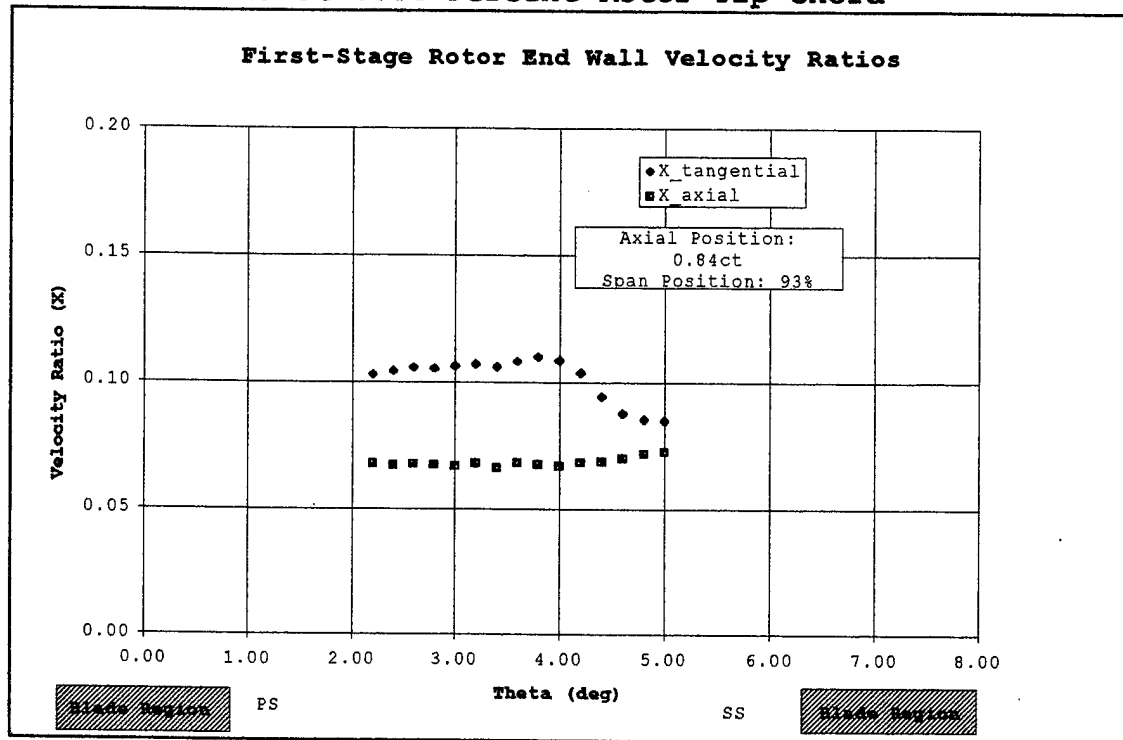


Figure 41. Velocity Ratio for
 0.84c_t and 93% Span

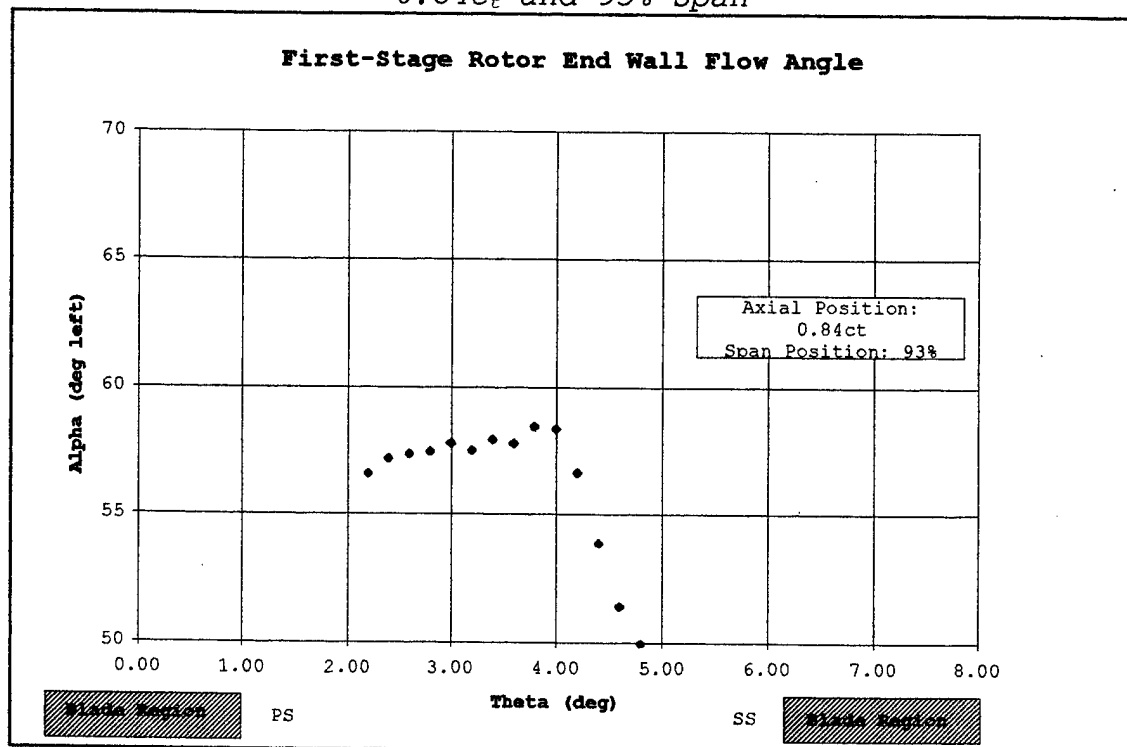


Figure 42. Absolute Flow Angle for
 0.84c_t and 93% Span

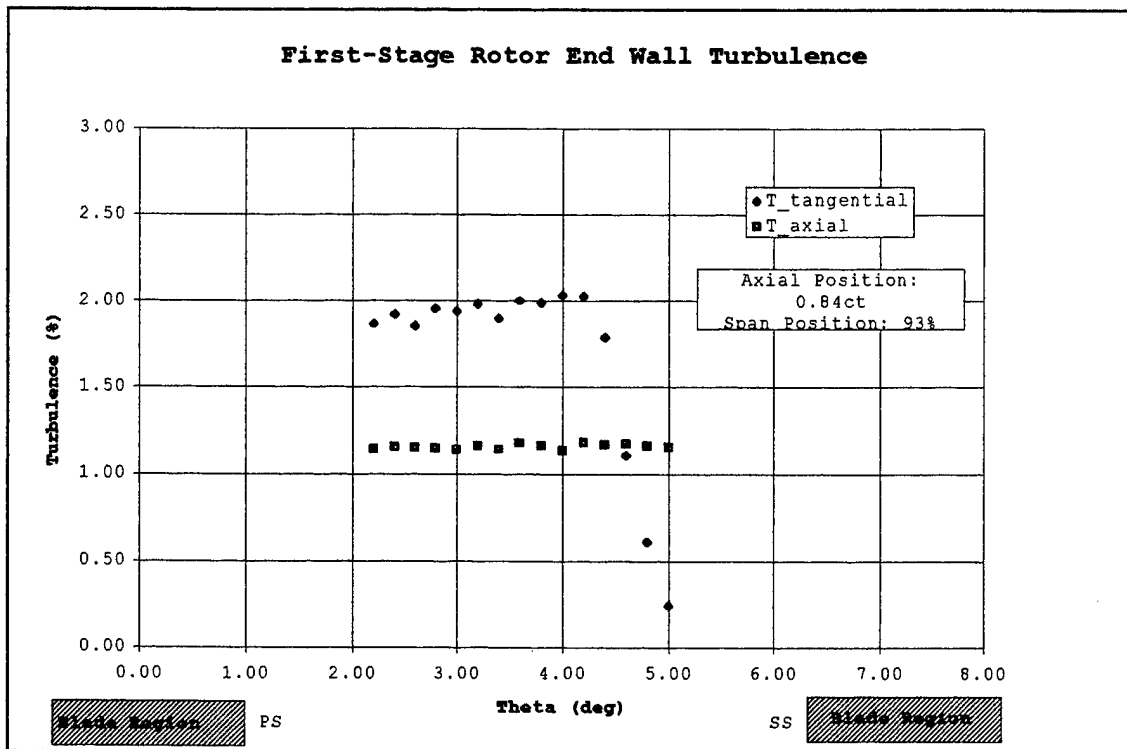


Figure 43. Turbulence Intensities for
0.84c_t and 93% Span

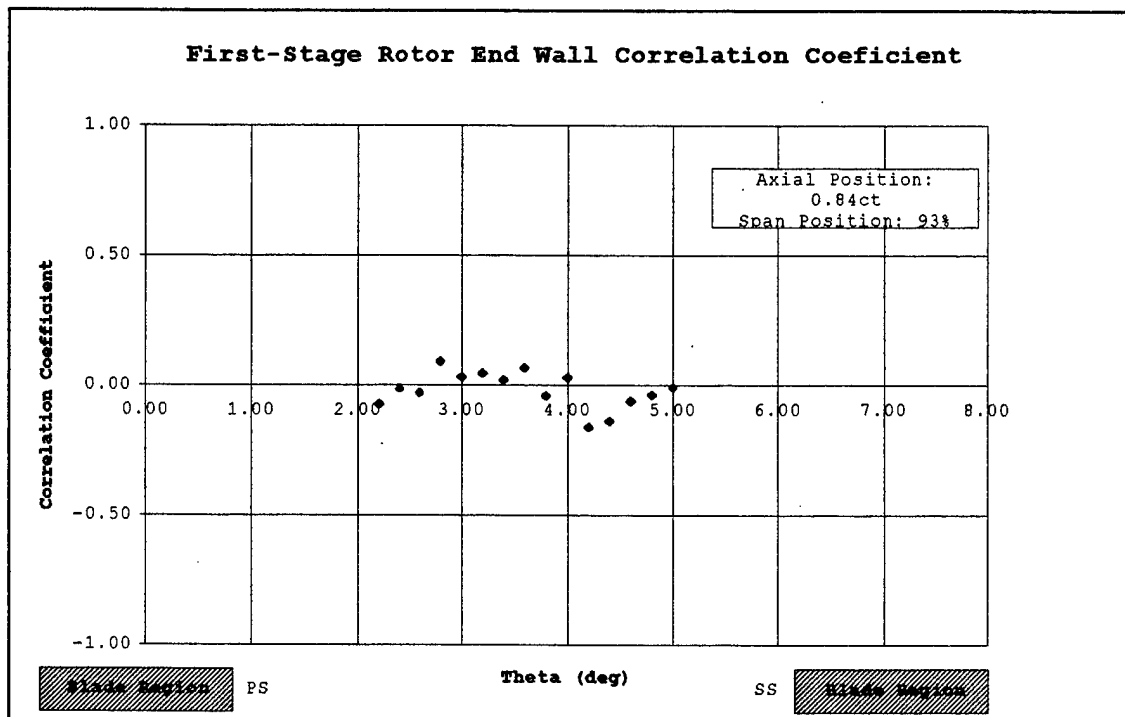


Figure 44. Correlation Coefficient for
0.84c_t and 93% Span

5. Window Averaging

The repeatability of a data set recorded using window averaging of all 50 windows (blade passages) were evaluated against a data set recorded from a single blade passage, without window averaging. The data sets were recorded sequentially under almost identical conditions. Cross plots were made of the velocity ratios, turbulence intensities, absolute flow angle, and correlation coefficient and are presented as Figures 45 through 48. Across the board, repeatability was outstanding. As an example, the maximum deviation in the velocity ratio data was only three percent, and most of the data points actually over-plotted. Within the scope of this evaluation, window averaging is a valid technique and was particularly useful when recording data within the middle and aft chord blade passages.

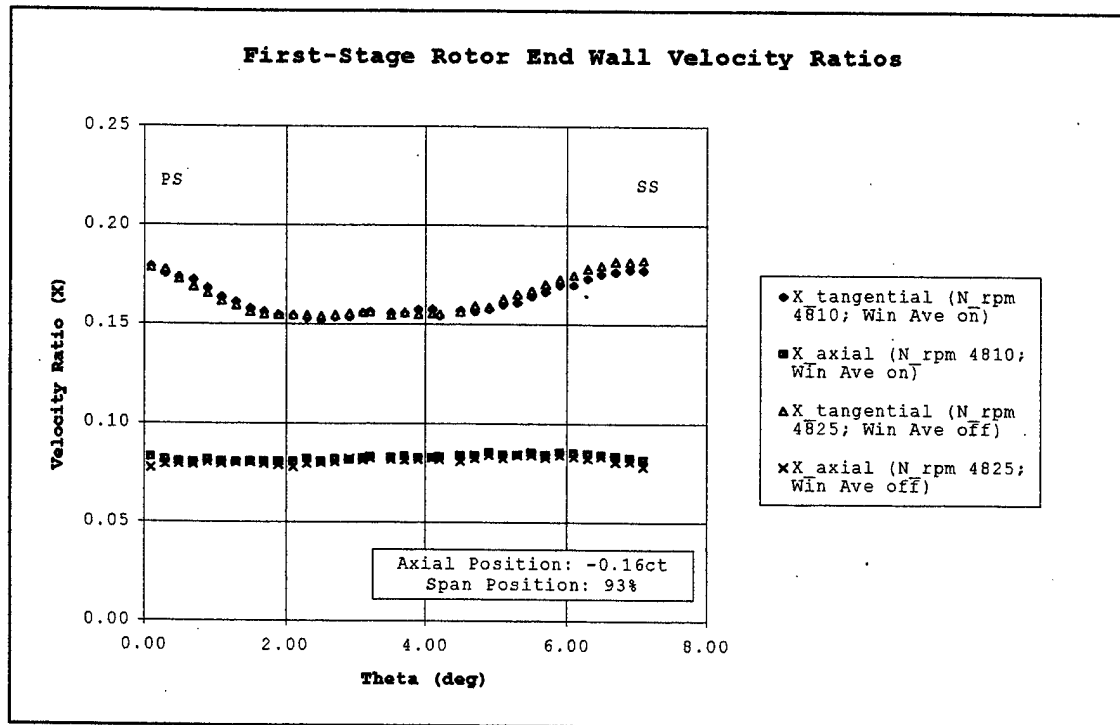


Figure 45. Velocity Ratios for $-0.16c_t$ and 93% Span (Window Averaging on/off)

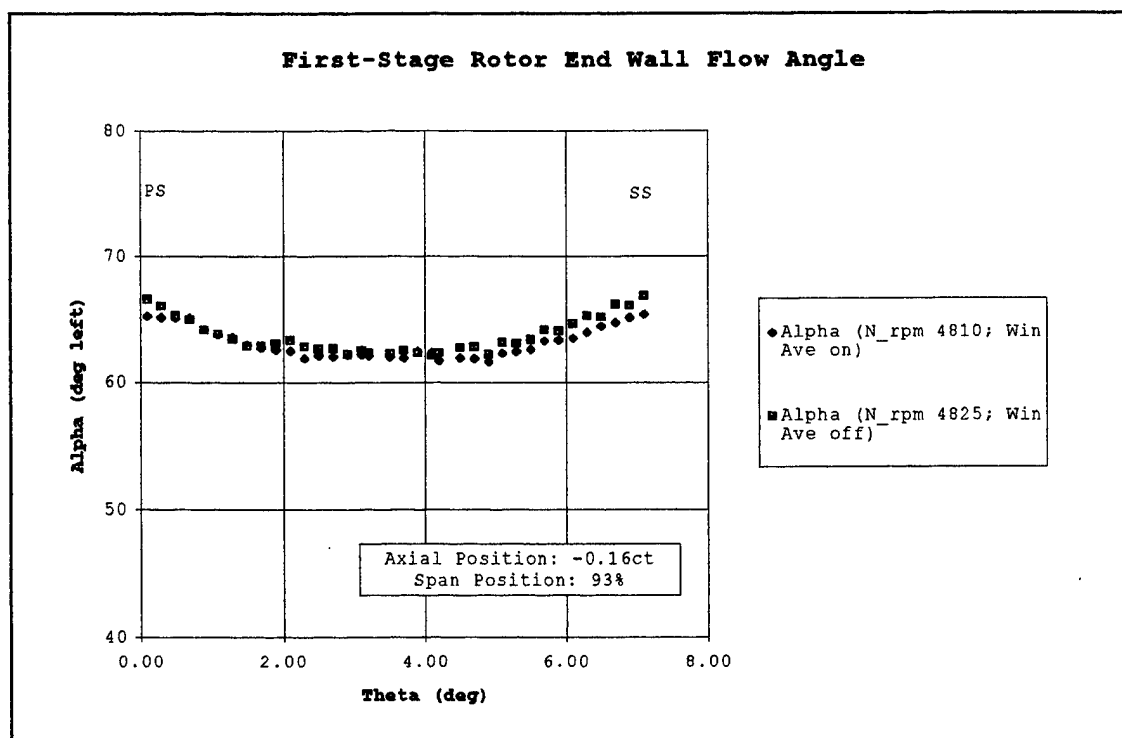


Figure 46. Absolute Flow Angle for $-0.16c_t$ and 93% Span (Window Averaging on/off)

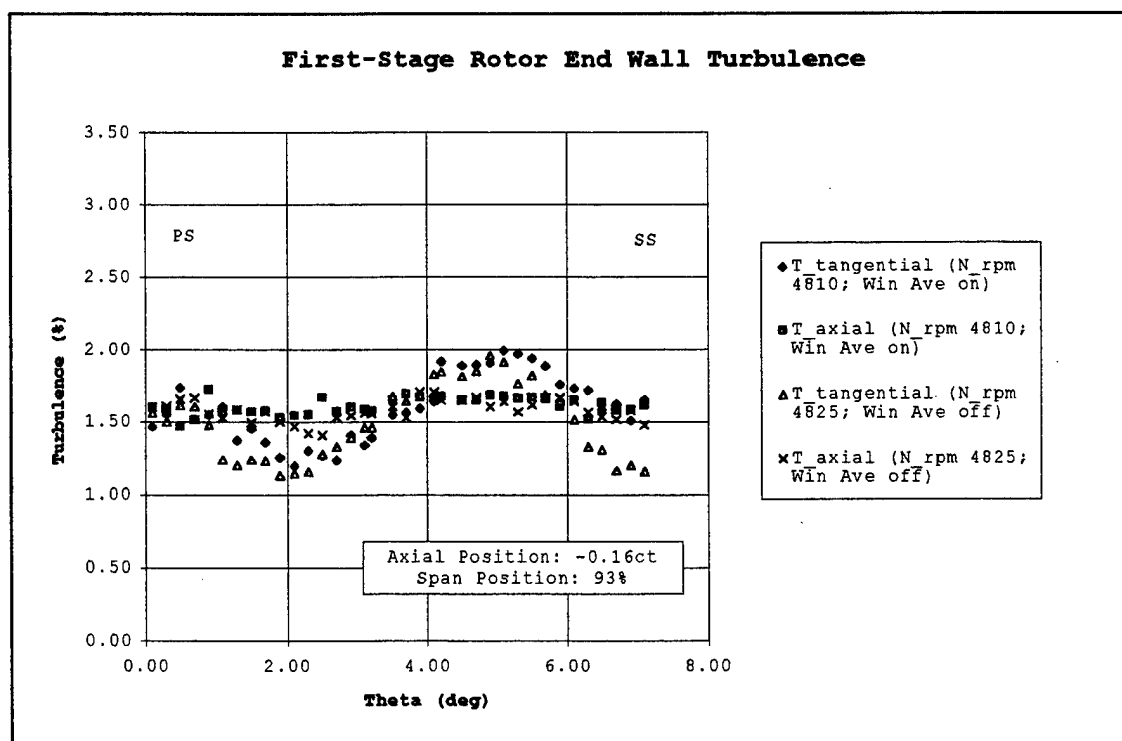


Figure 47. Turbulence Intensities for $-0.16c_t$ and 93% Span (Window Averaging on/off)

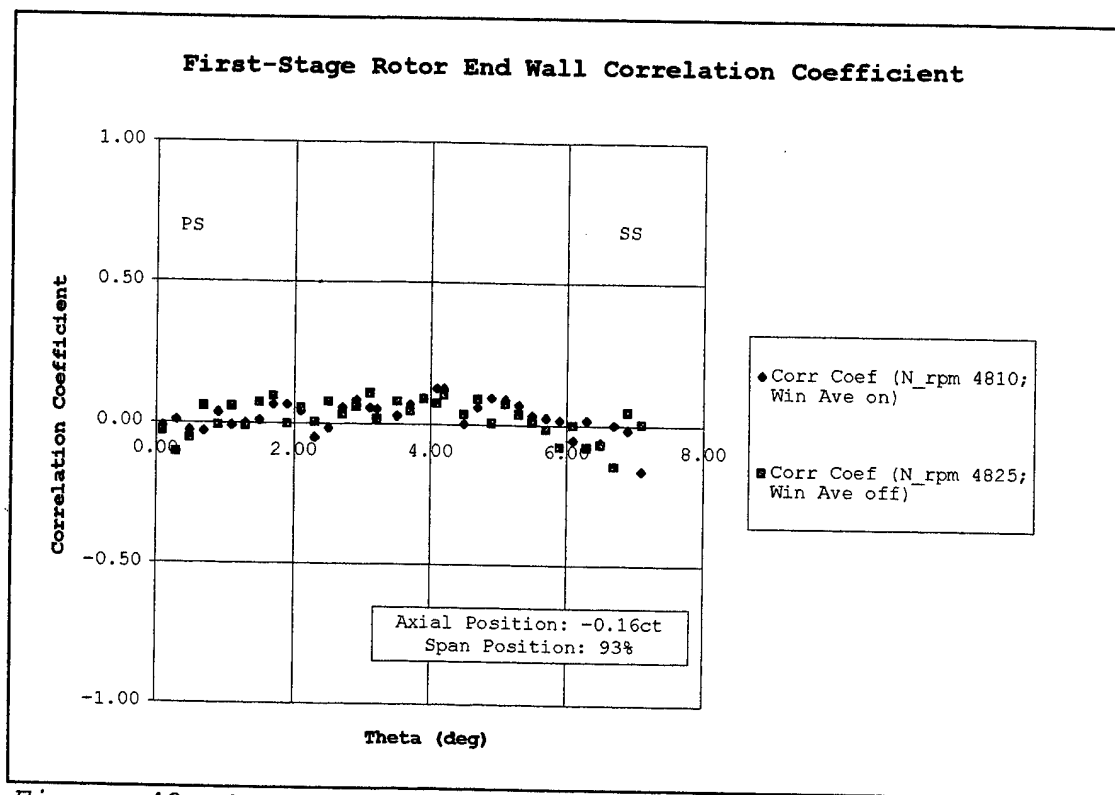


Figure 48. Correlation Coefficient for $-0.16c_t$ and 93% Span
(Window Averaging on/off)

V. CONCLUSIONS AND RECOMMENDATIONS

A. CONCLUSIONS

Modifications to the test cell were successful and adequate to facilitate installation of the LDV system hardware. They included the following items: relocation of the TTR bench and holding tank, addition of an inlet piping section, relocation of the Scanivalve into the test cell, incorporation of a closed-loop dynamometer cooling water system with heat exchanger, and installation of 220 VAC three-phase power for the LDV. Incorporation of the closed-loop dynamometer cooling water system, with heat exchanger, was a recommendation by Greco [Ref. 4: 1995]. The detailed TTR operation checklist, presented in Appendix E, was useful in safely and effectively operating the TTR. A TTR RPM of approximately 5000 was a good choice for LDV measurements, in that it was a stable speed and resulted in relatively cool bearing temperatures and low vibration levels.

Pressure-probe, velocity-profile data obtained at the stator inlet and rotor exit planes, were valid. Following the completion of probe measurements, the calibration values reported by Greco [Ref. 4; 1995] were verified in a free-jet calibration rig. First-stage, stator-inlet flow exhibited uniform Mach number and flow angle, with respect to radial position. The inlet-guide vane configuration most probably created circumferentially non-uniform flow characteristics at the stator-inlet plane. First-stage, rotor-exit characteristics varied with radial position. Rotor-exit data exhibited significant tip leakage and secondary flow within 20 percent span of the end wall.

LDV measurements were successfully conducted within the end wall region of the first-stage rotor, at five survey

locations. The three-hole, non-pressurized laser blank design was adequate for conducting LDV measurements; although, data could be affected by flow escaping through the access holes. LDV data indicated the presence of case-wall boundary layer effects, as well as tip leakage and secondary flows effects. Trends were noted in the data for both axial and spanwise directions. Velocity ratios were repeatable within two to seven percent, whereas axial velocity ratios were repeatable within four to 17 percent. Similarly, repeatability of tangential turbulence data was good; however, axial turbulence data varied by as much as 30 percent. The LDV data exhibited isotropic turbulence characteristics, in that, the correlation coefficient remained near zero and the axial and tangential turbulence intensities were, in most cases, roughly equivalent. This suggests that the survey location was in the free-stream stator exit flow and not directly within a wake zone. At the forward axial survey location, increased turbulence in the end wall region was consistent with tip leakage vortices and secondary flows. Window averaging is a valid technique and was particularly useful for recording data within the middle and aft-chord regions of blade passages.

B. RECOMMENDATIONS

If TTR operations require the use of the turbine-exit throttle valve, install a limit switch on the actuator to restrict aft movement of the back-pressure plate to a distance that will prevent damage to the forward main bearing temperature sensor. Install a pressure relief valve into the dynamometer cooling-system piping between the recirculation-pump output and the inlet control valve. This will prevent piping rupture in the event that either of the control valves are inadvertently closed. Hardware failures happen; therefore, frequent monitoring of both main bearing

and cooling water temperatures, especially when operating at rotational speeds above 3000 RPM, is prudent if system damage is to be prevented.

Additional Cobra probe velocity surveys should be conducted at the stator-inlet and rotor-exit planes to determine degree of circumferential non-uniformity.

Because of the sensitivity of the LDV system to extraneous reflections, background flare and backscatter, a field stop should be incorporated as a spatial filter for the receiving optics. With the field stop installed, conduct additional 2-D LDV measurements at $0.35c_t$ and $0.84c_t$ axial positions to ensure repeatability. Conduct 2-D LDV measurements using the pressurized laser blank, presented in Appendix B, Figures B4 and B5. Compare these data to the three-hole laser-blank data to determine if the flow escaping through the unsealed access holes has any significant effect on the measurements. Conduct 3-D LDV measurements using the TSI fiber-optics system and laser-window assembly shown in Appendix B, Figures B6 and B7. Concerning the data acquisition software, versions PHASE subsequent to 2.06 should allow a maximum DMA time out value greater than 999 seconds, to support measurements being made at slow (below 20 Hz) data rates. Incorporate the SSME HPFTP ADT second stage into the TTR, and map the two-stage turbine performance.

APPENDIX A. PROJECT PLANNING

Starting early was a key element in the accomplishment of this thesis. An early start allowed long-lead items to be completed with enough time remaining to finish the LDV measurements. Hardware modifications made to the test cell and TTR required six months to complete. Another two months were needed before the LDV system was up and running. Table A1 presents the program time-line and milestones chart.

LDV MEASUREMENTS OF THE SSME HPFTP ATD							
PROGRAM TASKS:	1996	1997				1998	
	Qtr	Qtr	Qtr	Qtr	Qtr	Qtr	Qtr
	4	1	2	3	4	1	2
Begin Thesis Project	▲						
Hardware Modification		▲	→				
Install LDV System			▲	→			
Shakedown Tests			▲	→			
Inlet & Exit Velocity Surveys				▲			
LDV Measurements				▲	→		
Write Report			▲	→		→	
Report Review & Approval						▲	→
Publication & Distribution							▲

Table A1. Thesis Milestone Chart

APPENDIX B. ENGINEERING DRAWINGS

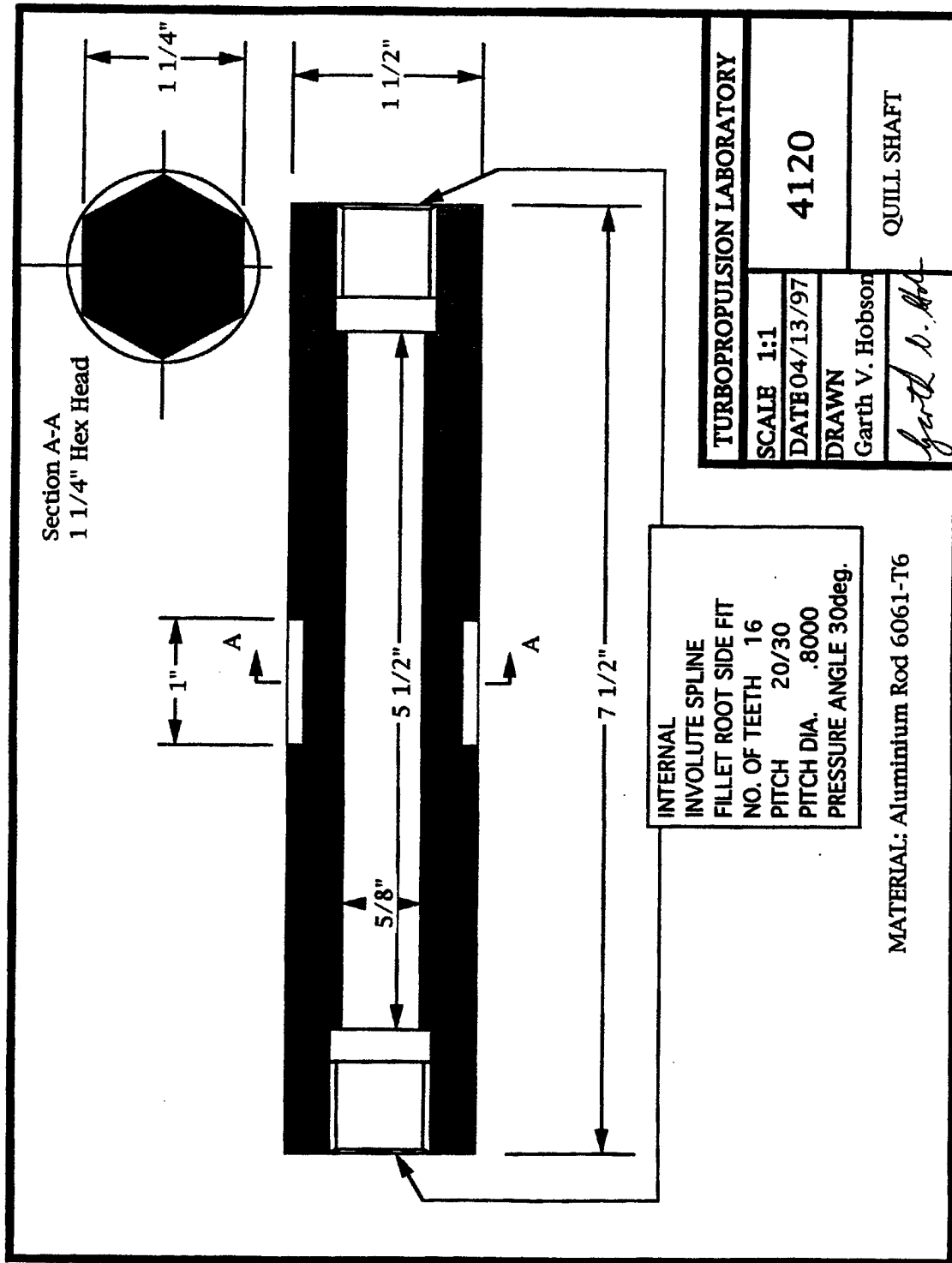


Figure B1. Quill Shaft

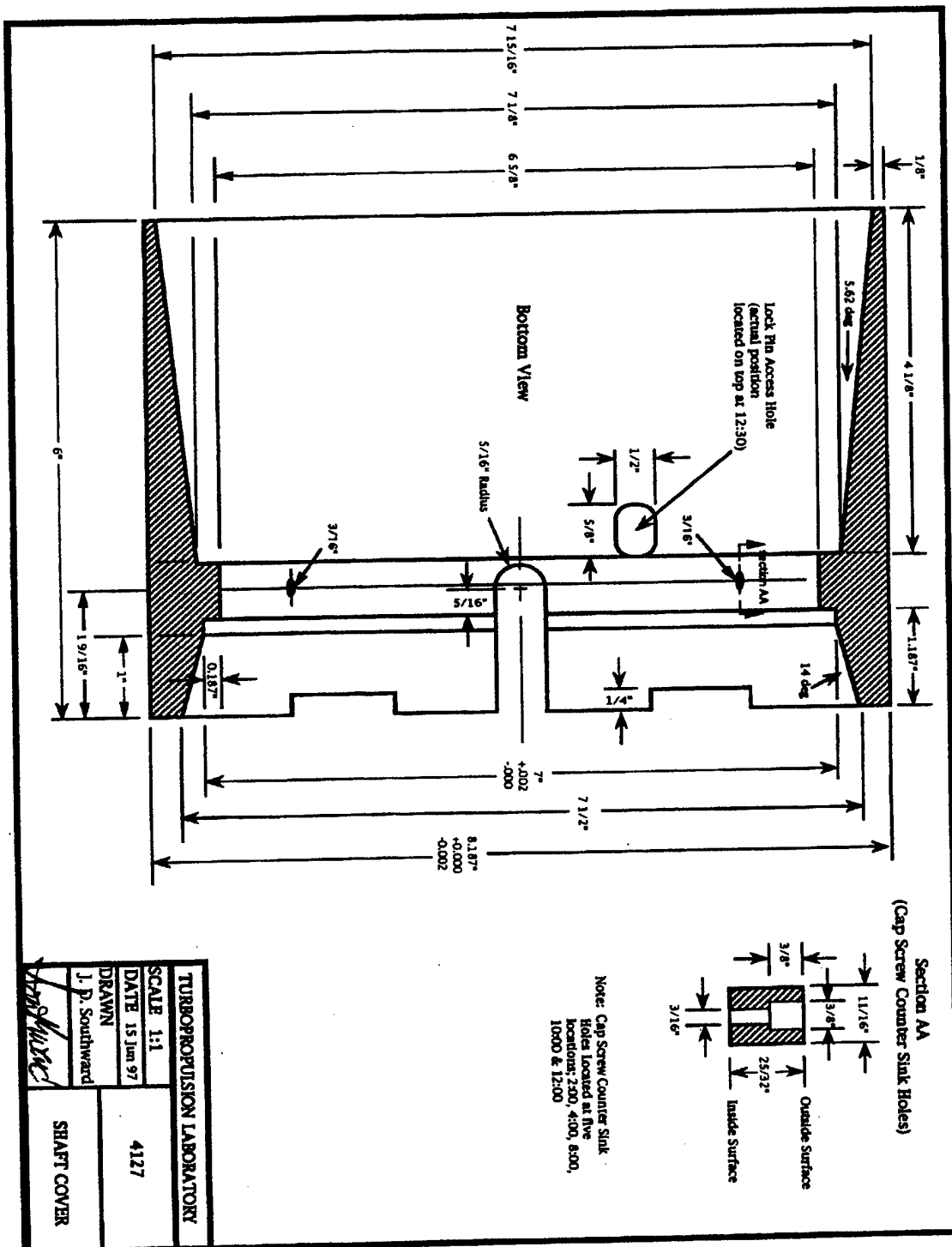


Figure B2. Shaft Cover

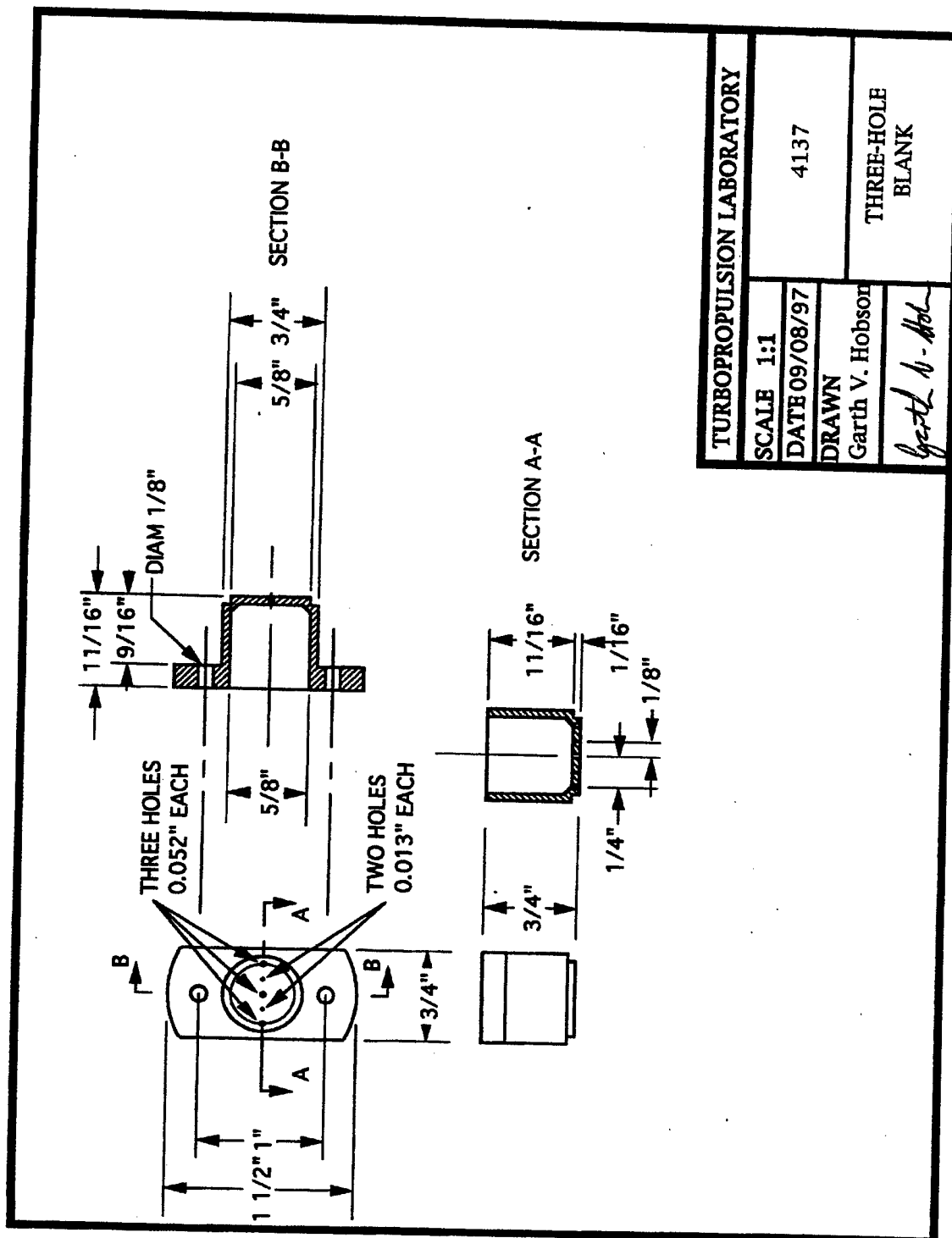


Figure B3. Three Hole Blank

TURBOPROPULSION LABORATORY			
SCALE 1:1	4137		
DATE 09/08/97	THREE-HOLE BLANK		
DRAWN Garth V. Hobson			
Garth V. Hobson			

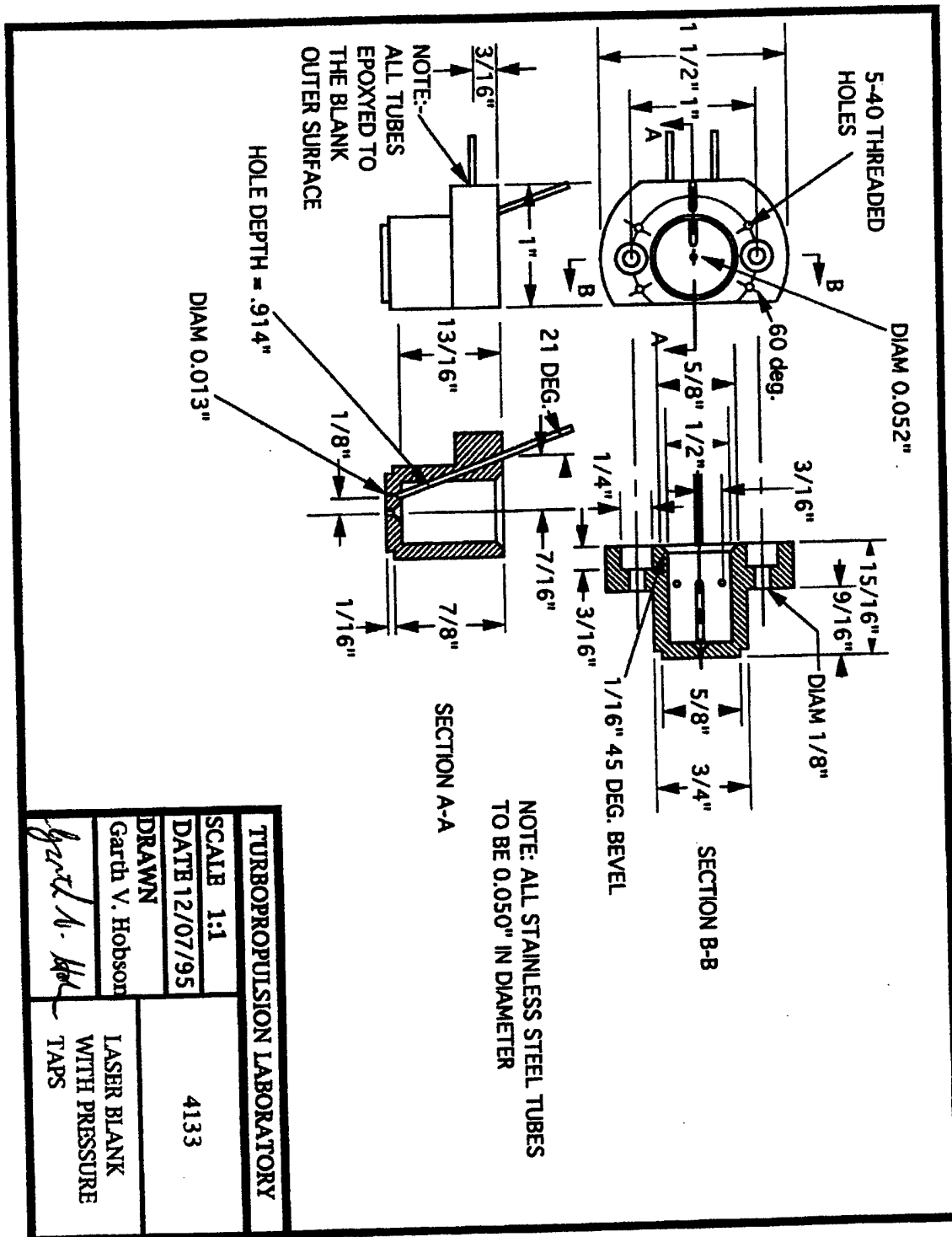


Figure B4. Laser Blank with Pressure Taps

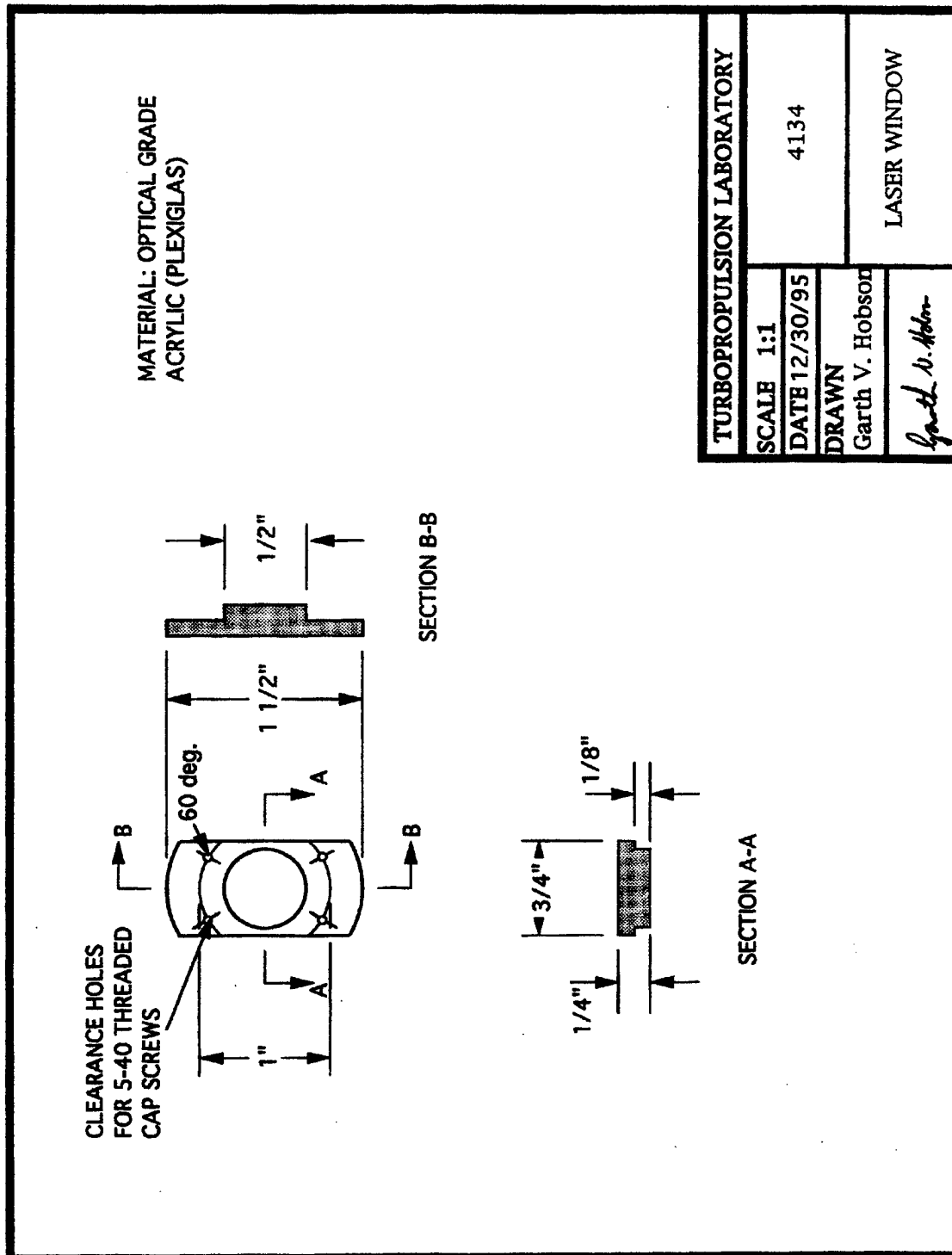


Figure B5. Laser Window

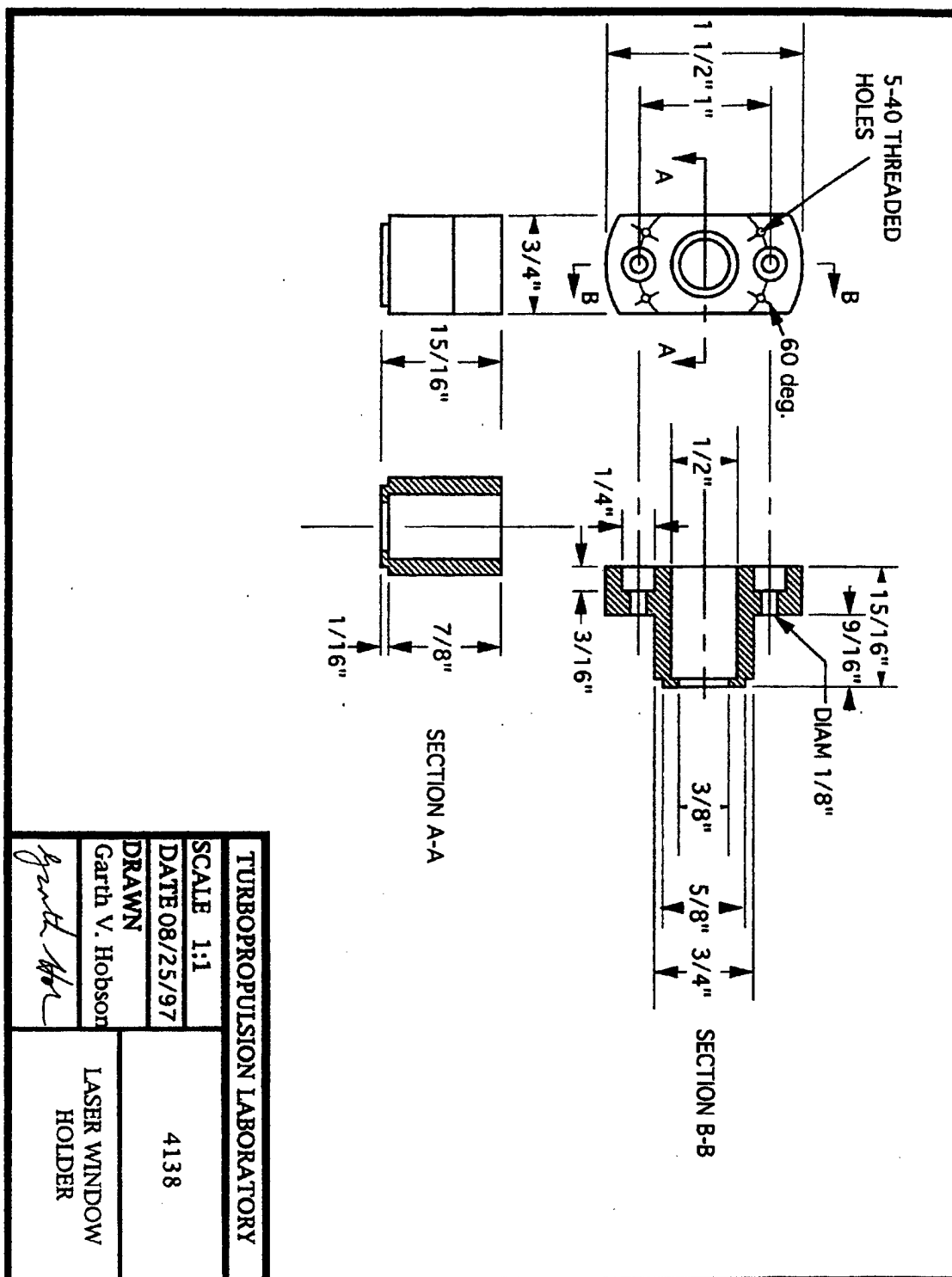
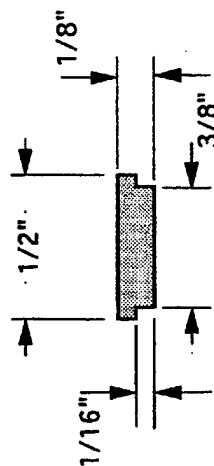
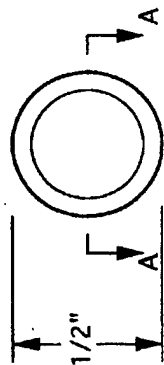


Figure B6. Laser Window Holder

MATERIAL: OPTICAL GRADE
ACRYLIC (PLEXIGLAS)



TURBOPROPULSION LABORATORY

SCALE 2:1

DATE 8/25/97

DRAWN

Garth V. Hobson

Garth V. Hobson

4139

WINDOW

Figure B7. Window

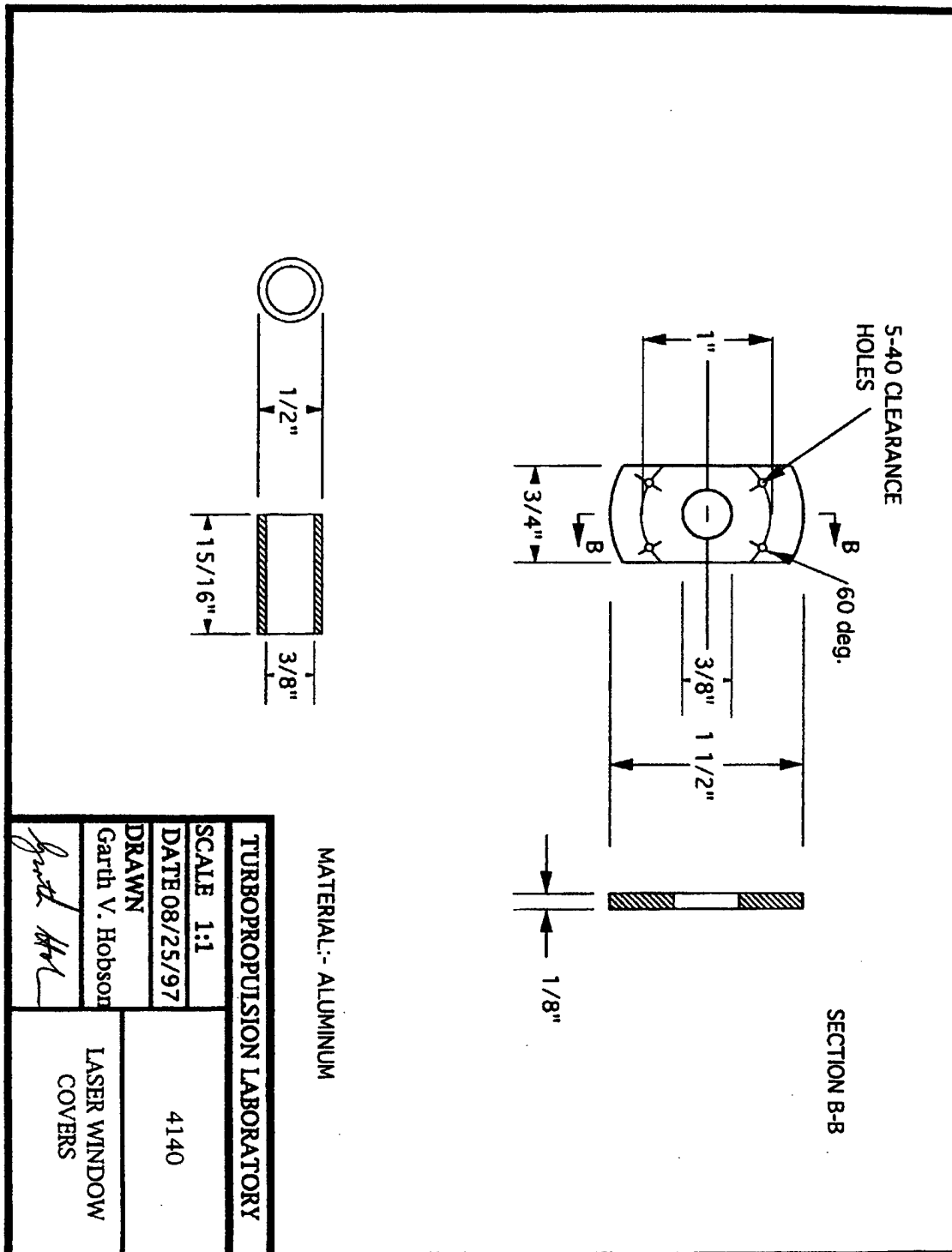


Figure B8. Laser Window Covers

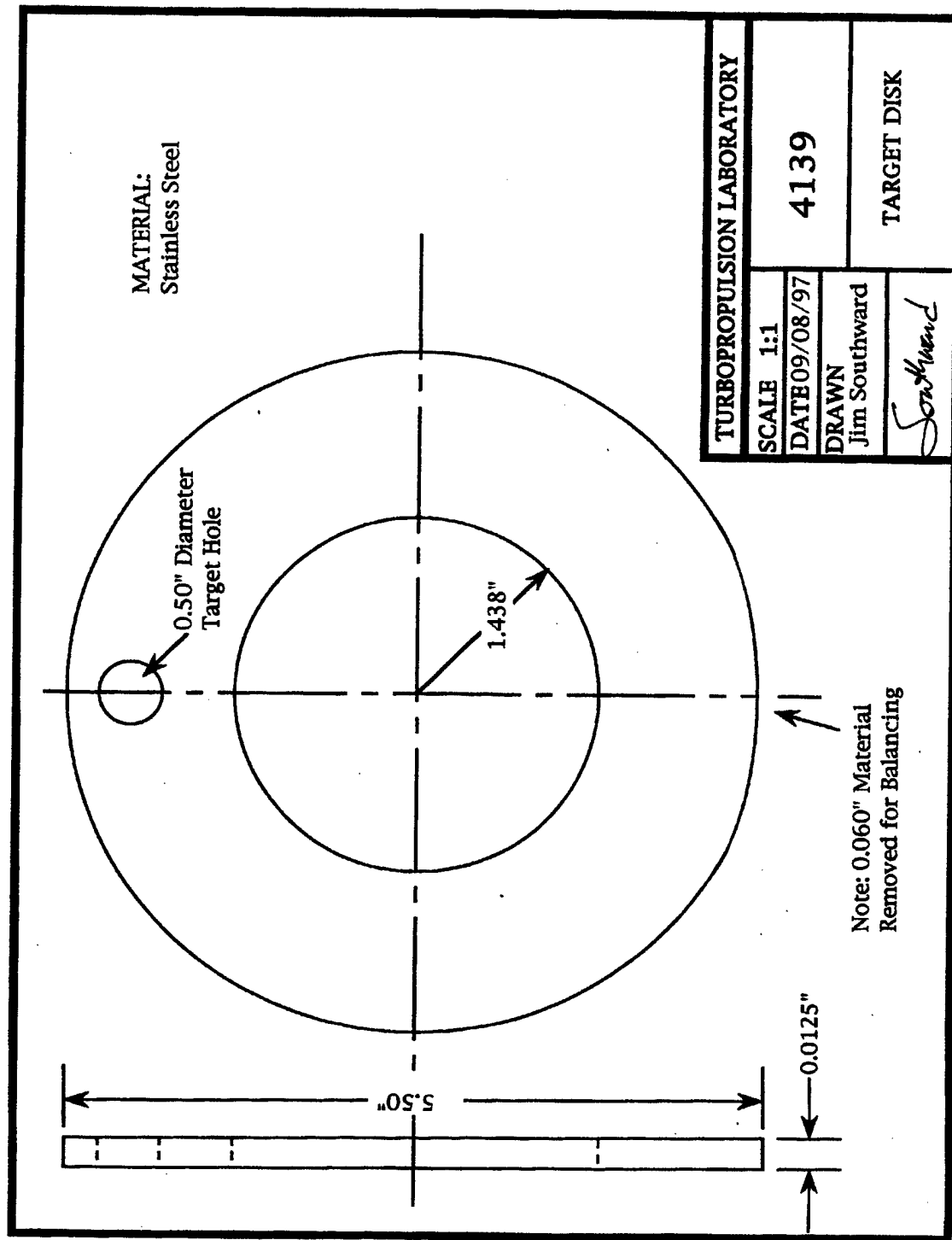


Figure B9. Target Disk

APPENDIX C. CALIBRATION DATA

A. Lebow Load Cell Calibration

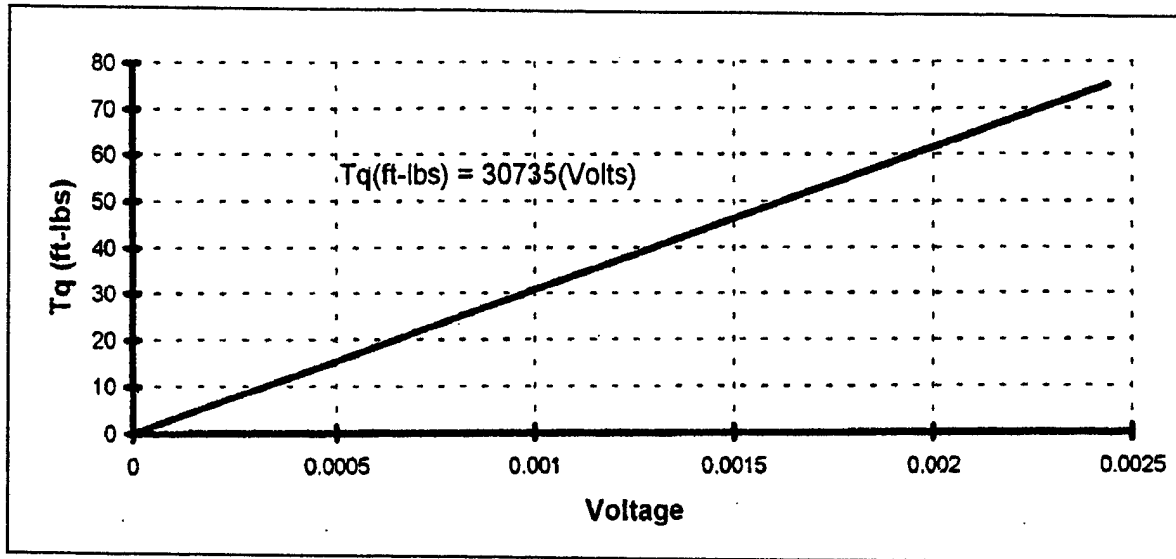


Figure C1. Lebow Load Cell Calibration

B. Cox Flow Meter Calibration

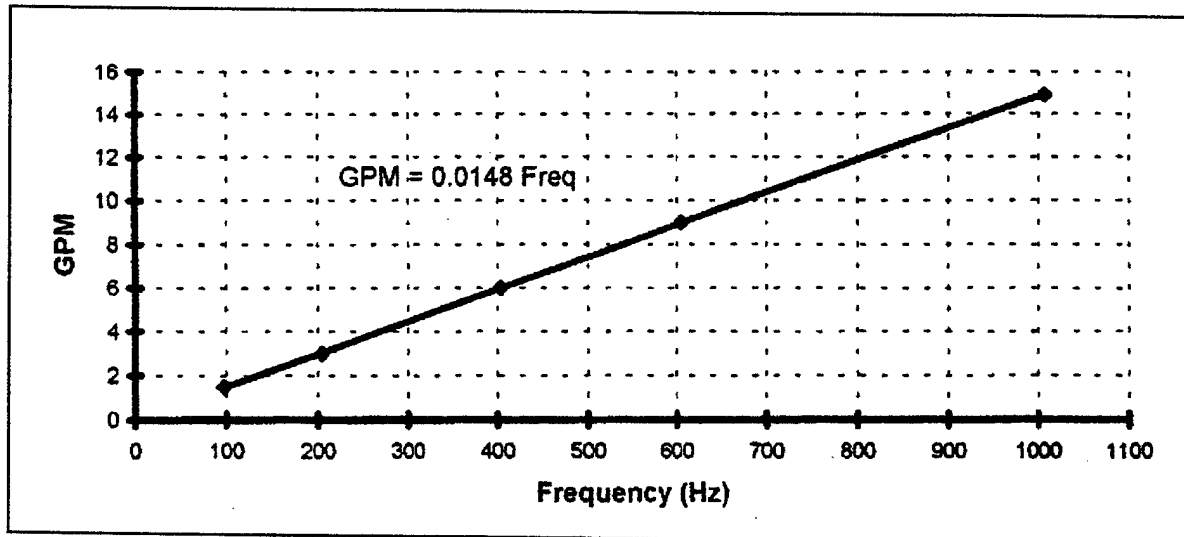


Figure C2. Cox Flow Meter Calibration

C. Type-J Thermocouple Calibration

Absolute temperature (T_T) for the type-J thermocouples installed in the TTR is given by

$$T_T = \alpha_0 + \alpha_1 V_T + \alpha_2 V_T^2 + \alpha_3 V_T^3 + \alpha_4 V_T^4 + \alpha_5 V_T^5$$

where, $\alpha_0 = -0.048868252$, $\alpha_1 = 19873.14503$, $\alpha_2 = -218614.5353$,
 $\alpha_3 = 11569199.78$, $\alpha_4 = -264917531.4$, $\alpha_5 = 2018441314$. V_T is defined as

$$V_T = V_S + V_R$$

where, V_S is the thermocouple voltage and V_R is the equivalent reference junction voltage. A first-order approximation of the above relationship was used in the TTR DAS program and is valid over the temperature range of 20 to 40 degrees C. A comparison of the linear approximation and the fifth-order relationship is provided in Figure C3.

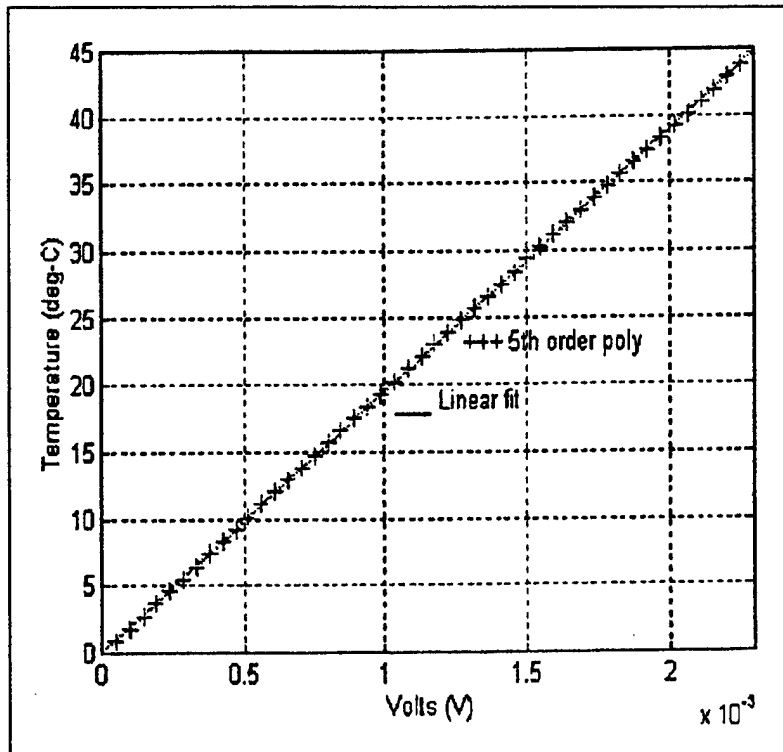


Figure C3. Type-J Thermocouple Calibration

D. Cobra Probe Calibration

Figure C4 presents the dimensionless velocity (X) plotted vs. dimensionless pressure coefficient (β) with the sixth order curve fit. The curve fit uses the equation

$$X = \alpha_0 + \alpha_1\beta + \alpha_2\beta^2 + \alpha_3\beta^3 + \alpha_4\beta^4 + \alpha_5\beta^5 + \alpha_6\beta^6$$

where, $\alpha_0=0.0662$, $\alpha_1=0.8443$, $\alpha_2=83.74$, $\alpha_3=-1962$, $\alpha_4=19342$,

$\alpha_5=-87713$, $\alpha_6=150585$, and $\beta = \frac{P_1 - P_{23}}{P_1}$.

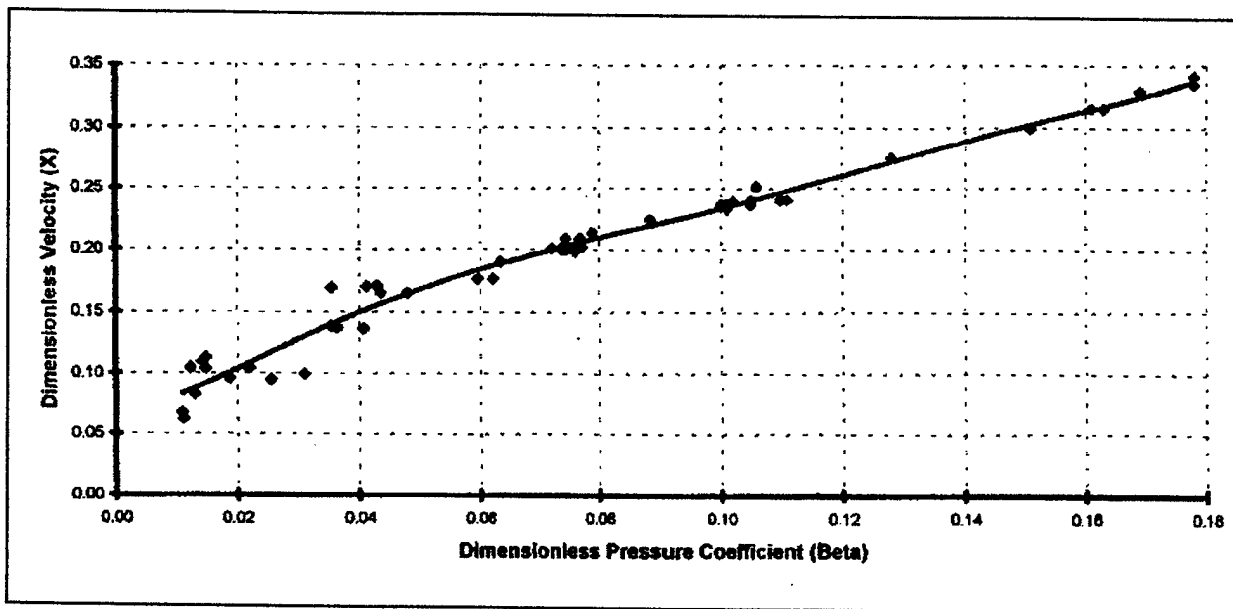


Figure C4. Cobra Probe Calibration

APPENDIX D. LabVIEW DAS PROGRAM DOCUMENTATION

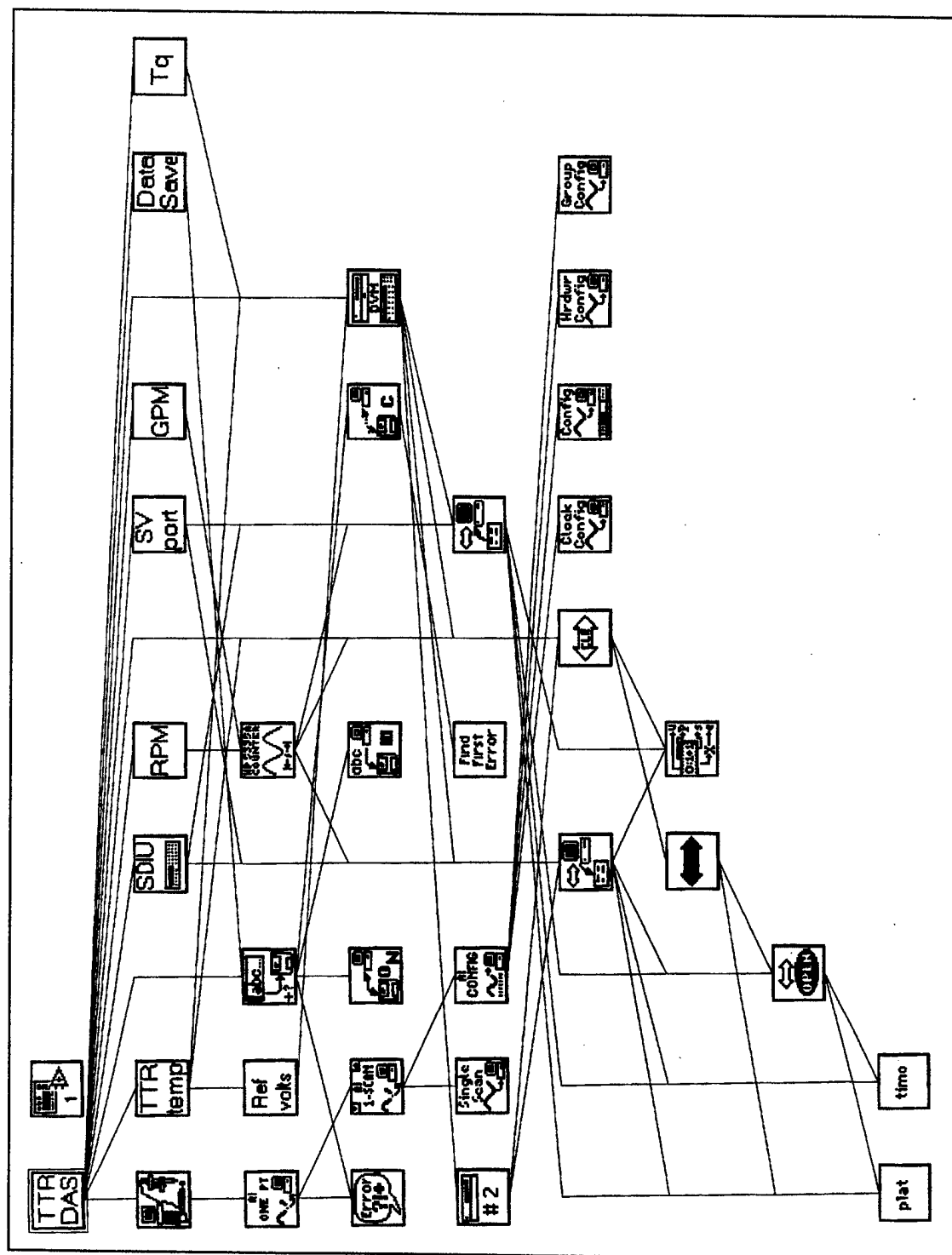


Figure D1. SSME_TTR.VI Icon Hierarchy

SSME HPFTP ATD data acquisition program

ATM Pressure (in Hg)		29.920		Ref Temp (deg-C)		0.00000		RPM		0.00000		Radial Position		0.0000	
Pressure (in H2O)		Scanrate		Port #		TT2 (deg-R)		Flow Rate (GPM)		0.00000		Swirl Angle		0.0000	
Tare	0.00000E+0	1	0.00000E+0	TT3 (deg-R)	0.00000	Torque (in-lbs)	0.00000	Throttle Position	0.0000						
Cal	0.00000E+0	2	0.00000E+0	TT4 (deg-R)	0.00000	Power #1 (HP)	0.00000	Ref Temp Ratio	0.00000						
P3	0.00000E+0	3	0.00000E+0	Inlet Water Temp	0.00000	Power #2 (HP)	0.00000	Ref Press Ratio	0.00000						
P4	0.00000E+0	4	0.00000E+0	Outlet Water Temp	0.00000	Power #3 (HP)	0.00000	Ref RPM	0.00000						
P2	0.00000E+0	5	0.00000E+0	Orifice Temp (deg-R)	0.00000	Ref HP	0.00000	Ref Mass Flow	0.00000						
P1	0.00000E+0	6	0.00000E+0												
P31	0.00000E+0	31	0.00000E+0												
P32	0.00000E+0	32	0.00000E+0												
P33	0.00000E+0	33	0.00000E+0												
P34	0.00000E+0	34	0.00000E+0												
Efficiency		Turbine Pressure Ratio		Mass Flow Rate (Vena)		Mass Flow (Flange)		Avg Mass Flow Rate (lbs/sec)							
0.00000		0.00000		0.00000		0.00000		0.00000							
Inlet (Vena)		0.00000E+0		0.00000		0.00000		0.00000							

Figure D2. SSME_TTR.VI Front Panel

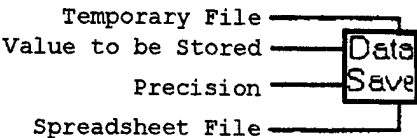
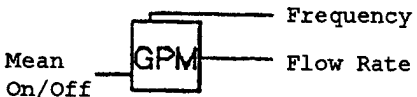

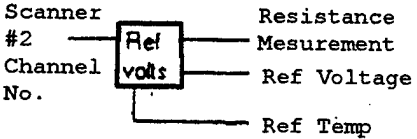

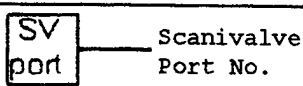
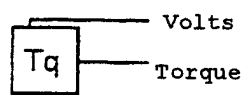
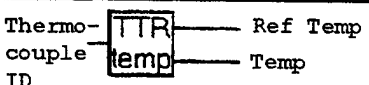
Sub_VI	Icon/Connection	Function
DATAFILE.VI		Stores measured & reduced data to two files; an Excel spreadsheet & a Temporary file which is deleted when data reduction is complete.
GPM.VI		Measures the frequency signal from the Cox flow meter through the HP Universal Counter.
POSITION.VI		Measures the linear potentiometer voltage from channels 13,14 &15 via the PC-LPM-16 A/D board.
REF_VLTS.VI		Determines the resistance at the reference junction (Ch 60) for calculation of reference temperature.
RPM.VI		Measures the frequency from the 30 tooth gear magnetic pick-up through the HP Universal Counter.
SV_PORT.VI		Determines what port the Scanivalve is on.
TORQUE.VI		Connects scanner #2 channel #33 to the DVM for voltage measurement of the Lebow load cell.
TTRTEMP.VI		Connects scanner #2 channels 60-66 to the DVM for reference temperature and thermocouple voltage measurement.

Table D1. SSME_TTR.VI Description of SubVI's

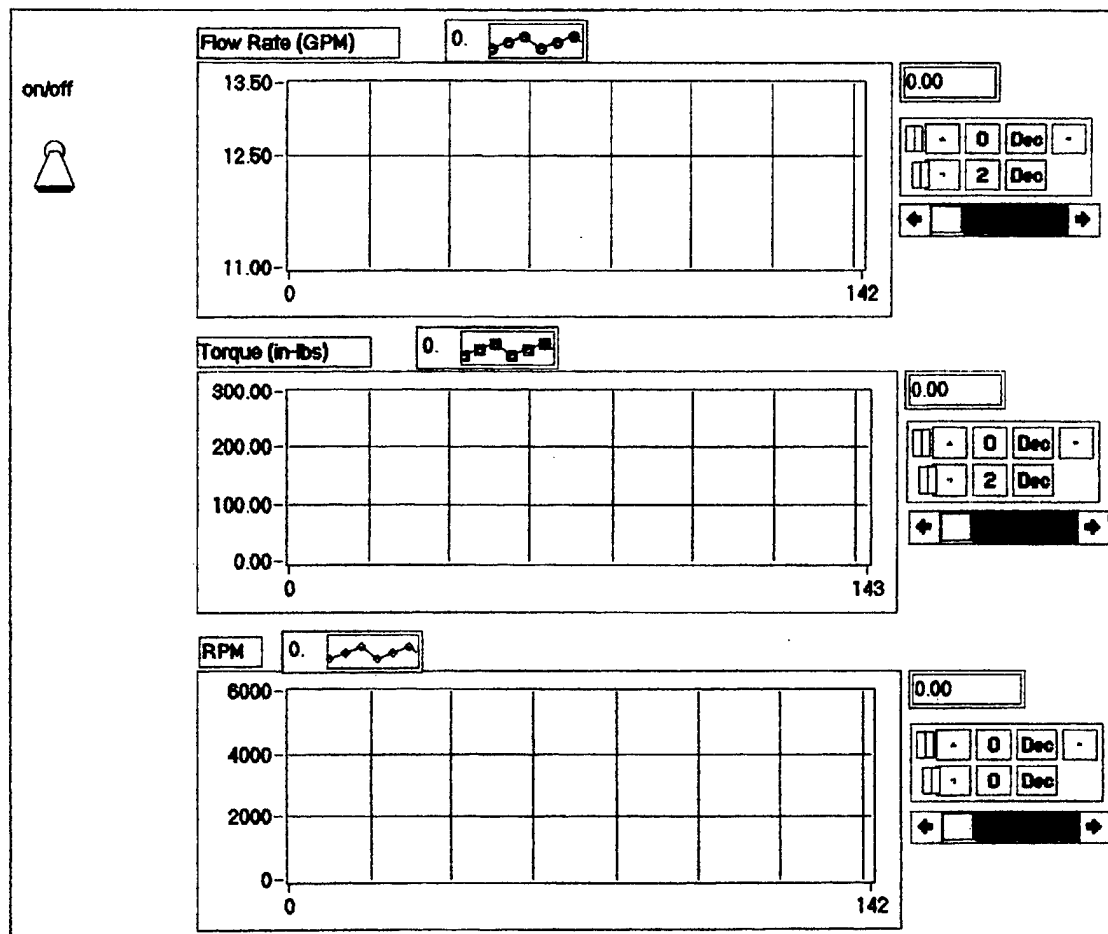


Figure D3. TTR_TEST.VI Front Panel

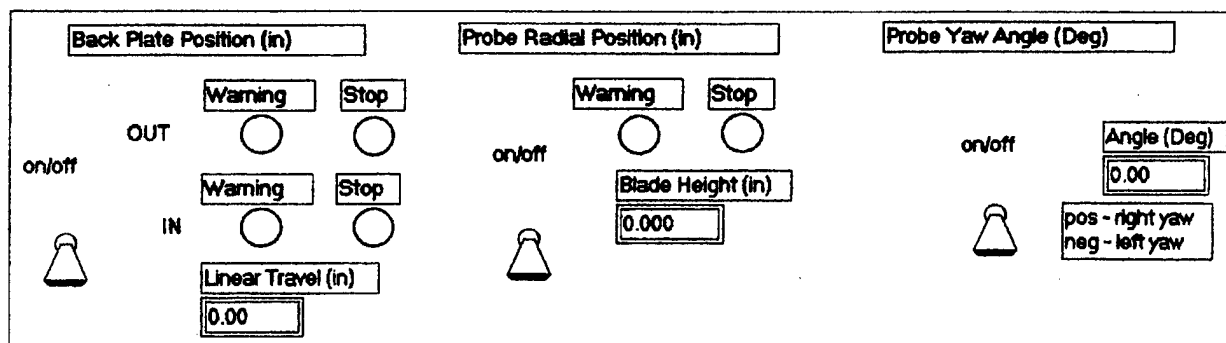


Figure D4. ACTUATOR.VI Front Panel

Turbine Velocity Profile

ATM Press (in Hg)

Tare

Cal

P2

P1

P23

RPM

Radial Position (inches)

Swirl Angle (degrees)

Beta

☒ **X**

Mach #

Prat

Figure D5. VEL_PRFL.VI Front Panel

105

APPENDIX D

APPENDIX E. CHECKLISTS

I. TTR OPERATION

A. TTR Pre-Start Checklist

- ☐ 1. Axial Compressor (A/C): Approximately two hours prior to having air "up and stable", start warming up oil and turn on cooling water (shop technician only)
- ☐ 2. Shop air (A/C room):
 - ☐ a. Drain Hose- place outside door
 - ☐ b. Outlet Valve (green handle)- close
 - ☐ c. Compressor Switch- on
 - ☐ d. Tank Drain Valve (bottom right with red handle)- open
 - ☐ e. Output Hose to green piping- check connected
 - ☐ f. Outlet Valve- open
- ☐ 3. TTR shop air (test cell):
 - ☐ a. Shop air valve(on green pipe)- open
 - ☐ b. Dynamometer valves- both full open
 - ☐ c. Oil Mist Filters- bleed
 - ☐ d. Oil Mist Regulator- off
 - ☐ e. Seed Particle Regulators- off
 - ☐ f. Plenum Manual Inlet Valve (green handle)- check closed
 - ☐ g. Alternate Source Air Hose- route and connect from compressor test cell to seed particle regulators using T-fitting
- ☐ 4. Cobra Probe- check retracted (if installed)
- ☐ 5. Throttle Actuator- connect control box in test

cell and check function, clean and lubricate as required, set to full open (if installed)

WARNING: DO NOT ALLOW THROTTLE ACTUATOR TO MOVE AFT INTO FORWARD BEARING TEMPERATURE SENSOR.

6. Calibration air (upper control room):

☐ a. Hose between regulator output and manual loading panel- disconnected

☐ b. Regulator- 25 psig

☐ 7. Throttle actuator control box in lower control room- check function

NOTE: TWO PERSONS REQUIRED; ONE AT CONTROL BOX AND ONE AT WINDOW. ABOVE WARNING GERMANE.

8. Dynamometer cooling water:

☐ a. Cooling Water- verify on

☐ b. Water Supply Valve (red handle in A/C room)- open

☐ c. Water Outlet Valve (green handle in A/C room)- open

☐ d. Heat Exchanger Cooling Water Supply Valve (red handle on white pipes in test cell)- check open

☐ e. Pump Outlet Valve (red handle)- open

☐ f. Holding Tank- check water level, wire indicator should be between marks

CAUTION: ENSURE PUMP OUTLET VALVE AND BOTH DYNAMOMETER VALVES ARE OPEN PRIOR TO TURNING ON SCAVENGE PUMP.

☐ g. Scavenge Pump- on

☐ h. Dynamometer Water Seal Valve (attached to dynamometer inlet valve)- check full open

- 9. Set-up Control Panel in upper control room:
 - ☐ a. Panel Breaker (below shelf)- on
 - ☐ b. RPM read out- check indicating zero RPM
 - ☐ c. Dump Valves- check both full open
 - ☐ d. TTR Valve (#5)- check closed
- ☐ 10. Run Log- start new one
- 11. Data Acquisition System Hardware Wiring:
 - ☐ a. GPIB Cables- connected from PC to DVM, SDIU to DVM, Universal Counter to DVM, & Scanner #2 to DVM.
 - ☐ b. Universal Counter Channels A & B- connect wire labeled "TTR RPM" to channel A, and wire labeled "TTR Flow Rate" to channel B
 - ☐ c. Scanivalve #1 Cable- connect black cable with large connector to junction box (Scanivalve position), and connect small gray wire cannon plug to SCU channel 20 (upper plug)
 - ☐ d. Scanivalve Pigtail- check connected between Scanivalve cable and cannon plug coming directly from Scanivalve transducer
 - ☐ e. SDIU Cable (gray with small black wire attached)- connect to junction box (SDIU position)
 - ☐ f. Solenoid Controller Wire Bundle (white)- connect to junction box (CTRL2 position)
 - ☐ g. 50-Pin Ribbon Cable- connect to upper slot on back of 486 PC
 - ☐ h. Turbine Torque Cannon Plug (gray wire)- connect to SCU channel 33, upper plug

- ☐ i. Cobra Probe Cannon Plug (white wire bundle)- connect to control box in lower control room
- ☐ j. Mass Flow Differential Pressure Transducer (DPT) (Scanivalve rack)- connect gray wire to SCU channel 24, upper plug
- ☐ 12. Instrumentation Master Power Switch- on
- ☐ 13. Instrumentation Power- check on for all components
- ☐ 14. Calibrate Mass Flow DPT Wheatstone Bridge:
 - ☐ a. Jumper Cable- connect between SCU channel 24 and DVM
 - ☐ b. Bridge Zero- adjust upper knob so that DVM reads zero volts
 - ☐ c. Check Line Hose- connect to either side of DPT
 - ☐ d. Check Line Switch- on
 - ☐ e. Calibration Pressure- set to 5 inHg
 - ☐ f. Wall Manometer- verify 5 inHg set
 - ☐ g. Bridge Span- adjust lower knob so that DVM reads 6.785E-3 volts
 - ☐ h. Calibration Air- off
 - ☐ i. Iterate- as required
 - ☐ j. Check Line Hose- disconnect from DPT and reconnect original hose
- ☐ 15. Calibrate Scanivalve DPT Wheatstone Bridge:
 - ☐ a. Calibration Pressure- set to 10 inHg
 - ☐ b. Wall Manometer- verify 10 inHg set
 - ☐ c. Jumper Cable- connect from SCU channel 20 to DVM
 - ☐ d. Scanivalve Port No. 1- select (check remote

- off, select #1, select port) and adjust upper knob so DVM reads zero
- ☐ e. Scanivalve Port No. 2- select and adjust lower knob so DVM reads 13.609E-3 volts
 - ☐ f. Iterate- as required
 - ☐ g. Jumper Cable- disconnect
16. Cobra Probe DPT- set ch. 22 to zero
17. Calibrate Lebow Load Cell:
- ☐ a. Jumper Cable- connect ch. 33 to DVM
 - ☐ b. Bridge Zero- set ch. 33 upper knob so DVM reads zero
 - ☐ c. Calibration Arm- attach to dynamometer
 - ☐ d. Weights- apply 31.44 lb. at 2 ft from center
 - ☐ e. Bridge Span- set to 2.197E-3 volts
 - ☐ f. Iterate- as required
 - ☐ g. Weights/Arm- remove
 - ☐ h. Jumper Cable- remove
18. Set up LabVIEW software on 486 PC:
- ☐ a. Open C:\labview\ttr\ssme_ttr.vi
- NOTE: REBOOT MAY BE REQUIRED IF INSUFFICIENT MEMORY ALERT APPEARS
- ☐ b. Using Notepad, open TTRdata.dat, SSMEdata.dat and vel_prfl.dat, and enter date in left column of each data file.
 - ☐ c. TTR_test.vi- open
 - ☐ d. Actuator.vi- open and run to get read out of Cobra probe position
 - ☐ e. Velprfl.vi- open

- ☐ 19. Dynamometer Outlet Water Temperature Read Out-check function
- ☐ 20. Dynamometer Outlet Valve- set to 50% using TTR Auto Control Panel in upper control room; select manual mode "M", press up arrow (right button), set with horizontal indicator

WARNING: ENSURE DYNAMOMETER OUTLET VALVE REMAINS AT LEAST 10% OPEN.

NOTE: 0% IS FULL OPEN AND 100% IS FULL CLOSED.

- ☐ 21. Plenum Inlet Sump Valve- bleed off water/dirt
- ☐ 22. Manual Valve (large green handle) to Plenum- open
- ☐ 23. Recirculation Water Pressure- check approximately 65 psig
- ☐ 24. Oil mist:
 - ☐ a. Regulator- set 30 psia (just prior to starting turbine)
 - ☐ b. Oil Drop Rate- check at one per second; adjust as required
- ☐ 25. Outside Gate- shut and lock

B. TTR Start Checklist

- ☐ 1. TTR_test.vi- run (click arrow in upper left corner)
 - ☐ 2. No. 5 valve- open to 20% (~ 800 rpm)
 - ☐ 3. Dump Valve No. 2- close (~ 1500 rpm)
- NOTE: MASS FLOW RATE NOW ACCURATE.
- ☐ 4. Test Cell- check
 - ☐ 5. No. 5 valve- open to 50%
 - ☐ 6. No. 1 dump valve- close as required to set approximately 3000 rpm

WARNING: CHANGE DUMP VALVE POSITIONS SLOWLY; MAINTAIN
SPEED COUNTER AT 3950 \pm 50.

- ☐ 7. Test Cell- check

CAUTION: DO NOT ENTER TEST CELL ABOVE 3000 RPM.

- ☐ 8. No. 5 valve- open to 80% and close #1 dump valve
as required for 5000 RPM
- ☐ 9. Accelerometers, Water and Bearing Temperatures-
monitor for normal indications
- ☐ 10. Run Log- record TTR operating conditions each hour

LIMITATIONS: DYNAMOMETER WATER TEMP < 125 DEG C

BEARING TEMP < 130 DEG C

ACCELEROMETERS NO CHANGE FROM NORMAL

C. TTR Shut-Down Checklist

- ☐ 1. Cobra Probe- retract
- ☐ 2. Dump Valve No. 1- open
- ☐ 3. Valve No. 5- close to 20%
- ☐ 4. Dump Valve No. 2- open
- ☐ 5. Test Cell- check
- ☐ 6. Valve No. 5- close
- ☐ 7. Dynamometer Exit Valve- open fully
- ☐ 8. Manual Plenum Inlet Valve- close
- ☐ 9. Scavenge Pump- off
- ☐ 10. Shop Air in Test Cell- secure
- ☐ 11. Advise shop technician to secure A/C and cooling
water
- ☐ 12. Close red and green cooling water valves
- ☐ 13. Complete post run inspection
- ☐ 14. Instrumentation master switch and console switch-
off

- ☐ 15. Calibration air- set zero
- ☐ 16. LabVIEW programs- close
- ☐ 17. Cannon Plugs on back of Control Box- disconnect

D. Emergency Shutdown

- ☐ 1. Dump Valves- both closed
- ☐ 2. No. 5 valve- close
- ☐ 3. Scavenge pump- off

II. LDV SYSTEM OPERATION

A. Start-Up

- ☐ 1. Laser Safety Signs- post at door entrance and at window
- ☐ 2. Hardware Connections- verify correct
- ☐ 3. Cooling Water Discharge Hose- route and connect
- ☐ 4. Beam Attenuator- open
- ☐ 5. Lens Cover- remove
- ☐ 6. Laser Start:
 - ☐ a. Power supply Switch Bar- on
 - ☐ b. Key Control- on
 - ☐ c. Water Flow Rate- adjust until all indicator lights are on, then open valve 1/2 turn more
- ☐ 7. Laser Power Supply:
 - ☐ a. Laser Power Meter Select Dial- 3 watts
 - ☐ b. Line Current Meter Select Dial- 50 amps
 - ☐ c. Light Control- check full Counter Clock Wise (CCW)
 - ☐ d. Current Control- check full CCW
 - ☐ e. Control Selector- current

- ☐ f. Power On- press
- ☐ g. Power INTLK Light- check on
- ☐ h. Ready Light- check on in 45-60 seconds
- ☐ i. Laser Start- press
- ☐ j. Current Control- set 0.5 watts (eye safe)
- 8. Traverse Table setup:
 - ☐ a. Power Supply Switch- on
 - ☐ b. Hand Control/Computer Control Switch- hand control
 - ☐ c. Sony Position Encoder- check on
- NOTE: DO NOT TURN OFF POWER OR REFERENCE POSITION WILL BE LOST.
- 9. Photomultiplier Power Supply set-up:
 - ☐ a. Power Switches- on
 - ☐ b. Current Control Knob- one O'clock position
- 10. Frequency Shifter set-up:
 - ☐ a. Power Switches- on
 - ☐ b. Frequency Shift Select- as required
 - ☐ c. Shift Direction- into flow; green up; blue down
- ☐ 11. IFA 750 Power-on
- ☐ 12. RMR Power- on
- ☐ 13. OPR Power Cord- plug in
- 14. Oscilloscope Set-up (OPR signal/burst signal):
 - ☐ a. Power- on
 - ☐ b. Vertical Mode- ALT (dual trace)
 - ☐ c. Trigger- slope
 - ☐ d. X10 Mag- press out
 - ☐ e. Ch 1 Volts/Div (vertical scale)- 2/0.1

- ☐ f. Ch 2 Volts/Div(horizontal scale)- 5/20m
- ☐ g. A & B Sec/Div- 10ms/0.1 μ s
- 15. 386 Computer (control room):
 - ☐ a. Video Monitor- on
 - ☐ b. Printer- on
 - ☐ c. CPU- on
 - ☐ d. Check Date- set as required
 - ☐ e. Change Directory- C:\>cd PHASE
 - ☐ f. Start program- C:\PHASE>PHASE
 - ☐ g. Program Menus- set up as required
- 16. 286 Computer (test cell):
 - ☐ a. Video Monitor- on
 - ☐ b. CPU- on
 - ☐ c. Check Data- set as required
 - ☐ d. Change Directory- C:\>cd FIND4 or PHASE (as required)
 - ☐ e. Start Program- C:\FIND4>FIND or PHASE (as required)
 - ☐ f. Program Menus- set up as required
- 17. Check Laser Optics:
 - ☐ a. Beam Crossing- check using microscope objective
 - ☐ b. External Seeding- attack external pipe, set 20 psia, select top jet only
 - ☐ c. Beam- focus in seeding output
 - ☐ d. Photomultipliers- set adjust screws for maximum data rate
 - ☐ e. Lens- clean (only if required)
- ☐ 18. Beam Reference Position- set

B. Measurement Preparation

- ☐ 1. Laser Blank/Window- clean
- ☐ 2. End Wall- clean
- ☐ 3. Seed Generators:
 - ☐ a. Regulators- 60 psig
 - ☐ b. Jet Valves- all three open
 - ☐ c. LPM Air- 80%
- ☐ 4. Current Control- as required
- ☐ 5. SSME_TTR.VI- run concurrent with each laser data set

C. Shutdown

- ☐ 1. Current Control- full CCW
- ☐ 2. TTS- move to reference position
- ☐ 3. Laser Power Supply:
 - ☐ a. Power Off- press
 - ☐ b. Key Control- off
 - ☐ c. Power Supply Switch Bar- off
- ☐ 4. Cooling Water- secure
- ☐ 5. Water Hose- secure
- ☐ 6. Laser Safety Sign- stow
- ☐ 7. OPR Power Cord- pull

APPENDIX F. FORTRAN CODE

```
c*      CDR James D. Southward, USN; updated 7 Feb. 98

c*      This FORTRAN program extracts selected data from a
c*      PHASE statistics file (*.s*) and creates a file
c*      (*.c*) that can be read by a commercial spreadsheet
c*      program, such as Excel. The user must tailor the
c*      following source code for each statistics file by
c*      changing the file names, setting arrays, and
c*      setting do loops. The code will reads both
c*      single processor and multiprocessor statistics;
c*      reference the PHASE Resolved Software manual for
c*      information on how data is stored. The number of
c*      data points contained in the statistics file is
c*      related to the number of bins plotted (reference
c*      PHASE Statistics/Graphics Setup menu). The first
c*      230 lines of the PHASE statistics file is header,
c*      which is skipped. The next 20*n lines are single
c*      processor data organized in 20 line blocks, and
c*      the last 7*n lines are the multiprocessor data
c*      organized in 7 line blocks. This code extracts
c*      u-mean, u-turb, v-mean, v-turb, Reynolds Stress,
c*      and Correlation coefficient.
```

program file

```
c*      *** declare variables & file names ***
c*      implicit integer (a - z)
c*      real sctr1(20),sctr2(7)
c*      *** set arrays equal to number of bins plotted***
c*      real theta(36),um(36),ut(36)
c*      real vm(36),vt(36),alpha(36),corr(36)
c*      character*40 fname, sfname
c*      character*20 dummy

c*      data untnum /9/
c*      data suntnum /19/

c*      *** set name of file to be processed ***
c*      fname = '1127fi.s01'
c*      *** set name of composite stats ASCII file ***
c*      sfname = '1127fi.c01'
c*      *** open data files ***
c*      open(unit=untnum,file=fname,access='sequential',
c*      >status='old')
c*      open(unit=suntnum,file=sfname,access='sequential',
c*      >status='unknown')
```

```

c*      *** skip file header ***
      do 100 i = 1, 230
        read(untnum, 399) dummy
100     continue
399     format(a20)

      write(*,*) 'Reading Statistics File '
      write(*,*) fname
        write(*,*) 'Creating Converted Statistics File'
        write(*,*) sfname

c*      *** write header to output file ***
      write(suntnum,*) 'File Name \',sfname

c*      *** read single component stats and store selected
c*      values. Set max loop value to number of bins
c*      plotted ***
      do 400 i = 1, 36

        do 300 j = 1, 20
          read (untnum, 500) sctr1(j)
300      continue

c*      *** two bin averaging (normally add 0.1, except
c*      when shifting) ***
      theta(i)= 0.1 + (i-1)*(0.2)
      um(i)=sctr1(4)
      ut(i)=sctr1(6)
      vm(i)=sctr1(14)
      vt(i)=sctr1(16)
400     continue

c*      *** read multiprocessor stats and store selected
c*      values. Set max loop value to number of bins
c*      plotted ***
      do 700 l=1, 36

        do 800 m=1, 7
          read (untnum, 501) sctr2(m)
800      continue

      alpha(l)=sctr2(5)
      corr(l)=sctr2(7)
700     continue

500     format(g13.5)
501     format(g13.5)

```

```

c*    *** write date to output file ***
      write(suntnum,601)
c*    *** set max loop value to number of bins plotted***
      do 200 k=1, 36
        write(suntnum, 600) theta(k), um(k),vm(k),
>ut(k),vt(k),alpha(k),corr(k)
200    continue
600    format(f5.2,' ',f8.2,' ',f8.2,' ',f8.2,' ',
>f8.2,' ',f8.3,' ',f8.5)
601    format('Theta      U-mean      ',
>'V-mean      U-turb      V-turb      Alpha      ',
>'Cuv')

c*    *** close the file ***
      close(untnum)
      close(suntnum)

      write(*,*) 'Complete'

      end

```


APPENDIX G. EQUATIONS AND CALCULATIONS

A. COORDINATES

1. Laser Access Hole Radial Axis

$$y' = D + 0.0625in. \quad (1)$$

2. TTS y-axis

$$y = y' / \cos(\phi) \quad (2)$$

3. TTS z-axis

$$z = y' \cdot \sin(\phi) \quad (3)$$

B. LDV DATA REDUCTION

1. Fringe Spacing

$$(4)$$

2. Velocity/Doppler Frequency Relationship

$$|f_D + f_s| = \frac{c_i}{d_f} \quad (5)$$

3. Measurement Volume Diameter

$$d_m = \frac{4 \cdot \lambda \cdot f}{\pi \cdot D_{e-2} \cdot \cos(\kappa)} \quad (6)$$

where, D_{e-2} is beam diameter of parallel beams measured in the beam expander prior to entering final lens.

4. Measurement Volume Length

$$l_m = \frac{4 \cdot \lambda \cdot f}{\pi \cdot D_{e-2} \cdot \sin(\kappa)} \quad (7)$$

5. Number of Fringes

$$N_F = \frac{d_m}{d_f} \quad (8)$$

6. Velocity

$$c = c_m + c' \quad (9)$$

where, c_m is the mean component and c' is the fluctuating component of c .

7. Absolute Flow Angle

$$\alpha = 90 - \arctan\left(\frac{c_{mz}}{c_{\theta z}}\right) \quad (10)$$

8. Axial Turbulence Intensity (referenced to component velocity)

$$\varepsilon_z = \frac{\sqrt{c_z'^2}}{c_{mz}} \quad (11)$$

9. Tangential Turbulence Intensity (referenced to component velocity)

$$\varepsilon_\theta = \frac{\sqrt{c_\theta'^2}}{c_{m\theta}} \quad (12)$$

10. Correlation Coefficient

$$c_{\theta z} = \frac{\overline{c_\theta' c_z'}}{\sqrt{c_\theta'^2} \sqrt{c_z'^2}} \quad (13)$$

C. DATA NORMALIZATION

1. Inlet Total Velocity

$$V_t = \sqrt{2 \cdot C_p \cdot T_{01}} \quad (14)$$

2. Non-dimensional Mean Axial Velocity

$$X_z = \frac{c_{mz}}{V_t} \quad (15)$$

3. Non-dimensional Mean Tangential Velocity

$$X_\theta = \frac{c_{m\theta}}{V_t} \quad (16)$$

4. **Axial Turbulence Intensity** (referenced to inlet total velocity)

$$T_z = \varepsilon_z \cdot X_z \quad (17)$$

5. **Tangential Turbulence Intensity** (referenced to inlet total velocity)

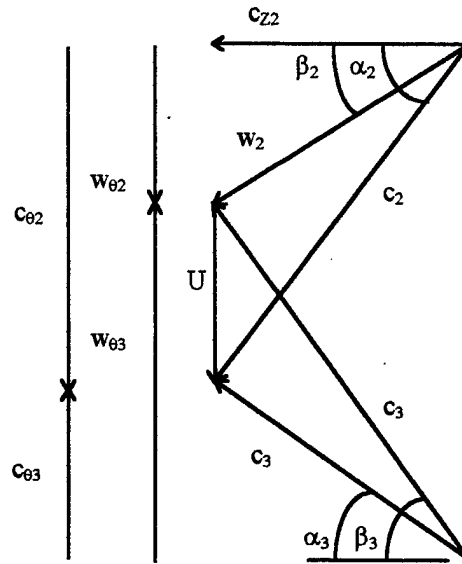
$$T_\theta = \varepsilon_\theta \cdot X_\theta \quad (18)$$

6. **Referred Rotational Speed**

$$N_{ref} = \frac{RPM}{\sqrt{\theta}} \quad (19)$$

where, $\theta = \frac{T_t}{T_{REF}}$

D. CALCULATIONS FOR 0.6 SPAN VELOCITY ANALYSIS



Calculate velocity at the stator inlet position;

$$\begin{aligned} C_1 &= C_{z1} = M \sqrt{\gamma \cdot R \cdot T_t} \\ &= (0.17) \sqrt{(1.4) (287) (309)} = 59.9 \text{ m/s} \end{aligned} \quad (20)$$

Calculate wheel speed;

$$U = \Omega \cdot r = (5043) \left(\frac{1}{60}\right) (2\pi) (0.1183) = 62.45 \text{ m/s} \quad (21)$$

Calculate static pressure and temperature;

$$P_t = 30.4 \text{ kPa} + 101.3 \text{ kPa} = 131.7 \text{ kPa}, \quad T_t = 311 \text{ K}$$

$$P = \frac{P_t}{\left(1 + \frac{\gamma - 1}{2} M^2\right)^{\gamma/\gamma-1}} = \frac{131.7}{\left(1 + \frac{0.4}{2} (0.17)^2\right)^{3.5}} = 121.9 \text{ kPa} \quad (22)$$

$$T = \frac{T_t}{\left(1 + \frac{\gamma - 1}{2} M^2\right)} = \frac{311}{\left(1 + \frac{0.4}{2} (0.17)^2\right)} = 309^\circ \text{K} \quad (23)$$

Calculate mass flow rate stator inlet annulus;

$$A_1 = \pi(r_{t1}^2 - r_{h1}^2) = \pi[(0.1307)^2 - (0.1012)^2] = 0.0215 \text{ m}^2 \quad (24)$$

$$\rho = \frac{P}{R \cdot T} = \frac{129.1}{(289)(309)} = 1.46 \text{ kg/m}^3 \quad (25)$$

$$\dot{m} = \rho \cdot c_{z1} \cdot A_1 = (1.46)(59.9)(0.0215) = 1.88 \text{ kg/m}^3 \quad (26)$$

Calculate C_{z2} for reduced annulus area, assuming density is constant across stator;

$$\begin{aligned} \dot{m} &= \rho \cdot c_{z2} \cdot A_2 = (1.46)(c_{z2})(0.0179) = 1.88 \\ \rightarrow c_{z2} &= 71.9 \text{ m/s} \end{aligned} \quad (27)$$

Use velocity triangle relationships to calculate rotor absolute flow angle;

$$\begin{aligned} c_{\theta 2} &= c_{z2} \cdot \arctan(\alpha_2) = 197.9 \text{ m/s} \\ \text{where, } \alpha_2 &= 70.0^\circ (\text{metal angle}) \end{aligned} \quad (28)$$

$$w_{\theta 2} = c_{\theta 2} - U = 197.9 - 62.5 = 135.4 \text{ m/s} \quad (29)$$

$$\beta_2 = \arctan\left(\frac{w_{\theta 2}}{c_{z2}}\right) = 62.0^\circ \quad (30)$$

Note that the rotor metal angle was 33 deg, giving a blade incidence of 29 deg. Design speed incidence was 15 degrees.

$$w_{\theta 3} = c_{z3} \cdot \tan(\beta_3) = (71.9)(2.605) = 187.3 \text{ m/s} \quad (31)$$

$$c_{\theta 3} = w_{\theta 3} - U = 187.3 - 62.5 = 124.8 \text{ m/s} \quad (32)$$

$$\alpha_3 = \arctan\left(\frac{c_{\theta 3}}{c_{z3}}\right) = \arctan\left(\frac{124.8}{71.9}\right) = 60^\circ \quad (33)$$

APPENDIX H. PRESSURE PROBE DATA

SSME HPTTP AND First-Stage Stator Inlet Velocity Survey													
RPMref=4853													
Tar (in H2O)	Cal (in H2O)	Pt2 (in H2O)	Cobra P1 (in H2O)	Cobra P23 (in H2O)	ATM (in Hg)	RPM	Beta	Dim Vel (X)	Mach (M)	Rad Pos (in)	Prat	Swirl (deg)	Rad Pos (in)
-1.93	135.88	122.82	121.89	118.07	29.84	5035.3	0.00719	0.07593	0.170	1.089	0.978	14.0	1.090
-1.84	135.83	122.98	121.76	118.02	29.84	5050.6	0.00705	0.07568	0.170	1.089	0.978	13.6	1.040
-1.94	135.86	123.06	121.96	118.26	29.84	5048.8	0.00699	0.07558	0.169	1.050	0.978	13.0	0.980
-1.95	135.73	122.38	121.75	118.21	29.84	5043.4	0.00668	0.07503	0.168	1.001	0.979	12.9	0.920
-1.98	136.03	122.73	121.81	118.31	29.84	5043.0	0.00661	0.07491	0.168	0.957	0.979	12.6	0.860
-1.87	135.92	122.47	121.88	118.32	29.84	5029.3	0.00673	0.07511	0.168	0.904	0.979	12.8	0.820
-1.98	135.93	122.67	121.97	118.40	29.84	5049.1	0.00675	0.07514	0.169	0.855	0.979	12.5	0.770
-1.98	135.97	122.48	121.91	117.93	29.84	5031.3	0.00750	0.07647	0.172	0.772	0.979	12.6	0.730
-1.97	135.93	122.57	121.89	118.04	29.84	5036.3	0.00726	0.07604	0.171	0.708	0.979	12.0	0.650
-1.98	135.93	122.86	122.05	118.19	29.84	5049.4	0.00729	0.07610	0.171	0.559	0.978	12.5	0.570
-1.97	135.94	122.44	121.95	118.05	29.84	5014.4	0.00737	0.07623	0.171	0.601	0.979	12.0	0.530
-1.96	135.91	122.31	121.83	118.06	29.84	5051.1	0.00712	0.07579	0.170	0.542	0.979	12.0	0.480
-1.95	135.91	123.15	122.27	118.40	29.84	5043.5	0.00730	0.07612	0.171	0.498	0.978	11.5	0.410
-1.93	135.80	122.18	122.12	118.28	29.84	5045.4	0.00723	0.07599	0.170	0.454	0.980	12.0	0.360
-1.90	135.84	123.14	122.39	118.40	29.84	5047.2	0.00752	0.07651	0.172	0.401	0.978	10.9	0.300
-1.89	135.91	122.54	122.19	118.20	29.84	5045.4	0.00754	0.07654	0.172	0.342	0.979	11.4	0.240
-1.89	136.04	122.84	122.36	118.24	29.84	5043.9	0.00778	0.07697	0.173	0.298	0.979	10.9	0.180
-1.88	136.00	123.24	122.48	118.36	29.84	5051.5	0.00777	0.07697	0.173	0.254	0.978	10.8	0.130
-1.90	135.96	122.41	122.35	118.16	29.84	5037.3	0.00791	0.07721	0.173	0.205	0.979	10.9	0.090
-1.89	135.93	123.13	122.45	118.23	29.84	5048.1	0.00796	0.07731	0.173	0.156	0.978	10.8	0.040
-1.89	135.92	123.00	122.44	118.13	29.84	5047.0	0.00813	0.07763	0.174	0.103	0.978		
-1.89	135.93	123.46	122.62	118.38	29.84	5052.9	0.00799	0.07737	0.174	0.054	0.978		
-1.90	136.00	123.03	122.47	118.35	29.84	5038.0	0.00777	0.07697	0.173	0.010	0.978		
-1.97	136.00	123.33	122.30	118.30	29.84	5041.9	0.00755	0.07657	0.172	0.015	0.978		

Note: Swirl angle was obtained on independent survey under same conditions.

SSME HPFTR ADR First-Stage Rotor Exit Velocity Survey														Sheet 1 of 2	
RPMref=4839															
Tar	Cal	Pc2	Cobra P1	Cobra P23	ATM	RPM	Beta	Dia Vel	Mach	Rad Pos	Prat	Swrl	Rad Pos		
(In H2O)	(In H2O)	(In H2O)	(In H2O)	(In H2O)	(In Hg)			(X)	(M)	(In)		(deg)	(In)		
-1.78	135.03	123.94	8.15	0.26	29.985	5045.3	0.01887	0.10102	0.227	0.986	0.755	-1.85	0.986		
-1.78	135.05	123.67	11.93	4.22	29.985	5073.2	0.01827	0.09959	0.224	0.947	0.763	-0.44	0.947		
-1.77	135.02	123.72	13.91	4.92	29.985	5062.7	0.02120	0.10659	0.24	0.913	0.763	-1.93	0.913		
-1.75	135.07	123.43	11.86	2.48	29.985	5063.1	0.02224	0.10908	0.245	0.894	0.758	-0.62	0.894		
-1.74	135.08	123.98	8.92	0.07	29.985	5073.3	0.02113	0.10643	0.239	0.884	0.754	11.51	0.884		
-1.75	135.13	124.19	6.65	-1.81	29.985	5077.4	0.02031	0.10445	0.235	0.859	0.751	16.44	0.859		
-1.72	135.03	124.30	4.92	-2.78	29.985	5069.8	0.01857	0.10029	0.225	0.82	0.75	31.11	0.82		
-1.72	135.02	124.50	4.85	-2.27	29.985	5071.3	0.01716	0.09659	0.218	0.811	0.751	34.28	0.811		
-1.71	135.00	123.87	7.17	-0.49	29.985	5060.6	0.01836	0.09981	0.224	0.767	0.754	42.28	0.767		
-1.71	135.02	124.13	13.68	3.51	29.985	5072.4	0.02402	0.11336	0.255	0.747	0.758	45.44	0.747		
-1.7	135.02	124.00	16.29	5.58	29.985	5069.6	0.02513	0.11603	0.261	0.723	0.761	49.83	0.723		
-1.68	135.00	124.26	18.87	7.43	29.985	5067.9	0.02670	0.11979	0.27	0.703	0.763	49.83	0.703		
-1.68	135.00	124.42	23.26	10.11	29.985	5066.5	0.03036	0.12840	0.289	0.674	0.765	51.59	0.674		
-1.67	135.00	124.44	25.06	11.19	29.985	5077.1	0.03191	0.13196	0.298	0.654	0.765	51.77	0.654		
-1.67	135.00	124.37	26.79	12.35	29.985	5072.6	0.03307	0.13461	0.304	0.62	0.767	53.09	0.62		
-1.66	135.10	124.14	27.59	12.55	29.985	5073.4	0.03440	0.13759	0.311	0.596	0.766	51.42	0.596		
-1.65	135.04	124.03	27.89	12.52	29.985	5080.2	0.03512	0.13918	0.314	0.576	0.766	51.42	0.576		
-1.64	135.02	124.00	27.74	12.51	29.985	5054.0	0.03482	0.13851	0.313	0.557	0.766	51.33	0.557		
-1.64	135.01	123.62	27.37	12.18	29.985	5080.8	0.03476	0.13838	0.312	0.523	0.766	49.57	0.523		
-1.62	134.99	124.58	27.03	11.92	29.985	5074.0	0.03458	0.13799	0.312	0.498	0.764	49.66	0.498		
-1.62	134.99	124.38	26.68	11.68	29.985	5072.1	0.03438	0.13754	0.31	0.479	0.764	49.57	0.479		
-1.61	134.99	124.21	26.4	11.54	29.985	5076.3	0.03407	0.13685	0.309	0.449	0.765	51.06	0.449		
-1.6	134.99	123.98	26.14	11.34	29.985	5058.6	0.03395	0.13658	0.308	0.42	0.765	52.82	0.42		
-1.59	134.98	123.98	25.87	10.94	29.985	5060.9	0.03429	0.13733	0.31	0.396	0.764	54.58	0.396		
-1.58	134.97	124.21	25.57	10.27	29.985	5072.8	0.03514	0.13920	0.314	0.381	0.761	56.16	0.381		
-1.57	135.06	124.74	25.27	10.15	29.985	5087.4	0.03477	0.13839	0.312	0.352	0.761	61.52	0.352		
-1.52	134.98	124.24	24.65	10.52	29.985	5080.2	0.03254	0.13341	0.301	0.322	0.764	64.78	0.322		
-1.54	134.97	124.25	24.43	10.16	29.985	5074.7	0.03286	0.13414	0.303	0.298	0.763	66.53	0.298		
-1.54	134.97	124.02	24.28	9.89	29.985	5073.3	0.03315	0.13477	0.304	0.278	0.763	68.38	0.278		

SSME HPFTP ADT First-Stage Rotor Exit Velocity Survey													Sheet 2 of 2	
RPMref=4839														
Tar (in H2O)	Cal (in H2O)	PT2 (in H2O)	Cobra P1 (in H2O)	Cobra P23 (in H2O)	ATM (in Hg)	RPM	Beta	Dim Vel (%)	Mach (M)	Rad Pos (in)	Prat	Swirl (deg)	Rad Pos (in)	
-1.53	134.87	123.97	24.2	9.58	29.985	5061.9	0.03370	0.13601	0.307	0.259	0.762	70.49	0.259	
-1.54	134.98	124.21	24.25	9.34	29.985	5077.3	0.03436	0.13749	0.31	0.22	0.76	72.16	0.22	
-1.54	134.99	124.41	24.43	8.94	29.985	5061.9	0.03569	0.14041	0.317	0.195	0.758	72.07	0.195	
-1.53	135.03	124.51	24.58	8.94	29.985	5078.3	0.03602	0.14115	0.319	0.166	0.758	73.74	0.166	
-1.53	135.03	124.44	24.75	9.05	29.985	5072.1	0.03613	0.14137	0.319	0.161	0.758	73.65	0.161	
-1.52	134.97	124.58	24.91	9.42	29.985	5063.8	0.03565	0.14032	0.317	0.122	0.759	73.65	0.122	
-1.52	134.96	124.53	25.1	9.57	29.985	5072.7	0.03572	0.14048	0.317	0.117	0.759	72.07	0.117	

APPENDIX I. PHASE MENU SETTINGS

I/O Port Selection:	
Traverse Controller	COM 1
Sony Position Enc.	COM 2
Printer Port	LPT 1
Proc./RMR I/O Port	COM 1
Color Link	Off

Hardware Selection:	
First Processor	IFA750
Second Processor	IFA750
Third Processor	NA
Master Interface	MI750
Rotary Encoder Type	1989

Table I1. I/O Port and Processor Selection

IFA 750 Operation Parameters	Manual Override
Number of Processors	2
Number of K-Data Points	20
Data Sampling Method	TBD on
Coincidence Window Width (μ sec)	1.2E5
DMA Time-out	999 Sec
Acquisition Mode	Coincidence
Sampling Time (μ sec)	100
Automatic Filter Selections	5-30 MHz 3-20 MHz
Number of C-Words	0
Single Measurement/Burst	Off
Transit Time Enable	Off
Minimum Threshold	10

Table I2. Processor Settings

Minimum Cycles/Burst	4
Signal to Noise Ratio	Very Low
Threshold Optimization	Off

Table I3. Manual Override Settings

	Processor 1	Processor 2
Fringe Spacing (Microns)	4.7591	4.5139
Frequency Shift (MHz)	-10 or 0	0
Half Angle (Degrees)	3.1	3.1
Focal Length (mm)	762	762
Beam Spacing (mm)	82.5	82.5
Wavelength (Nanometers)	514.5	488.0
Rotation x-y Plane (Degrees)	0.0	
Tilt y-z Plane (Degrees)	0.0	

Table I4. Optics Configuration

Application	Turbo Machinery
RMR Mode of Operation	Phase Lock Loop (PLL)
Lock Detect Sensitivity	+192 minutes
Encoder Pluses per Revolution	3600
Resolver Pulsed per Revolution	3600
Number of Sectors	50
Number of Windows	1 or 50
Window Width (points)	72 or as required
Delay to First Sector	0 or as required
Sector with Window Number 1	1

Table I5. Rotary Encoder Setup

APPENDIX J. LDV DATA

FIRST-STAGE ROTOR LDV DATA				Window Ave: off		
Date: 24 Sep 97				Axial Pos.: -0.16ct		
N ref: 4815				Span Pos.: 98%		
Vt= 798.8 m/s				t: 0.020 in		
Filter Settings: 5-30 MHz						
Theta	X_theta	X_axial	T_theta	T_axial	Alpha	Corr Coef
0.10	0.1793	0.0637	1.6299	1.6694	70.45	0.0022
0.30	0.1784	0.0654	1.6024	1.6617	69.87	-0.0275
0.50	0.1744	0.0644	1.8641	1.7768	69.72	0.0007
0.70	0.1703	0.0649	1.8507	1.7211	69.13	0.0011
0.90	0.1623	0.0659	1.8975	1.8738	67.92	0.0049
1.10	0.1560	0.0650	1.8192	1.8345	67.39	0.0632
1.30	0.1514	0.0649	1.8589	1.7259	66.81	0.0206
1.50	0.1488	0.0646	1.8585	1.6950	66.53	0.0519
1.70	0.1447	0.0659	1.8834	1.7483	65.50	0.0150
1.90	0.1436	0.0639	1.8700	1.6939	66.00	0.0237
2.10	0.1402	0.0654	1.8790	1.7347	64.99	0.0004
2.30	0.1376	0.0644	1.8797	1.6244	64.92	0.0502
2.50	0.1359	0.0644	1.8982	1.7287	64.64	0.0609
2.70	0.1350	0.0649	2.0015	1.6847	64.33	0.0522
2.90	0.1345	0.0650	2.0629	1.6155	64.19	0.0303
3.10	0.1343	0.0659	2.1520	1.6817	63.84	0.0181
3.30	0.1327	0.0648	2.1557	1.7625	63.98	0.0172
3.50	0.1302	0.0647	2.2023	1.7313	63.58	-0.0160
3.70	0.1291	0.0650	2.0713	1.7396	63.29	0.0801
3.90	0.1304	0.0645	2.0659	1.7266	63.69	-0.0161
4.10	0.1310	0.0649	2.1628	1.6701	63.63	0.0662
4.30	0.1328	0.0654	2.2649	1.7095	63.77	0.0420
4.50	0.1354	0.0650	2.4797	1.7624	64.37	-0.0020
4.70	0.1408	0.0650	2.5133	1.7241	65.22	0.0348
4.90	0.1426	0.0644	2.5481	1.6801	65.69	-0.0092
5.10	0.1476	0.0673	2.3805	1.8222	65.49	-0.0529
5.30	0.1553	0.0665	2.3558	1.6143	66.82	0.0113
5.50	0.1565	0.0663	2.3588	1.6939	67.03	0.0047
5.70	0.1606	0.0659	2.3020	1.5974	67.70	-0.0036
5.90	0.1667	0.0664	2.2306	1.5797	68.29	0.0132
6.10	0.1709	0.0649	2.0675	1.6480	69.19	-0.0487
6.30	0.1740	0.0658	1.8685	1.6423	69.28	-0.0409
6.50	0.1765	0.0650	1.6716	1.6461	69.79	-0.0417
6.70	0.1789	0.0658	1.5849	1.5666	69.80	-0.0867
6.90	0.1804	0.0643	1.4413	1.5736	70.37	-0.0772
7.10	0.1800	0.0646	1.4800	1.6637	70.26	-0.1493

FIRST-STAGE ROTOR LDV DATA				Window Ave: off		
Date: 24 Sep 97				Axial Pos.: -0.16ct		
N ref: 4825				Span Pos.: 93%		
Vt= 798.8 m/s				t: 0.020 in		
Filter Settings: 5-30 MHz						
Theta	X_theta	X_axial	T_theta	T_axial	Alpha	Corr Coef
0.10	0.1781	0.0772	1.5603	1.6002	66.56	-0.0316
0.30	0.1774	0.0789	1.4994	1.6084	66.02	-0.1043
0.50	0.1723	0.0793	1.6146	1.6580	65.28	-0.0554
0.70	0.1685	0.0788	1.6045	1.6652	64.95	0.0582
0.90	0.1652	0.0801	1.4799	1.5557	64.13	-0.0092
1.10	0.1613	0.0792	1.2371	1.5271	63.84	0.0572
1.30	0.1593	0.0798	1.2023	1.5818	63.38	-0.0106
1.50	0.1560	0.0800	1.2374	1.4951	62.86	0.0720
1.70	0.1549	0.0794	1.2331	1.5685	62.86	0.0947
1.90	0.1543	0.0786	1.1298	1.4996	63.02	-0.0029
2.10	0.1545	0.0777	1.1449	1.4684	63.30	0.0534
2.30	0.1543	0.0793	1.1590	1.4188	62.80	0.0036
2.50	0.1540	0.0798	1.2754	1.4069	62.62	0.0760
2.70	0.1546	0.0800	1.3295	1.5289	62.63	0.0312
2.90	0.1552	0.0819	1.3904	1.5410	62.17	0.0591
3.10	0.1557	0.0810	1.4618	1.5586	62.51	0.1069
3.30	0.1561	0.0819	1.4623	1.5547	62.31	0.0176
3.50	0.1544	0.0814	1.6749	1.6052	62.21	0.0795
3.70	0.1558	0.0811	1.6436	1.5304	62.51	0.0451
3.90	0.1549	0.0813	1.6834	1.7040	62.29	0.0890
4.10	0.1551	0.0821	1.8269	1.7079	62.10	0.0733
4.30	0.1551	0.0814	1.8452	1.6472	62.30	0.1034
4.50	0.1560	0.0805	1.8131	1.6478	62.72	0.0350
4.70	0.1592	0.0820	1.8517	1.6657	62.76	0.0893
4.90	0.1586	0.0837	1.9586	1.6044	62.16	0.0058
5.10	0.1625	0.0822	1.9106	1.6400	63.15	0.0732
5.30	0.1650	0.0838	1.7611	1.5667	63.08	0.0367
5.50	0.1669	0.0838	1.8196	1.6204	63.34	0.0079
5.70	0.1701	0.0825	1.6859	1.6665	64.13	-0.0172
5.90	0.1726	0.0839	1.6450	1.6677	64.08	-0.0779
6.10	0.1745	0.0827	1.5128	1.6403	64.65	0.0000
6.30	0.1778	0.0819	1.3278	1.5641	65.25	-0.0792
6.50	0.1795	0.0831	1.3070	1.5342	65.17	-0.0694
6.70	0.1813	0.0801	1.1624	1.5151	66.16	-0.1453
6.90	0.1814	0.0804	1.1989	1.5773	66.08	0.0470
7.10	0.1823	0.0781	1.1560	1.4783	66.82	0.0042

FIRST-STAGE ROTOR LDV DATA				Window Ave: On		
Date: 24 Sep 97				Axial Pos: -0.16ct		
N ref: 4810				Span Pos: 93%		
Vt: 799.1 m/s				t: 0.020		
Filter Settings: 5-30 MHz						
Theta	X_theta	X_axial	T_theta	T_axial	Alpha	Corr Coef
0.30	0.1519	0.0804	1.2640	1.6684	62.111	-0.0161
0.50	0.1534	0.0816	1.2350	1.5699	62.005	0.0561
0.70	0.1535	0.0811	1.4091	1.6018	62.151	0.0825
0.90	0.1554	0.0820	1.3393	1.5850	62.189	0.0560
1.10	0.1563	0.0829	1.3876	1.5757	62.045	0.0522
1.30	0.1555	0.0826	1.5470	1.6466	62.012	0.0288
1.50	0.1555	0.0830	1.5659	1.6908	61.907	0.0701
1.70	0.1574	0.0823	1.5925	1.6706	62.403	0.0924
1.90	0.1574	0.0824	1.6403	1.6577	62.362	0.1271
2.10	0.1541	0.0829	1.9168	1.6727	61.712	0.1247
2.30	0.1570	0.0837	1.8897	1.6484	61.922	0.0034
2.50	0.1563	0.0836	1.8975	1.6493	61.863	0.0609
2.70	0.1578	0.0853	1.9104	1.6840	61.596	0.0946
2.90	0.1599	0.0840	1.9921	1.6735	62.292	0.0892
3.10	0.1608	0.0840	1.9693	1.6627	62.408	0.0694
3.30	0.1641	0.0852	1.9386	1.6693	62.577	0.0345
3.50	0.1664	0.0838	1.8857	1.6552	63.274	0.0256
3.70	0.1699	0.0853	1.7581	1.6048	63.343	0.0185
3.90	0.1697	0.0847	1.7344	1.6484	63.475	-0.0520
4.10	0.1730	0.0845	1.7182	1.5146	63.964	0.0168
4.30	0.1752	0.0838	1.5823	1.6333	64.451	-0.0592
4.50	0.1764	0.0832	1.6243	1.5797	64.737	0.0010
4.70	0.1776	0.0824	1.5082	1.5825	65.124	-0.0149
4.90	0.1773	0.0813	1.6539	1.6140	65.369	-0.1623
5.10	0.1789	0.0824	1.4653	1.6019	65.261	-0.0132
5.30	0.1754	0.0813	1.5522	1.5879	65.137	0.0084
5.50	0.1735	0.0805	1.7355	1.4655	65.122	-0.0265
5.70	0.1722	0.0800	1.5151	1.5131	65.072	-0.0293
5.90	0.1681	0.0812	1.5479	1.7215	64.200	0.0373
6.10	0.1636	0.0806	1.6032	1.5684	63.785	-0.0080
6.30	0.1612	0.0801	1.3715	1.5807	63.577	-0.0007
6.50	0.1577	0.0806	1.4541	1.5678	62.941	0.0100
6.70	0.1561	0.0805	1.3613	1.5754	62.709	0.0642
6.90	0.1547	0.0803	1.2534	1.5256	62.588	0.0649
7.10	0.1542	0.0803	1.1968	1.5417	62.485	0.0435
7.30	0.1531	0.0819	1.3015	1.5503	61.872	-0.0497

FIRST-STAGE ROTOR LDV DATA				Window Ave: off		
Date: 24 Sep 97				Axial Pos.: -0.16ct		
N ref: 4833				Span Pos.: 88%		
Vt: 798.8 m/s				t: 0.020 in		
Filter Settings: 5-30 MHz						
Theta	X_theta	X_axial	T_theta	T_axial	Alpha	Corr Coef
0.10	0.1828	0.0908	0.9928	1.5642	63.58	0.0575
0.30	0.1819	0.0896	1.2712	1.5879	63.77	0.0063
0.50	0.1752	0.0917	1.4387	1.4620	62.39	-0.1879
0.70	0.1717	0.0871	1.4049	1.6296	63.10	0.0880
0.90	0.1679	0.0897	1.4640	1.4588	61.89	0.0306
1.10	0.1657	0.0882	1.4580	1.5893	61.97	-0.0295
1.30	0.1663	0.0909	1.2608	1.5080	61.34	0.0279
1.50	0.1635	0.0883	1.3568	1.5789	61.62	0.0414
1.70	0.1609	0.0902	1.2161	1.5927	60.73	-0.0838
1.90	0.1589	0.0888	1.1136	1.5359	60.80	0.0475
2.10	0.1565	0.0902	0.9075	1.5514	60.04	0.0341
2.30	0.1540	0.0888	0.9427	1.4709	60.03	-0.0914
2.50	0.1537	0.0896	0.9146	1.4513	59.77	0.0213
2.70	0.1543	0.0892	0.9271	1.5185	59.96	-0.0301
2.90	0.1542	0.0892	0.9116	1.4330	59.97	0.0358
3.10	0.1551	0.0896	0.9368	1.4715	59.99	0.0586
3.30	0.1556	0.0902	0.9553	1.4896	59.89	0.0446
3.50	0.1567	0.0912	0.9935	1.4637	59.80	0.0032
3.70	0.1581	0.0905	0.9521	1.5828	60.21	0.0642
3.90	0.1591	0.0916	0.9863	1.4577	60.08	0.0791
4.10	0.1605	0.0915	0.9567	1.4761	60.31	-0.0459
4.30	0.1613	0.0917	0.9452	1.4793	60.38	0.0164
4.50	0.1630	0.0921	0.9881	1.5438	60.54	-0.0163
4.70	0.1643	0.0926	1.0157	1.5072	60.59	0.0411
4.90	0.1663	0.0922	1.0160	1.4996	60.99	0.0221
5.10	0.1670	0.0928	1.0720	1.5455	60.95	0.0154
5.30	0.1684	0.0920	1.0892	1.5546	61.35	0.0327
5.50	0.1699	0.0934	1.0361	1.4684	61.21	0.0310
5.70	0.1730	0.0925	1.0724	1.5094	61.87	-0.0125
5.90	0.1751	0.0935	1.0350	1.5177	61.92	-0.0738
6.10	0.1759	0.0927	1.0394	1.5224	62.20	-0.1049
6.30	0.1781	0.0928	1.0278	1.5772	62.49	-0.0335
6.50	0.1804	0.0920	0.9780	1.4873	62.98	0.0557
6.70	0.1816	0.0927	0.9627	1.4746	62.95	-0.0355
6.90	0.1831	0.0917	0.9832	1.4658	63.39	-0.1010
7.10	0.1829	0.0914	1.0244	1.4631	63.45	-0.0267

FIRST-STAGE ROTOR LDV DATA				Window Ave: on		
Date: 27 Nov 97				Axial Pos: -0.16		
N ref: 4846				Span Pos: 98%		
Vt: 796.1 m/s				t: 0.020 in		
Filter Settings: 3-20 MHz						
Theta	X_theta	X_axial	T_theta	T_axial	Alpha	Corr Coef
0.10	0.1836	0.0754	2.1973	0.8412	67.68	0.0362
0.30	0.1802	0.0749	2.4688	0.8205	67.42	-0.0006
0.50	0.1753	0.0759	2.3529	0.9050	66.60	-0.1304
0.70	0.1712	0.0748	2.5394	0.8928	66.39	-0.1540
0.90	0.1621	0.0763	2.2030	0.9916	64.79	-0.0162
1.10	0.1522	0.0768	1.7393	0.8844	63.21	-0.1212
1.30	0.1479	0.0759	1.7575	1.0028	62.85	-0.0871
1.50	0.1471	0.0759	1.6537	0.9417	62.72	0.0518
1.70	0.1460	0.0761	1.6168	0.9083	62.49	0.0869
1.90	0.1437	0.0755	1.6366	0.9310	62.28	-0.0169
2.10	0.1439	0.0765	1.6136	0.9334	62.01	0.0659
2.30	0.1438	0.0758	1.6273	0.8833	62.19	-0.0688
2.50	0.1410	0.0753	1.7050	0.8913	61.91	0.0572
2.70	0.1421	0.0758	1.7645	0.8895	61.91	-0.0509
2.90	0.1417	0.0755	1.8621	0.9370	61.95	0.0020
3.10	0.1377	0.0750	1.7463	0.9583	61.42	0.1365
3.30	0.1394	0.0749	1.9487	0.9532	61.76	0.0849
3.50	0.1391	0.0747	1.9815	0.9451	61.77	-0.0325
3.70	0.1381	0.0755	2.0405	0.9277	61.33	0.0116
3.90	0.1391	0.0757	2.0939	0.9198	61.45	-0.0153
4.10	0.1376	0.0755	2.2208	0.8925	61.25	0.0102
4.30	0.1394	0.0747	2.3406	0.9178	61.80	0.0138
4.50	0.1410	0.0745	2.2989	0.8974	62.14	0.0101
4.70	0.1447	0.0752	2.4722	0.9467	62.55	0.0314
4.90	0.1475	0.0756	2.4368	0.9129	62.87	0.0305
5.10	0.1491	0.0753	2.3965	0.9326	63.22	0.0508
5.30	0.1544	0.0746	2.4307	0.9393	64.23	0.0248
5.50	0.1565	0.0750	2.3995	0.9429	64.39	0.0180
5.70	0.1603	0.0752	2.4609	0.9230	64.88	0.0742
5.90	0.1653	0.0755	2.4239	0.9174	65.46	0.0070
6.10	0.1673	0.0751	2.3740	0.9329	65.82	0.0270
6.30	0.1715	0.0751	2.2240	0.8945	66.35	0.0470
6.50	0.1750	0.0757	2.3041	0.9313	66.60	-0.0210
6.70	0.1785	0.0749	2.3526	0.8728	67.23	-0.0774
6.90	0.1819	0.0744	2.1842	0.9007	67.74	0.0351
7.10	0.1816	0.0748	2.3012	0.8972	67.63	0.0636

FIRST-STAGE ROTOR LDV DATA				Window Ave: on		
Date: 27 Nov 97				Axial Pos: -0.16		
N ref: 4849				Span Pos: 93%		
Vt: 795.9 m/s				t: 0.020 in		
Filter Settings: 3-20 MHz						
Theta	X_theta	X_axial	T_theta	T_axial	Alpha	Corr Coef
0.10	0.1830	0.0756	2.0754	0.8548	67.56	0.0439
0.30	0.1791	0.0748	2.4821	0.9191	67.32	-0.1509
0.50	0.1733	0.0758	2.6615	1.0053	66.37	0.0974
0.70	0.1619	0.0763	2.1797	0.7459	64.76	0.0602
0.90	0.1545	0.0752	1.7642	0.9386	64.04	0.0255
1.10	0.1530	0.0736	1.9337	0.9924	64.32	-0.1663
1.30	0.1512	0.0748	1.3248	0.9245	63.69	-0.0448
1.50	0.1514	0.0757	1.3264	0.8889	63.43	-0.0333
1.70	0.1509	0.0761	1.2494	0.8463	63.24	-0.1008
1.90	0.1491	0.0754	1.2537	0.9770	63.18	-0.0079
2.10	0.1506	0.0771	1.1790	0.8818	62.89	0.0496
2.30	0.1496	0.0763	1.3136	0.9169	62.99	0.0784
2.50	0.1511	0.0755	1.2947	0.9069	63.44	0.0035
2.70	0.1514	0.0757	1.2866	0.9263	63.42	-0.0683
2.90	0.1526	0.0755	1.3367	0.8868	63.66	-0.0110
3.10	0.1520	0.0760	1.4108	0.9392	63.44	-0.0056
3.30	0.1535	0.0751	1.4277	0.8866	63.92	0.0489
3.50	0.1542	0.0754	1.3907	0.9060	63.95	0.0402
3.70	0.1538	0.0754	1.6396	0.8938	63.90	-0.0028
3.90	0.1533	0.0751	1.6969	0.9247	63.91	-0.0199
4.10	0.1541	0.0751	1.7660	0.8812	64.01	0.0144
4.30	0.1544	0.0754	1.7727	0.9484	63.96	0.0256
4.50	0.1543	0.0756	1.9492	0.9027	63.90	0.0594
4.70	0.1566	0.0747	2.0105	0.9468	64.51	0.0556
4.90	0.1587	0.0752	1.8922	0.9368	64.66	-0.0483
5.10	0.1607	0.0751	1.9041	0.9524	64.95	0.0105
5.30	0.1624	0.0753	1.9913	0.9168	65.12	-0.0013
5.50	0.1660	0.0754	1.8603	0.9087	65.56	0.0309
5.70	0.1672	0.0753	1.9174	0.9290	65.74	0.0042
5.90	0.1697	0.0755	1.9106	0.9781	66.02	0.0251
6.10	0.1746	0.0755	1.7301	0.9872	66.62	-0.0080
6.30	0.1772	0.0762	1.8237	0.9740	66.73	0.0555
6.50	0.1804	0.0760	1.7933	0.9044	67.16	-0.0598
6.70	0.1815	0.0754	1.8241	0.9414	67.43	-0.0575
6.90	0.1839	0.0765	2.0868	0.9401	67.41	-0.0516
7.10	0.1852	0.0750	2.0463	1.0175	67.94	0.0723

FIRST-STAGE ROTOR LDV DATA				Window Ave: on		
Date: 27 Nov 97				Axial Pos: -0.16		
N ref: 4846				Span Pos: 88%		
Vt: 796.7 m/s				t: 0.020 in		
Filter Settings: 3-20 MHz						
Theta	X_theta	X_axial	T_theta	T_axial	Alpha	Corr Coef
0.10	0.1888	0.0761	2.0148	0.8712	68.05	0.0961
0.30	0.1861	0.0757	2.5251	0.9785	67.87	-0.0278
0.50	0.1784	0.0780	2.7808	0.9397	66.39	-0.1553
0.70	0.1766	0.0763	2.7515	0.9733	66.64	0.1793
0.90	0.1685	0.0765	2.7292	0.9416	65.58	0.0064
1.10	0.1605	0.0780	2.3048	0.9846	64.09	0.1456
1.30	0.1564	0.0768	2.1179	0.8659	63.84	0.0150
1.50	0.1534	0.0782	1.6625	0.8835	62.99	0.0587
1.70	0.1524	0.0760	1.3651	0.8891	63.49	-0.0730
1.90	0.1520	0.0775	1.1568	0.8685	62.97	0.0461
2.10	0.1523	0.0760	1.0552	0.8894	63.49	-0.0730
2.30	0.1508	0.0770	1.0601	0.8714	62.96	0.0108
2.50	0.1510	0.0760	1.0451	0.9000	63.30	0.1189
2.70	0.1513	0.0768	1.0409	0.8770	63.09	0.0600
2.90	0.1521	0.0768	1.0737	0.8791	63.19	0.0409
3.10	0.1520	0.0756	1.0611	0.8830	63.56	-0.0588
3.30	0.1531	0.0759	1.0917	0.8985	63.64	0.0056
3.50	0.1535	0.0758	1.0992	0.9260	63.71	0.0615
3.70	0.1550	0.0757	1.1022	0.9287	63.98	0.0168
3.90	0.1559	0.0754	1.1658	0.9001	64.19	0.0250
4.10	0.1570	0.0760	1.1632	0.9569	64.17	-0.0491
4.30	0.1574	0.0755	1.1918	0.9344	64.39	-0.0357
4.50	0.1595	0.0759	1.1609	0.9028	64.54	-0.0246
4.70	0.1607	0.0755	1.2612	0.9536	64.83	0.0094
4.90	0.1625	0.0756	1.2672	0.9400	65.04	0.0778
5.10	0.1632	0.0762	1.3331	0.9843	64.96	0.0451
5.30	0.1654	0.0764	1.4257	1.0080	65.22	0.0158
5.50	0.1667	0.0762	1.4516	0.9838	65.43	0.0060
5.70	0.1690	0.0765	1.5194	0.9913	65.65	0.0087
5.90	0.1721	0.0760	1.5130	0.9546	66.18	-0.0007
6.10	0.1742	0.0763	1.5450	0.9709	66.34	0.0386
6.30	0.1776	0.0760	1.6072	0.9559	66.84	-0.0196
6.50	0.1814	0.0762	1.5236	0.9568	67.20	0.0879
6.70	0.1834	0.0763	1.6527	0.9121	67.41	-0.0820
6.90	0.1858	0.0762	1.6942	0.9498	67.69	-0.0087
7.10	0.1887	0.0761	1.7904	1.0634	68.04	0.0642

FIRST-STAGE ROTOR LDV DATA				Window Ave: on		
Date: 9 Jan 98				Axial Pos.: 0.35ct		
N ref: 4842				Span Pos.: 93%		
Vt: 795.6 m/s				t: 0.020 in.		
Filter Settings: 3-30 MHz						
Theta	X_theta	X_axial	T_theta	T_axial	Alpha	Corr Coef
2.90	0.1032	0.0745	1.911	1.470	54.15	0.0398
3.10	0.1021	0.0739	1.899	1.430	54.10	0.0464
3.30	0.1018	0.0735	1.915	1.426	54.17	0.0733
3.50	0.1015	0.0725	1.994	1.514	54.45	0.0532
3.70	0.0989	0.0722	1.895	1.501	53.85	0.0953
3.90	0.0967	0.0727	1.879	1.426	53.05	0.1110
4.10	0.0974	0.0731	1.977	1.377	53.10	0.0862
4.30	0.1001	0.0736	2.086	1.397	53.65	0.0369

FIRST-STAGE ROTOR LDV DATA				Window Ave: on		
Date: 20 Jan 98				Axial Pos.: 0.84ct		
N ref: 4841				Span Pos.: 93%		
Vt: 792.8 m/s				t: 0.020 in.		
Filter Settings: 3-30 MHz						
Theta	X_theta	X_axial	T_theta	T_axial	Alpha	Corr Coef
2.20	0.1027	0.0677	1.8674	1.1420	56.60	-0.0733
2.40	0.1042	0.0672	1.9197	1.1535	57.18	-0.0126
2.60	0.1056	0.0676	1.8528	1.1514	57.37	-0.0286
2.80	0.1053	0.0672	1.9556	1.1456	57.46	0.0919
3.00	0.1061	0.0669	1.9401	1.1369	57.78	0.0323
3.20	0.1068	0.0680	1.9813	1.1614	57.50	0.0462
3.40	0.1058	0.0663	1.8968	1.1390	57.94	0.0201
3.60	0.1081	0.0681	2.0022	1.1784	57.79	0.0677
3.80	0.1098	0.0674	1.9885	1.1600	58.44	-0.0402
4.00	0.1085	0.0669	2.0333	1.1358	58.35	0.0297
4.20	0.1036	0.0682	2.0253	1.1803	56.63	-0.1606
4.40	0.0943	0.0688	1.7891	1.1681	53.88	-0.1376
4.60	0.0876	0.0699	1.1071	1.1705	51.42	-0.0604
4.80	0.0855	0.0718	0.6094	1.1619	49.96	-0.0367
5.00	0.0848	0.0726	0.2451	1.1529	49.46	-0.0069

APPENDIX K. TTR AND SSME DATA

TTR DATA (sheet 1 of 2)											
Tar	Cal	P2	P3	P4	P31	P32	P34	vena	Ref Temp		
[in H2O]	[in H2O]	[in H2O]	[in H2O]	[in H2O]	[in H2O]	[in H2O]	[in H2O]	[in H2O]	[deg C]		
9/24/97											
-1.24	135.09	123.88	23.34	123.98	-1.29	168.89	-1.30	166.91	165.74		
-2.14	135.06	123.16	22.60	123.24	-2.18	167.16	-2.19	164.46	164.73		
-4.12	135.00	120.94	20.66	121.28	-4.18	165.74	-4.19	162.87	162.93		
-5.70	134.94	117.78	18.26	118.21	-5.74	162.76	-5.74	160.15	159.30		
-6.45	134.84	117.93	17.70	118.38	-6.50	162.26	-6.49	159.93	159.49		
-7.26	134.84	116.26	16.79	117.07	-7.31	161.05	-7.31	158.21	158.50		
-7.55	134.81	115.87	16.49	116.23	-7.61	160.48	-7.61	157.53	157.15		
11/27/97											
-4.33	135.33	120.72	19.60	120.62	-4.43	165.87	-4.44	163.30	162.99		
-6.77	135.33	118.28	17.42	118.71	-6.84	162.86	-6.84	160.23	160.02		
-8.23	135.20	116.44	15.76	116.60	-8.31	161.35	-8.31	159.06	158.84		
-8.75	135.30	115.99	15.36	116.78	-8.81	160.94	-8.82	157.70	157.81		
-11.44	135.14	113.39	12.80	113.10	-11.50	156.79	-11.49	154.42	154.28		
1/9/98											
-12.88	135.17	110.95	11.31	111.74	-12.92	152.68	-12.92	150.19	149.86		
1/20/98											
-1.27	135.97	120.17	22.30	119.96	-1.41	-1.43	-1.44	135.08	-1.49		

TTR DATA (sheet 2 of 2)									
TT2	TT3	TT4	Water In	Water Out	Orifice	Torque	Speed	Flow	
[deg R]	[deg R]	[deg R]	[deg R]	[deg R]	[deg R]	[in-lbs]	[RPM]	[GPM]	
3.13	29.84	566.76	566.69	544.08	533.48	542.72	575.93	5080.68	
3.10	30.16	570.38	570.05	547.46	536.20	545.40	577.79	5067.93	
3.06	30.74	572.35	572.31	549.47	536.91	546.23	578.60	5076.31	
3.07	31.19	572.41	572.37	549.73	537.00	546.13	578.46	5053.02	
2.96	31.40	572.01	572.04	549.45	536.76	545.99	577.97	5067.18	
2.97	31.64	572.14	572.19	549.67	536.89	546.09	578.21	5046.75	
3.01	31.76	572.41	572.31	549.90	536.72	545.95	578.35	5057.47	
3.11	22.33	567.63	567.45	545.24	542.85	552.25	575.45	5072.86	
3.16	22.50	568.04	567.82	545.66	541.21	550.63	574.79	5072.90	
3.11	22.66	567.59	567.45	545.40	541.81	551.25	575.20	5071.71	
3.14	22.80	568.21	568.01	545.69	541.78	551.22	575.55	5071.43	
3.07	23.54	568.97	568.81	546.79	541.84	551.20	575.97	5056.69	
2.00	27.56	567.39	567.48	545.09	541.91	551.14	575.45	5064.32	
3.12	24.96	563.67	563.28	541.27	618.06	626.91	571.55	5046.03	

SOME DATA												
Press Ratio	Mass Flow [kg/m^3]	Efficiency	Ref Speed [RPM]	Mass Flow [kg/m^3]	Vena	Ref Pwr [HP]	Ref Press Ratio	Ref Temp Ratio	Power 1 [HP]	Power 2 [HP]	Power 3 [HP]	Flange Flow [kg/m^3]
9/24/97												
1.31	3.26	53.64	4860.65	2.62	16.74	1.30	1.05	23.71	22.72	25.04	16.60	9.93
1.31	3.23	53.52	4833.59	2.61	16.60	1.30	1.05	23.46	22.60	24.99	16.52	9.88
1.31	3.22	53.57	4832.64	2.60	16.71	1.30	1.05	23.71	22.79	24.98	16.52	9.87
1.31	3.22	53.63	4810.20	2.61	16.45	1.30	1.05	23.17	22.38	24.76	16.49	9.85
1.31	3.16	53.13	4825.23	2.56	16.50	1.30	1.05	23.41	22.48	24.23	16.51	9.84
1.31	3.17	53.11	4805.16	2.57	16.43	1.30	1.05	23.41	22.36	24.19	16.48	9.82
1.31	3.18	53.20	4814.55	2.58	16.45	1.29	1.05	23.53	22.37	24.29	16.47	9.83
11/27/97												
1.31	3.27	53.37	4849.67	2.61	16.50	1.31	1.05	23.45	22.61	24.74	16.73	10.00
1.31	3.29	53.04	4848.04	2.63	16.51	1.31	1.05	23.63	22.63	24.87	16.70	9.99
1.31	3.26	52.93	4848.67	2.61	16.47	1.31	1.05	23.48	22.54	24.50	16.70	9.98
1.31	3.28	53.35	4845.88	2.62	16.49	1.31	1.05	23.40	22.61	24.96	16.67	9.98
1.31	3.24	52.87	4828.48	2.59	16.41	1.31	1.05	23.08	22.46	24.28	16.65	9.94
1/9/98												
1.31	2.61	53.52	4841.95	2.09	16.46	1.31	1.05	23.28	22.50	19.83	16.55	9.58
1/20/98												
1.30	2.75	54.84	4841.39	2.21	16.35	1.30	1.04	22.31	22.14	20.77	15.63	9.19

LIST OF REFERENCES

1. Sutton, G.P., "Rocket Propulsion Elements, An Introduction to the Engineering of Rockets", Sixth Edition, John Wiley & Sons Inc., 1992.
2. Studevan, C.C., "Design of a Cold-Flow Test Facility for the High-Pressure Fuel Turbopump Turbine of the Space Shuttle Main Engine", Master's Thesis, Naval Postgraduate School, Monterey, California, December 1993.
3. Rutkowski, R.J., "Cold-flow Simulation of the Alternate Turbopump Development Turbine of the Space Shuttle Main Engine High Pressure Fuel Turbopump", Master's Thesis, Naval Postgraduate School, Monterey, California, March 1994.
4. Greco, P.A., "Turbine Performance Mapping of the Space-Shuttle Main Engine High-Pressure Fuel Turbopump", Master's Thesis, Naval Postgraduate School, Monterey, California, September 1995.
5. Malak, M.F., Hamed, A., and Tabakoff, W., "Three-Dimensional Flow Field Measurements in a Radial Inflow Turbine Scroll Using LDV", ASME of Turbomachinery, vol. 109, No. 2, pp 163-169, April 1987.
6. Stauter, R.C., Dring, R.P., and Carta, P.O., "Temporally and Spatially Resolved Flow in a Two-Stage Axial Compressor: Part I-Experiment", ASME Journal of Turbomachinery, vol. 113, No. 2, pp 219-226, April 1991.
7. Stauter, R.C., "Measurement of the Three-Dimensional Tip Region Flowfield in an Axial Compressor", ASME paper No. 92-GT-211, June 1992.
8. Skoch, G.J., Prahst, P.S., Wernet, M.P., Wood, J.R., and Strazisar, A.J., "Laser Anemometer Measurements of the Flow Field in a 4:1 Pressure Ratio Centrifugal Impeller", ASME paper No. 97-GT-342, June 1997.
9. Binder, A., Forster, W., Mach, K., and Rogge, H., "Unsteady Flow Interaction Caused by Stator Secondary Vortices in a Turbine Rotor", ASME Journal of Turbomachinery, Vol 109, pp 251-257, 1987.

10. Zaccaria, M.A., Lakshminarayana, B., "Unsteady Flow Field Due to Nozzle Wake Interaction With the Rotor in an Axial Flow Turbine: Part I-Rotor Passage Flow Field", International Gas Turbine Institute paper No. 95-GT-295, March 1995.
11. Kahn, "Waterbrake Dynamometer", Instructional Manual Model 061-109, Part Number 9755, 1976.
12. AIRPAX Corporation, "TACHTROL 3 Tachometer", Operations Manual, 1994.
13. Electro Sensors, "Proximity Switches 600 Series", ES600, Revision B, April 1991.
14. Electro Sensors, "Digital Signal Conditioner SA420", ES334, 1997.
15. National Instruments, "Getting Started with Your AT-GPIB/TNT and the NI-488.2 Software for Windows", User's Manual, Part Number 320719B-01, August 1994.
16. National Instruments, "DAQ PC-LPM-16", User's Manual, Part Number 320287-01, November 1993.
17. Hewlett-Packard Company, "Model 3456A Digital Voltmeter," User's Manual, Revision B, Part Number 03456-90054, February 1982.
18. Hewlett-Packard Company, "Model 3495A Scanner", Programming and Service Manual, Part Number 03495-90012, August 1978.
19. Hewlett-Packard Company, "5335A Universal Frequency Counter", User's Manual, Fourth Edition, Part Number 05335-90021, August 1988.
20. National Instruments, "LabVIEW for Windows", User Manual, Part Number 320534-01, August 1993.
21. Murray, K. D., "Automation and Extension of LDV Measurements of Off-Design Flow in a Subsonic Cascade Wind Tunnel", Master's Thesis, Naval Postgraduate School, Monterey, California, June 1989.
22. TSI, "System 9100-7 Laser Doppler Velocimeter", Instruction Manual, Part Number 1990157, Revision A, 1984.

23. TSI, "Laser Doppler Velocimetry Optical Components", Part Number 1990381, Revision A, 1990.
24. TSI, "Model 9500 Traverse Table System Hardware and Software", Instruction Manual, Part Number 1990229, Revision B, January 1987.
25. TSI. "Model 9306 Six-Jet Atomizer", Instruction Manual, Part Number 1990143, Revision D, January 1992.
26. TSI, "Model 9180 Frequency Shift System", Instruction Manual, Part Number 1990145, Revision B, 1984.
27. TSI, "Model 1989A High-Speed Rotating Machinery Resolver", Instruction Manual, Part Number 1990303, Revision D, June 1992.
28. TSI, "Model IFA 755 Digital Burst Correlator", Instruction Manual, Part Number 199077, Revision B, January 1997.
29. TSI, "Phase Resolved Software (Phase)", Instruction Manual, Part Number 1990564, Preliminary Revision 2, March 1992.
30. Hill, P.G., Peterson, C.R., "Mechanics and Thermodynamics of Propulsion", Addison-Wesley, Second Edition, 1992.

INITIAL DISTRIBUTION LIST

		No. of Copies
1.	Defense Technical Information Center..... 8725 John J. Kingman Rd., Ste 0944 Ft. Belvoir, VA 22060-6218	2
2.	Dudley Knox Library..... Naval Postgraduate School 411 Dyer Rd. Monterey, CA 93943-5101	2
3.	Department Chairman, Code AA..... Department of Aeronautics and Astronautics Naval Postgraduate School 699 Dyer Road, Rm. 137 Monterey, CA 93943-5107	1
4.	Dr. Garth V. Hobson, PhD., Code AA/HG..... Department of Aeronautics and Astronautics Naval Postgraduate School 699 Dyer Road, Rm. 137 Monterey, CA 93943-5106	5
5.	Dr. Raymond P. Shreeve, PhD., Code AA/SF..... Department of Aeronautics and Astronautics Naval Postgraduate School 699 Dyer Road, Rm. 137 Monterey, CA 93940-5106	1
6.	Naval Air Warfare Center..... AIR-4.4.T (Attn: Mr. C. Gordon) Propulsion and Power Engineering, Building 106 Patuxent River, MD 20670-5304	1
7.	Naval Air Warfare Center Aircraft Division..... AIR-4.4.3.1 (Attn: D. Parish) Propulsion and Power Engineering, Building 106 Patuxent River, MD 20670-5304	1
8.	James D. Southward..... 1308 Evelyn Ct. N.E. Albuquerque, NM 87112	2